

5-20-2005

## Late Quaternary Louisiana Shelf-Margin Deltaic Deposition, North-Central Gulf of Mexico

Casey Mobley  
*University of New Orleans*

Follow this and additional works at: <https://scholarworks.uno.edu/td>

---

### Recommended Citation

Mobley, Casey, "Late Quaternary Louisiana Shelf-Margin Deltaic Deposition, North-Central Gulf of Mexico" (2005). *University of New Orleans Theses and Dissertations*. 237.  
<https://scholarworks.uno.edu/td/237>

This Thesis is protected by copyright and/or related rights. It has been brought to you by ScholarWorks@UNO with permission from the rights-holder(s). You are free to use this Thesis in any way that is permitted by the copyright and related rights legislation that applies to your use. For other uses you need to obtain permission from the rights-holder(s) directly, unless additional rights are indicated by a Creative Commons license in the record and/or on the work itself.

This Thesis has been accepted for inclusion in University of New Orleans Theses and Dissertations by an authorized administrator of ScholarWorks@UNO. For more information, please contact [scholarworks@uno.edu](mailto:scholarworks@uno.edu).

LATE QUATERNARY LOUISIANA SHELF-MARGIN DELTAIC DEPOSITION,  
NORTH-CENTRAL GULF OF MEXICO

A Thesis

Submitted to the Graduate Faculty of the  
University of New Orleans  
in partial fulfillment of the  
requirements for the degree of

Master of Science  
in  
The Department of Geology and Geophysics

by

Casey Ryan Mobley

B.S. University of Kentucky, 2001

May, 2005

## TABLE OF CONTENTS

List of Figures .....	iv
List of Tables .....	vi
Abstract .....	vii
Introduction .....	1
Gulf of Mexico Geologic Framework and Processes .....	2
Structural Elements .....	4
Faulting .....	4
Diapirism .....	4
Late Quaternary Glaciation and Sea-level Fluctuation .....	8
Depositional Response to Sea-level Fluctuation .....	9
Regional History .....	15
Texas Shelf .....	15
Eastern Texas Shelf .....	17
Central Louisiana Shelf-Mississippi Canyon .....	19
Mississippi-Alabama Shelf .....	23
Louisiana Shelf .....	25
Summary .....	28
Methods .....	29
Data Sets .....	29
Geotechnical Foundation Borehole Data .....	29
High-resolution Seismic Profile Data .....	32
West Delta 96 Lease Block Survey Report .....	34
Seismic Sequence Stratigraphy .....	37
Seismic Sequence Analysis .....	38
Seismic Facies Analysis .....	40
Internal Seismic Facies Reflection Patterns .....	42
External Seismic Facies Forms .....	46
Analysis of Relative Change of Sea Level .....	47
Arguments Against Seismic Sequence Stratigraphy .....	53
In Defense of Seismic Sequence Stratigraphy .....	54
Results .....	56
Modern Bathymetry .....	56
Structural Features .....	56
Seismic Sequence Analysis .....	59
Horizons .....	60
Horizon A .....	60
Horizon B .....	61
Horizon C .....	68
Horizon D .....	68
Horizon E .....	69
Seismic Facies Units .....	69
Basal Package .....	69

Package 1 .....	70
Package 2 .....	70
Package 3 .....	80
Package 4 .....	80
Late Wisconsin Unconformity .....	81
Summary .....	85
Discussions .....	87
Late Quaternary Shelf-Margin Delta .....	87
Seismic Characteristics .....	87
Depositional History .....	89
Comparison to Regional Studies.....	92
Paleodrainage Patterns .....	94
Pearl River Scenario .....	98
Conclusions.....	101
References.....	102
Vita.....	107



## LIST OF FIGURES

Figure 1: Physiographic map of Gulf of Mexico basin.....	3
Figure 2: Miss. River Canyon/ Mississippi Fan.....	5
Figure 3: Diagrammatic structural cross-section of northern GOM basin .....	6
Figure 4: Structural features of onshore and offshore Louisiana.....	7
Figure 5: Sea-level change, glacial cycles, and oxygen isotope stages .....	10
Figure 6: Late Pleistocene-Holocene sea-level curves .....	11
Figure 7: Depositional systems response to eustatic flux .....	12
Figure 8: Fluvio-deltaic depositional patterns during a cycle of sea-level change.....	13
Figure 9: Map of Holocene Miss. River deltaic plain and related features .....	14
Figure 10: Shelf-margin deltas described by Suter and Berryhill (1985).....	16
Figure 11: Basemap of northwestern GOM shelf-margin, Morton and Suter (1996) .....	18
Figure 12: Diagrams of lowstand deltaic deposition models.....	20
Figure 13: Basemap of Mississippi Canyon, from Goodwin and Prior (1989) .....	22
Figure 14: Basemaps used in Kindinger (1989b), Lagniappe delta.....	24
Figure 15: Basemap of Coleman and Roberts (1988a) dataset.....	26
Figure 16: Diagrammatical representation of MC 268 borehole .....	30
Figure 17: Basemap of study area showing location of datasets .....	33
Figure 18: Basemap of West Delta 96 lease block survey report .....	35
Figure 19: West Delta 96 lease block survey report seismic profile .....	36
Figure 20: Idealized depositional sequence .....	39
Figure 21: Idealized seismic sequence.....	40
Figure 22: Seismic reflector patterns .....	41
Figure 23: Oblique and sigmoid progradational reflection configurations.....	43
Figure 24: External forms of seismic facies units.....	47
Figure 25: Vail et al. (1977a) diagrams for relative sea-level rise.....	49
Figure 26: Vail et al. (1977a) diagrams for relative sea-level fall and stillstand.....	51
Figure 27: Vail et al. (1977a) depositional models.....	52
Figure 28: Bathymetric map of study area.....	57
Figure 29: Structural map of study area.....	58
Figure 30: Seismic profile of <i>Acadiana</i> 89 Line 19, updip direction .....	62
Figure 31: Seismic profile of <i>Acadiana</i> 86 Lines 31-33, downdip direction.....	63
Figure 32: Seismic profile of <i>Acadiana</i> 89 Line 19, updip direction .....	64
Figure 33: Seismic profile of <i>Acadiana</i> 89 Line 1, downdip direction .....	65
Figure 34: Seismic profile of <i>Acadiana</i> 89 Line 21, downdip direction .....	66
Figure 35: Seismic profile of <i>Acadiana</i> 89 Line 22, updip direction .....	67
Figure 36: Time-structure map of Horizon A .....	71
Figure 37: Time-structure map of Horizon B .....	72
Figure 38: Time-structure map of Horizon C .....	73
Figure 39: Time-structure map of Horizon D .....	74
Figure 40: Time-structure map of Horizon E .....	75
Figure 41: Isochron map of Package 1 .....	76

Figure 42: Isochron map of Package 2 .....	77
Figure 43: Isochron map of Package 3 .....	78
Figure 44: Isochron map of Package 4 .....	79
Figure 45: Diagram illustrating the correlation of Horizon A with the LWU .....	83
Figure 46: Map of relic channels observed in seismic data .....	88
Figure 47: Paleogeographic map of late Pleistocene northern GOM shelf .....	90
Figure 48: Map of northern GOM shelf paleodrainage networks.....	91
Figure 49: Map of late Pleistocene paleodrainage networks, LA shelf .....	95
Figure 50: Cross-sections showing paleodrainage patterns .....	96
Figure 51: Proposed paleodrainage map.....	99

## LIST OF TABLES

Table 1: Oxygen isotope stages, boundaries, and durations .....	31
---	----

## ABSTRACT

This study focuses on establishing a depositional framework model for an area of the Louisiana shelf, north-central Gulf of Mexico. The depositional history of the study area is poorly understood, especially within the last cycle of major eustatic fluctuation (~18,000 yrs BP to present). Data sets include pre-existing and previously unanalyzed two-dimensional, high-resolution seismic profile records (*Acadiana 86* and *Acadiana 89*), geotechnical foundation boring data (Coleman and Roberts, 1988a), and an industry lease block survey report (Cole, 1983). Seismic sequence stratigraphic methods are used in this study to analyze seismic profile data.

Seismic sequence analysis results indicate the presence of five unconformable surfaces and five seismic facies units. Correlation of seismic profile data with lithologic and chronologic data indicates that these seismic facies units represent shelf-margin deltaic deposits formed during the last sea-level lowstand (~18,000 yrs BP). The Pearl River is the most likely fluvial source for these deltaic sediments.

## INTRODUCTION

The northern Gulf of Mexico has been an area of focus for sedimentary geology for more than a half century. Numerous studies conducted in the Gulf of Mexico basin have resulted in an in-depth understanding of fluvial and deltaic response to changes in sea level (Fisk, 1944; Kolb and Van Lopik, 1958; Frazier 1967; Frazier 1974; Suter and Berryhill, 1985; Coleman and Roberts, 1988a; Kindinger, 1988; Penland et al., 1991; Sydow and Roberts, 1994; Morton and Suter, 1996; Anderson et al., 2004; and many others). A substantial body of this research has been focused on establishing a depositional framework for deltaic sediments deposited on the northern Gulf of Mexico shelf and shelf edge within the last cycle of major eustatic fluctuation (~18,000 yrs BP – present).

The modern Mississippi River Deltaic Plain, located in southern Louisiana, has been the focus of much of this work due to its well-preserved regressive stratigraphy as well as to the effects of transgression due to relative sea-level rise on this regressive package (Fisk, 1944; Frazier, 1974; Penland et al., 1991; Stanley et al., 1996). Similar studies have been performed on other fluvio-deltaic systems along the northern Gulf of Mexico shelf (most recently Anderson et al., 2004). However, many uncertainties regarding both the timing and the nature of deposition persist for areas of the northern Gulf of Mexico shelf and shelf-edge environments.

The primary objective of this study is to develop an understanding of the stratigraphic framework of an area extending from the mid shelf and across the shelf edge to the upper slope in the north-central Gulf of Mexico. The study area represents a portion of the Louisiana shelf where the most recent late Quaternary depositional history

has not been previously studied in detail. Bathymetric maps of the Louisiana shelf edge to upper slope in this area show large-scale lobate features similar in morphology to submerged delta lobes deposited by the Mississippi River during the early Holocene (Fig. X) (Maringoin lobe; Frazier, 1974). Genesis and timing of these submerged morphologic features is unknown. Preliminary interest in these submerged features provided the basis for this study.

### *Gulf of Mexico Geologic Framework and Processes*

The Gulf of Mexico basin is in the western northern hemisphere; bounded by the United States to the east, north and west, by Mexico to the west and south, and flanked by Cuba to the southwest. It is elongate along a northeast-southwest axis, with restricted marine communication to the Atlantic Ocean along the southeast (Fig. 1). Major physiographic provinces of the Gulf include shelf and slopes of East Mexico, Texas-Louisiana, West Florida, and the Yucatan peninsula (Fig. 1). Physiographic regions of particular interest to this study are the Louisiana Shelf and Mississippi Canyon (sometimes referred to as the Mississippi Trough) (Fig. 2).

The Gulf of Mexico basin began forming in the Late Triassic with fragmentation of the Pangean supercontinent (Salvador, 1991b). Rifting lasted until the Late Jurassic, resulting in a large area of attenuated continental crust (transitional crust). Oceanic crust (5-6 km thick) underlies the center of the basin, whereas thin transitional crust (8-15 km thick) underlies much of the slope and shelf regions, and thick transitional crust (20-40 km thick) extends to the margins of the basin (Fig. 3) (Buffler and Thomas, 1994). Mesozoic through Cenozoic sedimentary packages deposited by retrogradational and

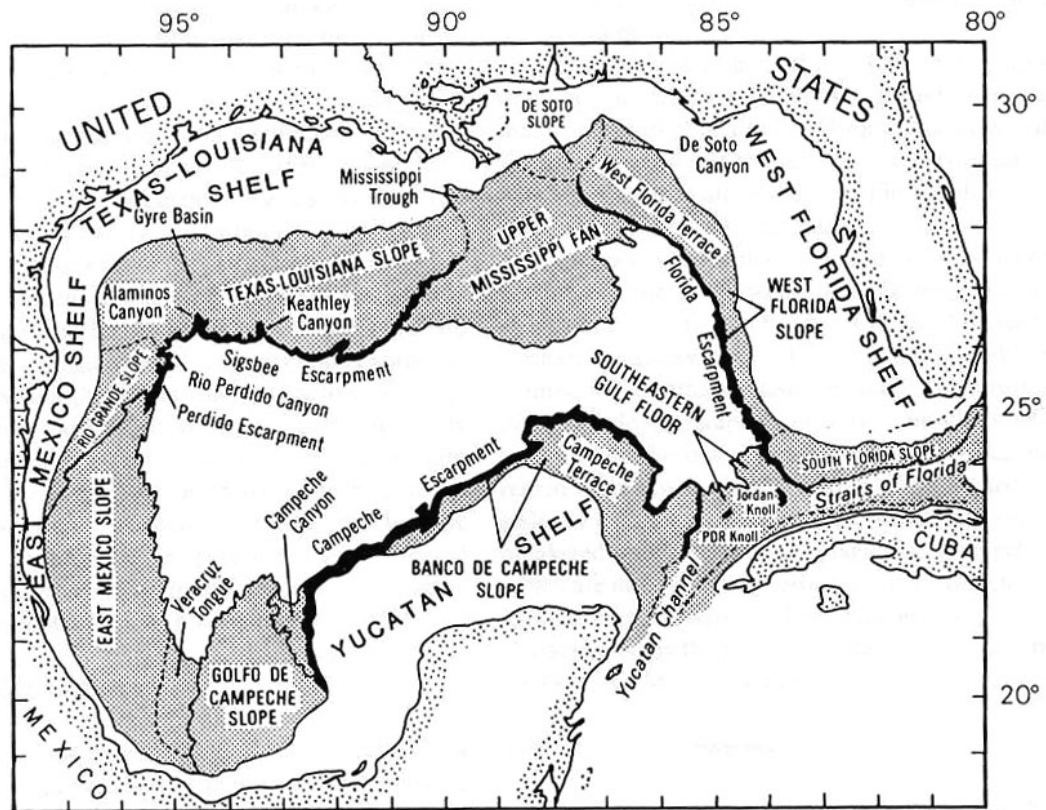


Figure 1. Map of the Gulf of Mexico basin showing the primary physiographic provinces of the region and salient features discussed in the text. (Modified from Coleman et al., 1991). This study focuses on the area indicated by a boxed outline across the continental shelf south of the Barataria Bight.

progradational depocenters overlie Late Triassic to Early Jurassic basement rocks (Fig. 3).

### *Structural Elements*

#### *Faulting*

A common structural feature within the Cenozoic sedimentary package is the existence of numerous, laterally continuous and typically down-to-the-south faults. Locally, these faults indicate as much as 500 m of throw, with consequential thickening of as much as several thousand meters in sedimentary units located on the downthrown side (Lopez, 1990). These normal faults are common along the slope and shelf areas (Fig. 3).

#### *Diapirism*

Upper Jurassic Louann salt is located stratigraphically below the Cenozoic sedimentary packages (Fig 3). Deformation within the Louann salt has influenced substantially the overlying stratigraphic framework (Ewing, 1991).

Sedimentary loading of the salt at depth has resulted in diapirism, a consequence of density contrast between the salt and overlying compacted sedimentary units. This has led to the piercement of overlying strata as salt is extruded upward to form diapirs and in some cases laterally to form large salt massifs (Nelson, 1991). The existence of many of the diapirs is expressed in the modern bathymetry as local highs. They have directly influenced depositional styles and thickness of some sedimentary units because of the seafloor relief they created prior to, during, or after deposition (Suter and Berryhill, 1985; Kindinger, 1988; Morton and Suter, 1996). Figure 4 shows the distribution of major salt bodies on the slope, shelf, and in-shore segments of Louisiana.



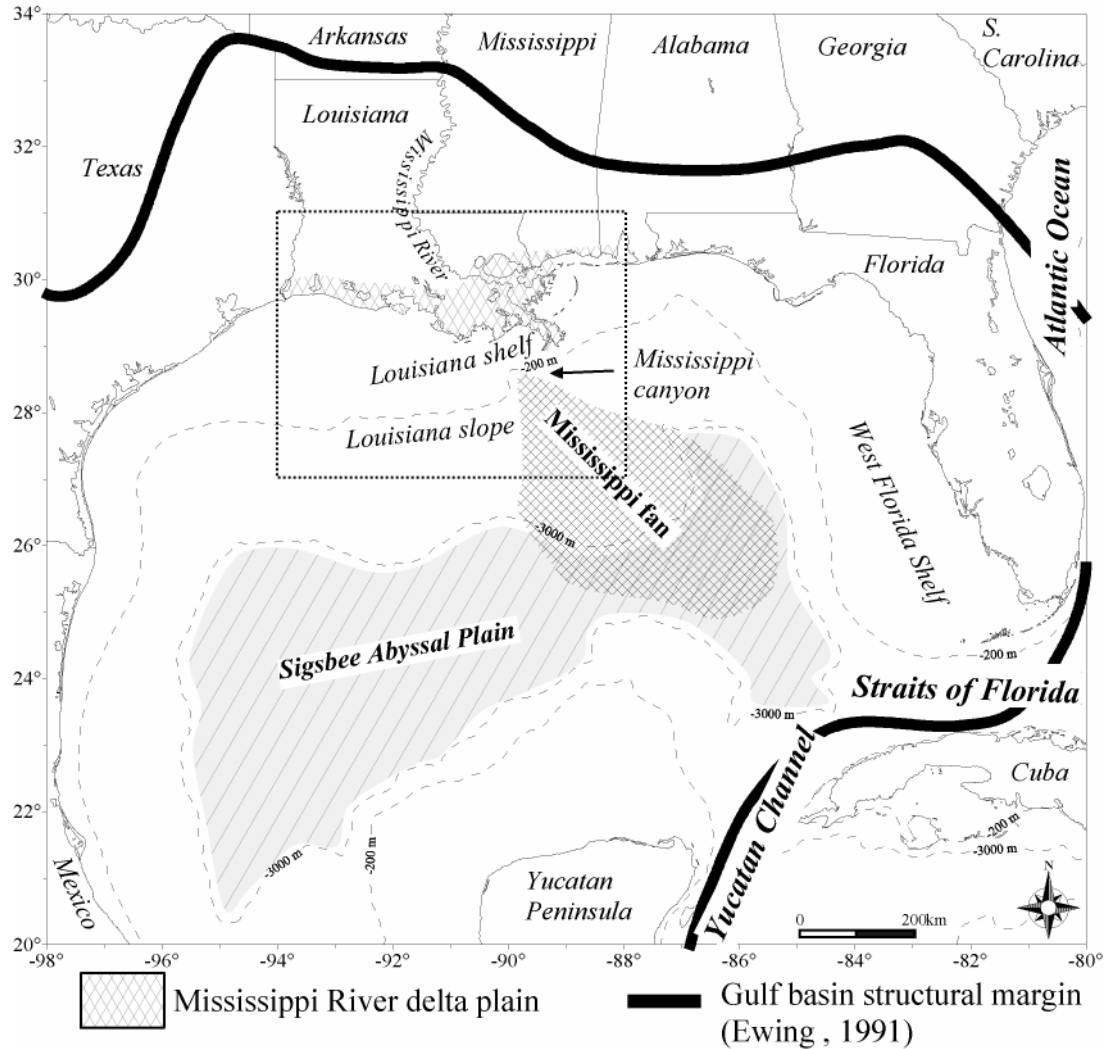


Figure 2. Map of Gulf of Mexico basin showing the structural margins of the basin as defined by (Ewing, 1991). The Mississippi Canyon forms a large embayment along the continental margin that is indicated by the north to northwest indentations of the isobaths. Note the downdip relationship and location of the Mississippi Fan relative to the Mississippi Canyon, which served as the thalweg for sediment delivered to the fan during periods of sea-level lowstand.

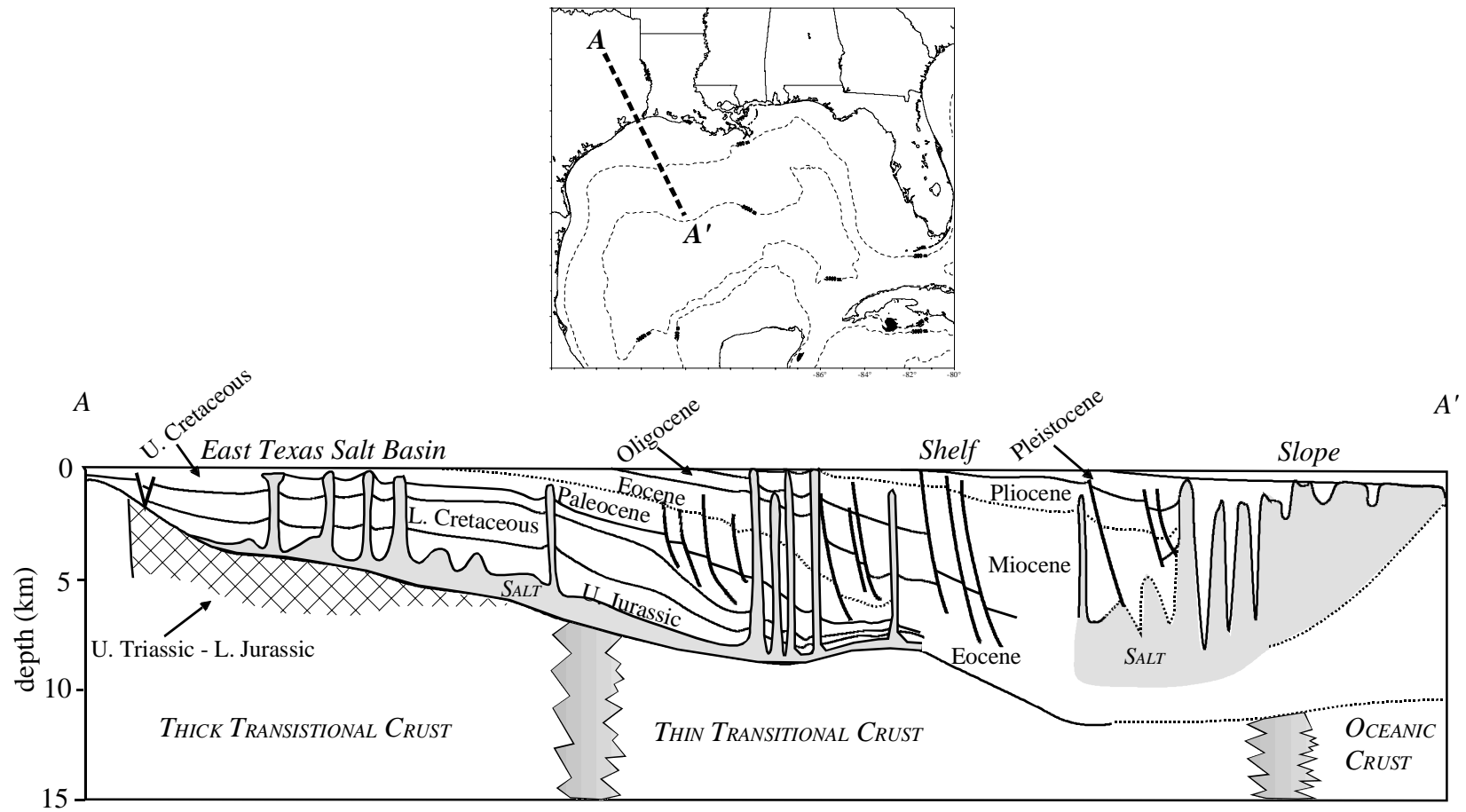


Figure 3. Diagrammatic cross section of the northern Gulf of Mexico Basin. Upper Jurassic salt deposits and down-to-south movement of Cenozoic growth faults are responsible for deformation of overlying stratal layers (modified from Salvador, 1991b).

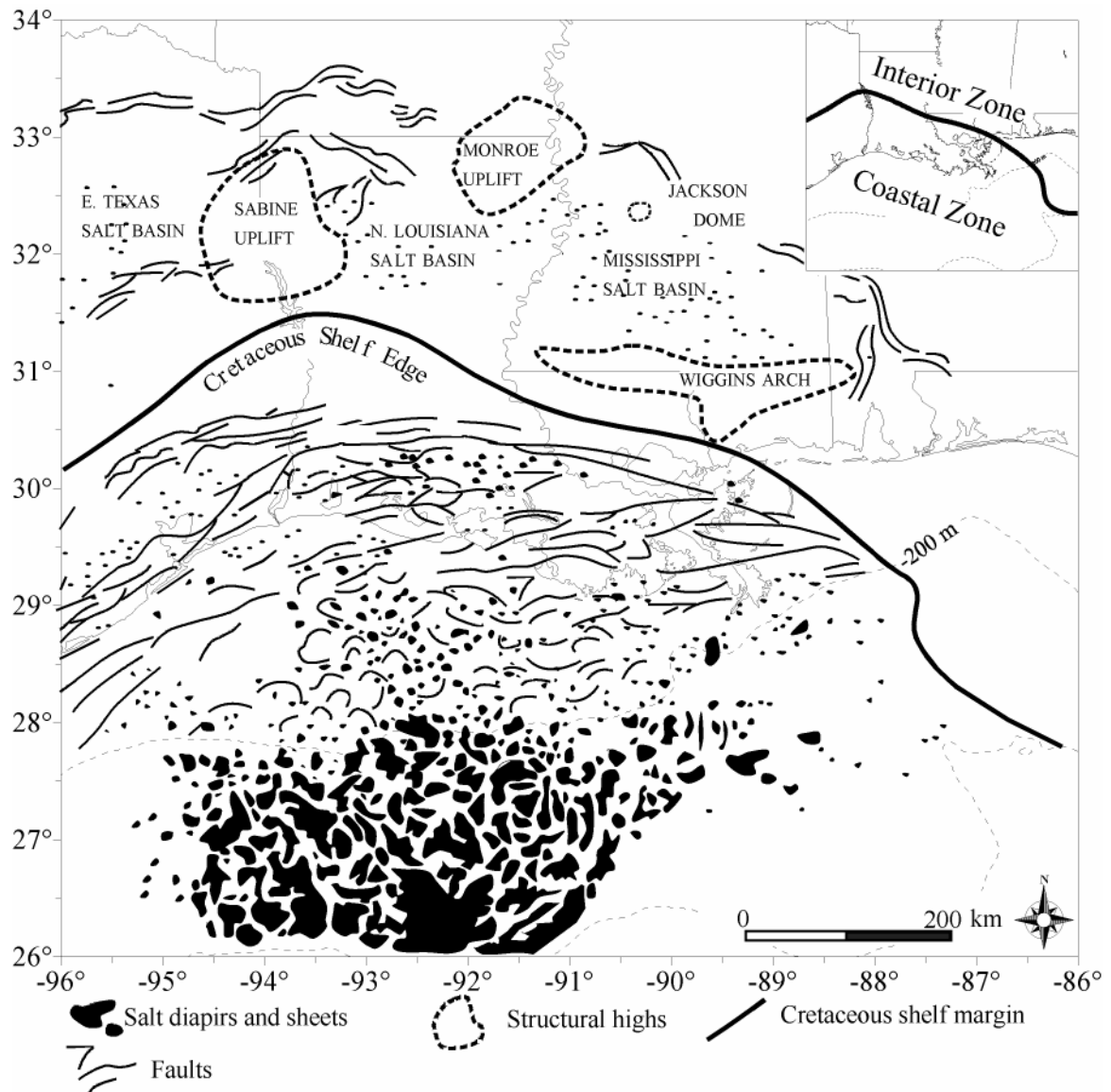


Figure 4. Map of onshore and offshore Louisiana showing position of salt bodies, faults, structural highs and salt basins. Several east-west oriented faults are present in the near shore vicinity of the study area, as well as several salt bodies located on the shelf-margin.

### *Late Quaternary Glaciation and Sea-level Fluctuation*

Glacial cycles directly influenced changes in sea level throughout Quaternary time (Chappell and Shackleton, 1986). Glacial and interglacial stages documented in terrestrial domains correspond well with periods of sea-level lowstand and highstand indicated by stratigraphic relationships and oxygen isotope data ( $^{16}\text{O}$  to  $^{18}\text{O}$  ratios) (Fig. 5) (Chappell and Shackleton, 1986; Martinson et al., 1987).

Global-scale cycles of climatic cooling have resulted throughout the Cenozoic in wide spread continental-scale glaciations. This process affects ocean waters in the following ways: 1) a net loss of water from major ocean basins because of preferential evaporation of  $^{16}\text{O}$  and storage of this isotope in snowfall when waxing ice sheets prevent its return through glacial melting; 2) relative enrichment of ocean basins in the  $^{18}\text{O}$  isotope as  $^{16}\text{O}$  -enriched water becomes stored in ice sheets; and 3) a decrease in elevation of sea level as water is removed from the global ocean basins. During global warming cycles, or interglacial stages, continental ice sheets melt thereby releasing large volumes of  $^{16}\text{O}$  -enriched water into drainage basins that result in rapid rise in sea level (Imbrie et al., 1984).

Four late Quaternary glacial stages have been identified on the North American continent. In order of decreasing age they are the Illinoian, Sangamonian, Wisconsinan, and Holocene. These glacial stages are correlated to six oxygen isotope stages (Fig. 5). Oxygen isotope stages are determined on basis of the ratio between  $^{16}\text{O}$  to  $^{18}\text{O}$  (Chappell and Shackleton, 1986). Of particular interest to this study is the Late Wisconsinan glacial stage that took place approximately 22,000 - 18,000 yrs BP (Fig. 5). This glacial stage is linked to a sea-level lowstand that is indicated as oxygen isotope stage 2 (Fig. 5). The

Holocene interglacial stage is responsible for the most recent transgression and current highstand conditions (Fig. 5).

Many independent researchers have constructed sea-level curves for Late Pleistocene-Holocene time (Curran, 1960; Ballard and Uchupi, 1970; Nelson and Bray, 1970; Frazier, 1974; Fairbanks, 1989; Penland et al., 1991; and, Tornqvist et al., 2004) (Fig. 6). Several of these curves indicate sea level fell 90 to 160 meters (m) below present elevation between 20,000 and 15,000 yrs BP, and then rose rapidly until approximately 5,000 yrs BP when current highstand conditions were achieved. Except for Fairbanks and Tornqvist et al., are all relative sea level (RSL) curves derived from stratigraphic relationships. This study utilizes the lowstand timing of Fairbanks (1989), which suggests that sea level was 120 +/-5 m below present elevation during the last glacial maximum at approximately 18,000 yrs BP. This curve is based on radiocarbon-dated coral reef samples collected from offshore Barbados. The timing and elevation of this curve correlate well with results from a similar study performed in the Pacific Ocean basin (Chappell and Shackleton, 1986).

#### *Depositional Response to Sea-level Fluctuation*

Fluvio-deltaic systems are sensitive to glacio-eustatic changes (Fig. 7). Depocenters shift geographic location as base level changes in response to glacial-interglacial cycles. Significantly, depositional character and the resulting stratigraphic relationships of fluvio-deltaic sedimentary packages also change as the location of depocenters shift through time.

One response of fluvio-deltaic systems to eustatic fall is a basinward translation of the systems as sea level falls during glaciation. Large portions of the shelf may be

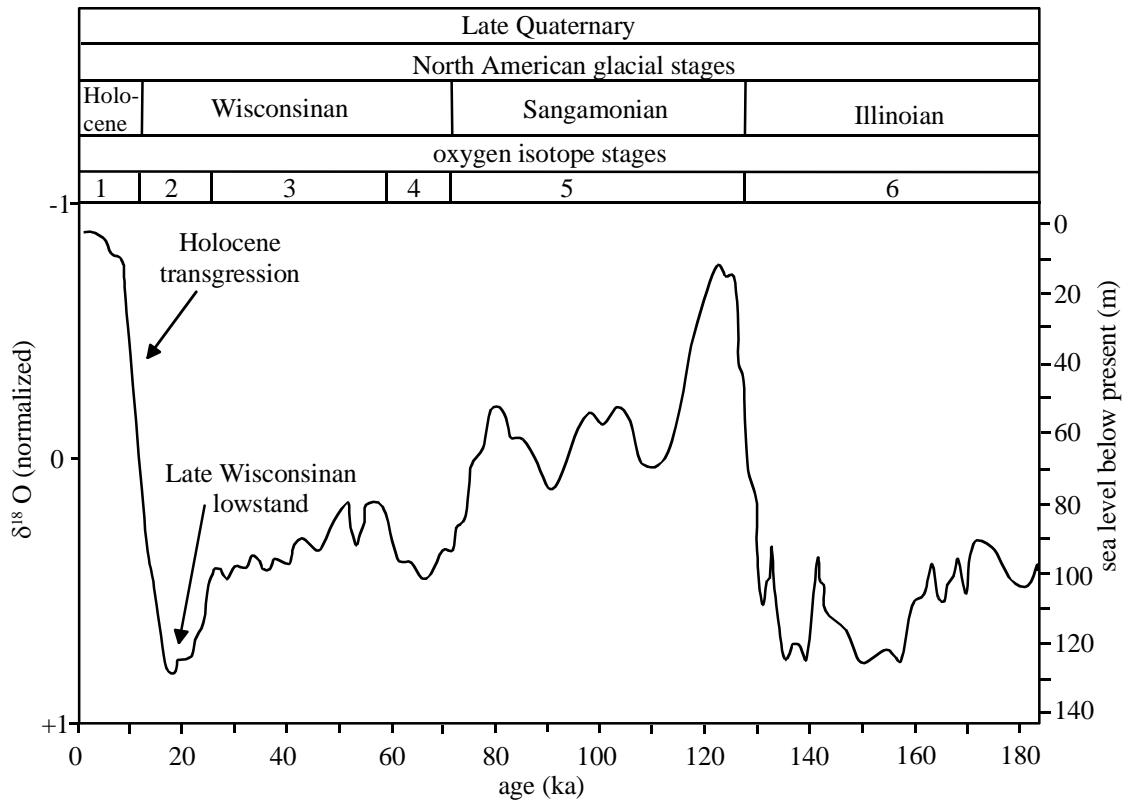


Figure 5. Late Quaternary North American glacial stages correlate well with oxygen isotope data to show patterns in sea-level fluctuation are linked to growth and decay of continental ice sheets (modified from Morton and Suter, 1996).

exposed as sea level falls creating an erosional surface classically referred to as a lowstand unconformity (Fig. 8). Stream extension and incision may also occur across the shelf as sea level falls and reaches lowstand. During maximum lowstand the greatest amount of deposition takes place on the shelf-margin, continental slope, and in the deep basin (Coleman et al., 1991) (Fig. 8). Large fluvio-deltaic systems such as the Mississippi River produce incised alluvial valleys on the shelf that can be linked downdip to an incised canyon on the shelf edge and large submarine fan on the basin floor (Coleman et al., 1991) (Fig. 9).

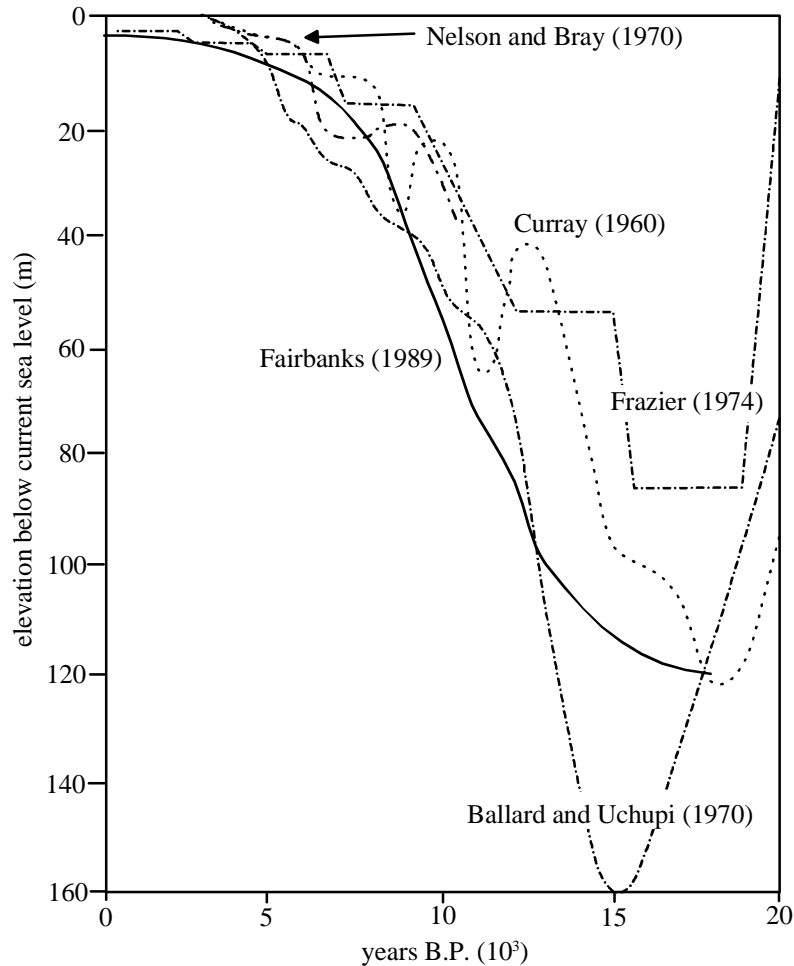


Figure 6. Chart showing the relationships of multiple sea-level curves for the last 20,000 years in the Gulf basin. Variations in the curves exist but overall the trends indicate that sea level fell to elevations of approximately 90 to 160 m below present sea level during the Late Wisconsin glacial maximum at approximately 18,000 to 15,000 yr BP. Subsequent rise in sea level was not monotonic and more likely stair-stepped in some fashion (Fairbanks, 1989). Graphs from Curray (1960), Ballard and Uchupi (1970), Nelson and Bray (1970), Frazier (1974), and Fairbanks (1989).

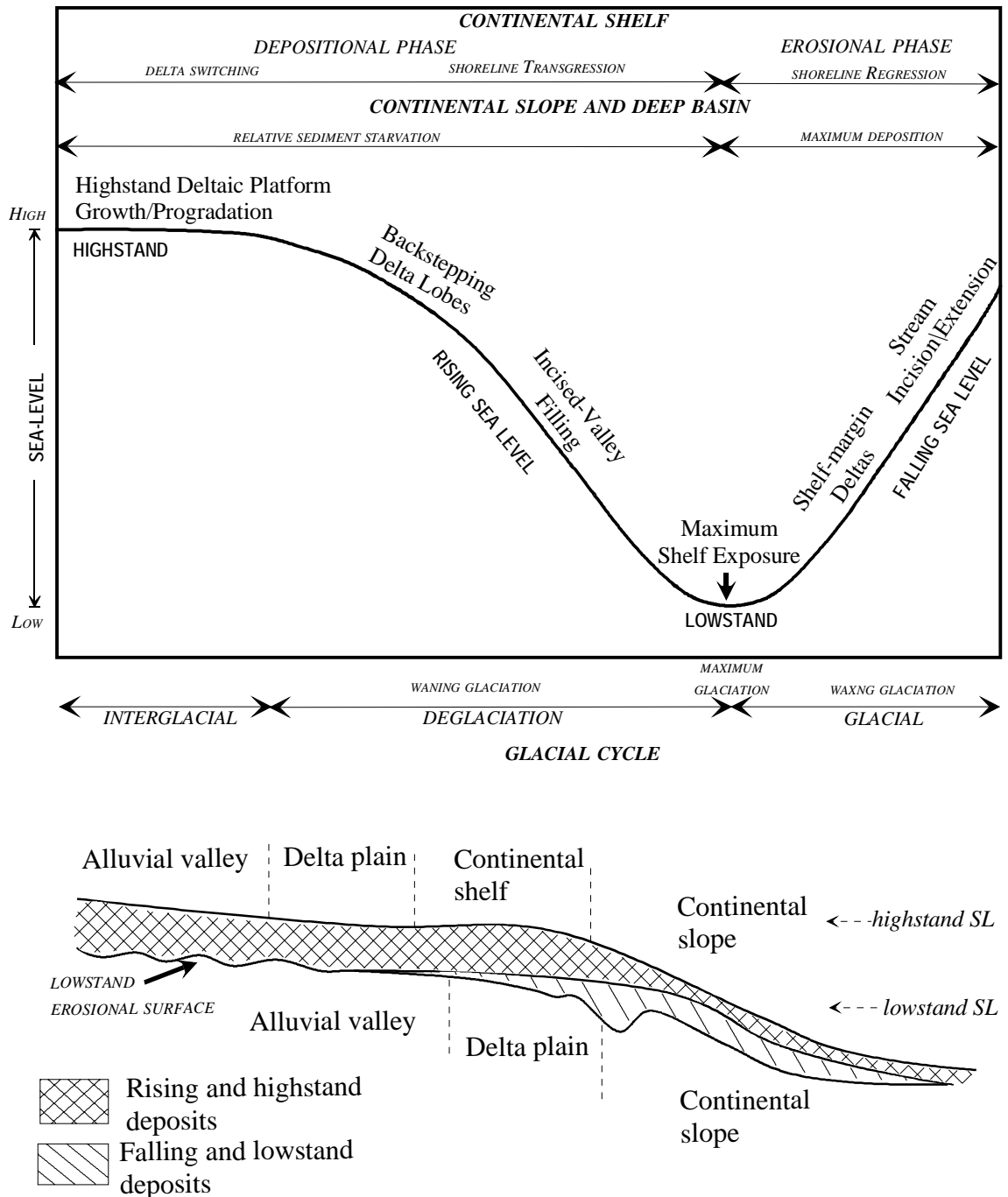


Figure 7. Diagram showing relationship of glacial cycles, eustatic fluctuations, and response of depositional systems to these forcing mechanisms. During sea-level fall streams can incise into the exposed shelf forming a well-defined lowstand erosional surface. Deposition takes place on the shelf margin, continental slope, and deep basin while erosion occurs on the continental shelf. Maximum shelf exposure is concomitant with maximum lowstand conditions.



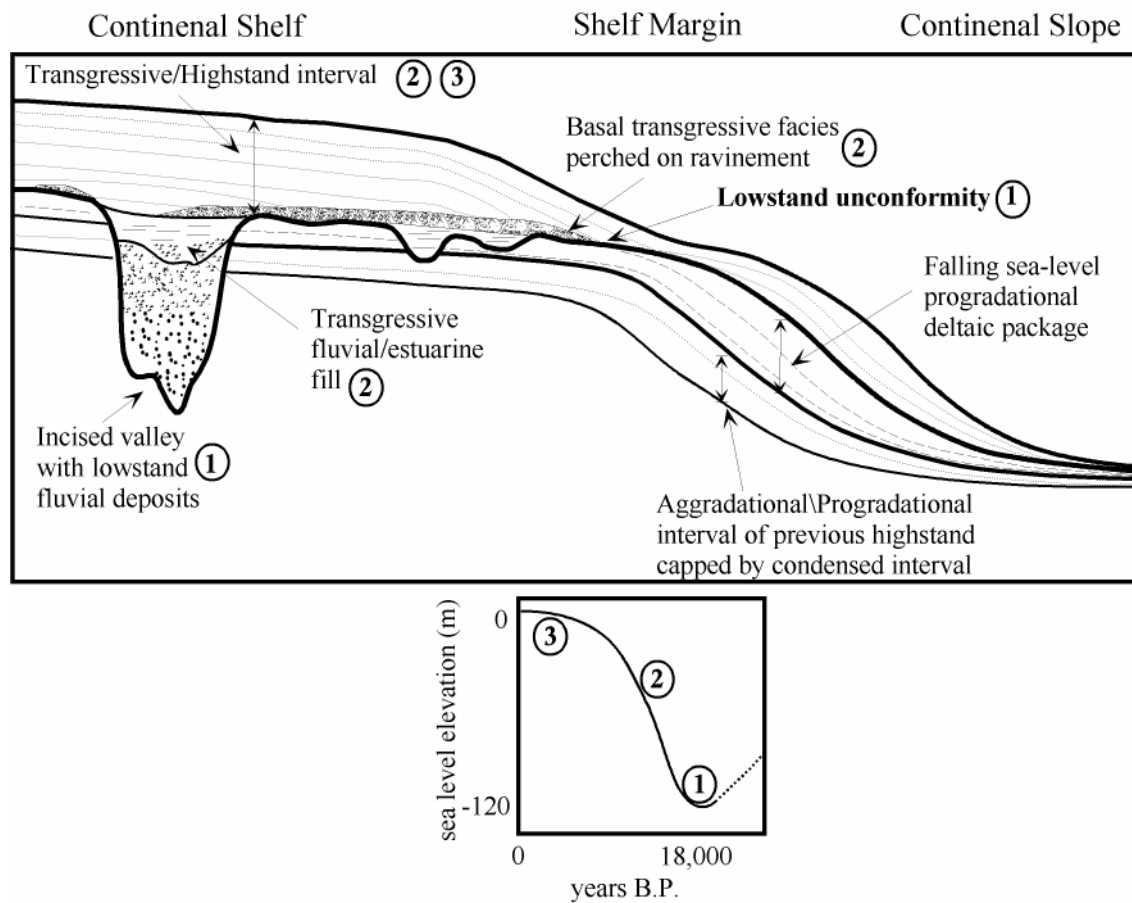


Figure 8. Schematic representation of fluvio-deltaic deposition on the continental shelf and slope during a cycle of sea-level change. Key positions of sea level are labeled in increasing order as sea level rises: 1) lowstand, 2) transgression, and 3) highstand.

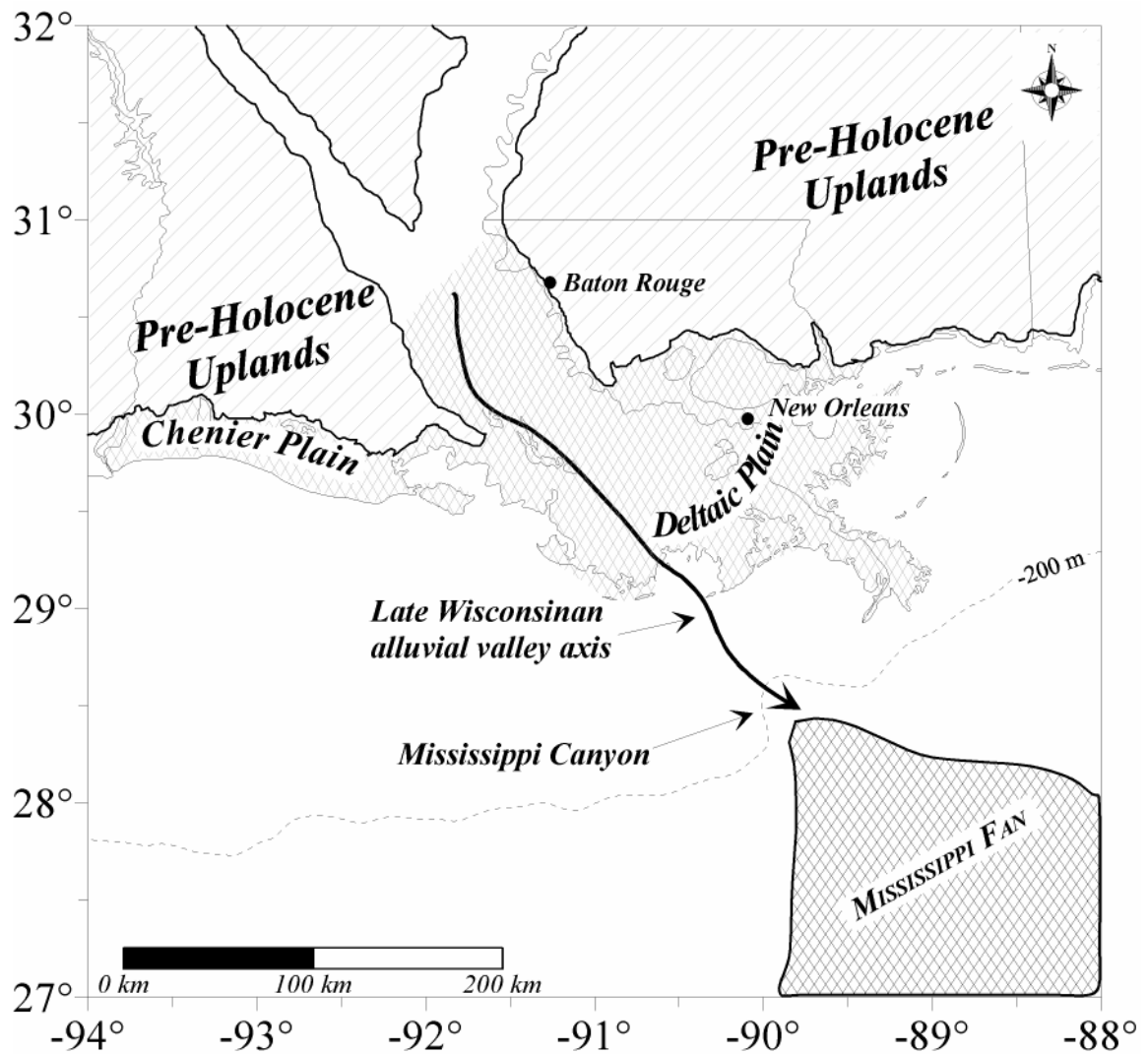


Figure 9. Map showing the extent of the Holocene Mississippi Delta Plain and Chenier Plain. Dark arrow indicates thalweg of the Mississippi River during the last glacial maximum and sea-level lowstand (from Fisk and McFarlan, 1955). The bordering dashed lines mark the walls of the Mississippi River incised valley.

Deglaciation and subsequent rise in sea level result in a landward shift of depocenters. This stage is marked by river valley aggradation and deposition of basal transgressive facies directly on top of lowstand erosional surfaces (Coleman et al., 1991). During sea-level rise fluvio-deltaic deposition decreases in slope and shelf-margin areas as depocenters migrate backward, instead depositing retrogradational deltas on the shelf (Fig. 7).

During interglacial sea level stabilizes and highstand conditions are achieved, allowing for fluvio-deltaic platform growth and progradation. Delta switching occurs on the continental shelf while the continental slope, whereas deep basins become relatively starved of sediment (Fig. 8).

### *Regional History*

This section summarizes the work of existing depositional framework studies that examine late Quaternary fluvio-deltaic sedimentation on the northern Gulf of Mexico shelf. Five selected studies are presented here, each analyzing a specific shelf-edge segment or area along a west-to-east transect. The purpose of this section is to provide the reader with an understanding of regional depositional architecture in order to more fully establish a context for the results of this study.

#### *Texas Shelf*

Suter and Berryhill (1985) examined 35,000 km of trackline of single-channel, high-resolution, seismic reflection profile data collected from the Texas and Louisiana shelf and upper continental slope. They identified five shelf-margin deltas: the Rio Grande River delta, the Mississippi River delta, and three deltas labeled A, B, and C of unknown fluvial origin (Fig. 10). The presence of steep internal clinoform reflection

patterns connected to a well-developed network of ancient channels was the basis for their determination that these sedimentary packages were fluvially derived. Age determination for these sedimentary packages, based on stratigraphic relationships and limited radiocarbon dates, ranges from 18,000 to 10,500 years BP. These dates suggest deposition of these units occurred during the time of the Late Wisconsin glacial maximum through Holocene transgression.

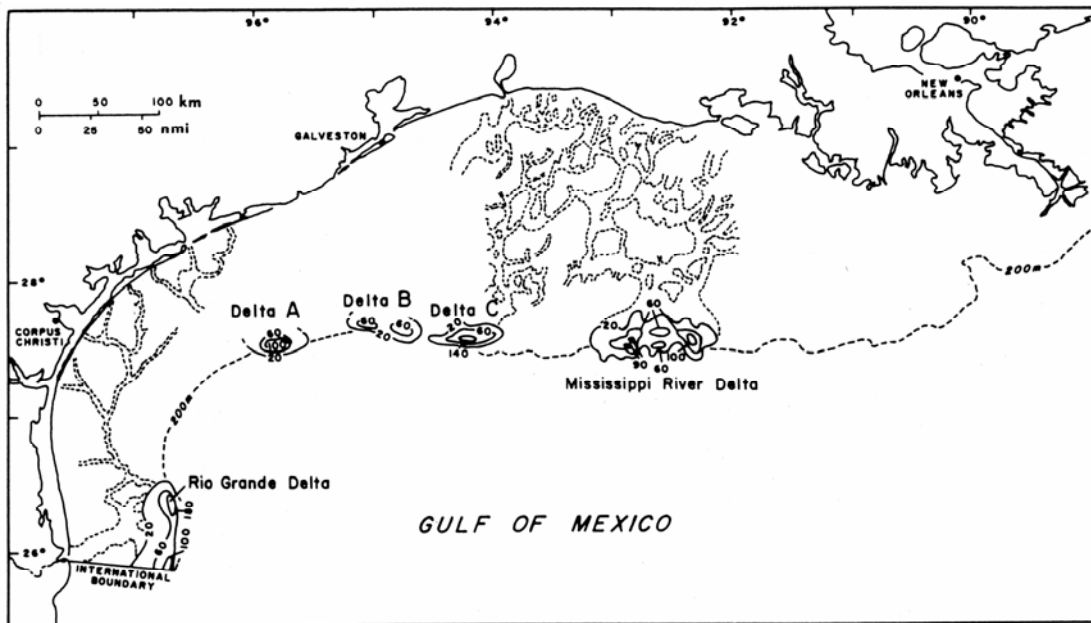


Figure 10. Map showing location of shelf-margin deltas identified by Suter and Berryhill (1985) and their associated paleodrainage networks. Contours indicate thickness of shelf-margin deltaic sediments (in meters).

The Rio Grand River delta, delta A, and delta B are similar in architecture. They exhibit a multilobate constructional framework. Locally, seismic reflection profiles across these depocenters show features suggestive of syn- and post-depositional slumping and sliding in their delta-front environments. The presence of sheet-like sandy deposits

indicated in cores suggest shoreline erosion took place during transgression of the depocenters.

Delta C exhibits no multilobate architecture. Clinoform patterns show that a diapirically formed basin controlled the style of deposition. Once this basin filled, sediment bypass began and sedimentation took place directly onto the continental slope, forming a linked downslope submarine fan.

The late Wisconsin to early Holocene Mississippi River delta is located on the southwest Louisiana shelf. It is multilobate and linked to a large channel complex. Delta lobes fill diapirically controlled basins, and channel distribution patterns are controlled by diapiric structures. Suter and Berryhill (1985) recognized this as the Mississippi River delta due to the presence of the large channel complex linked to this delta and proximity of the delta to a Pleistocene-age Mississippi River depocenter. Two submarine troughs are recognized downslope of this delta. Based on stratigraphic relationships, these troughs pre-date the Late Wisconsin lowstand and may have existed during the last three lowstands. These valleys served as conduits of mass-sediment transport.

#### *Eastern Texas Shelf*

Morton and Suter (1996) analyzed an area of the eastern Texas outer shelf and upper slope (Fig 11). Data sets within their study included more than 100 foundation borings and single channel, high-resolution sparker seismic profiles. Foundation borehole depths exceed 90 m (295 ft) and provide lithologic information, such as sediment composition, color, and textures. More than 2400 km of high-resolution seismic reflection profiles were also used in this study.

They identified three stacked deltaic sequences of Wisconsin age (120,000 yr BP and younger). A more refined absolute-age determination is limited by the presence of the *Trimosina* fault zone in the southern portion of the study area. Active faulting and diapirism along this structural trend complicate establishing accurate chronostratigraphic control. Sequence thickness, axial direction of major fluvial channels, and shelf-margin delta lobe geometry for all three deltaic intervals is attributed to this fault zone.

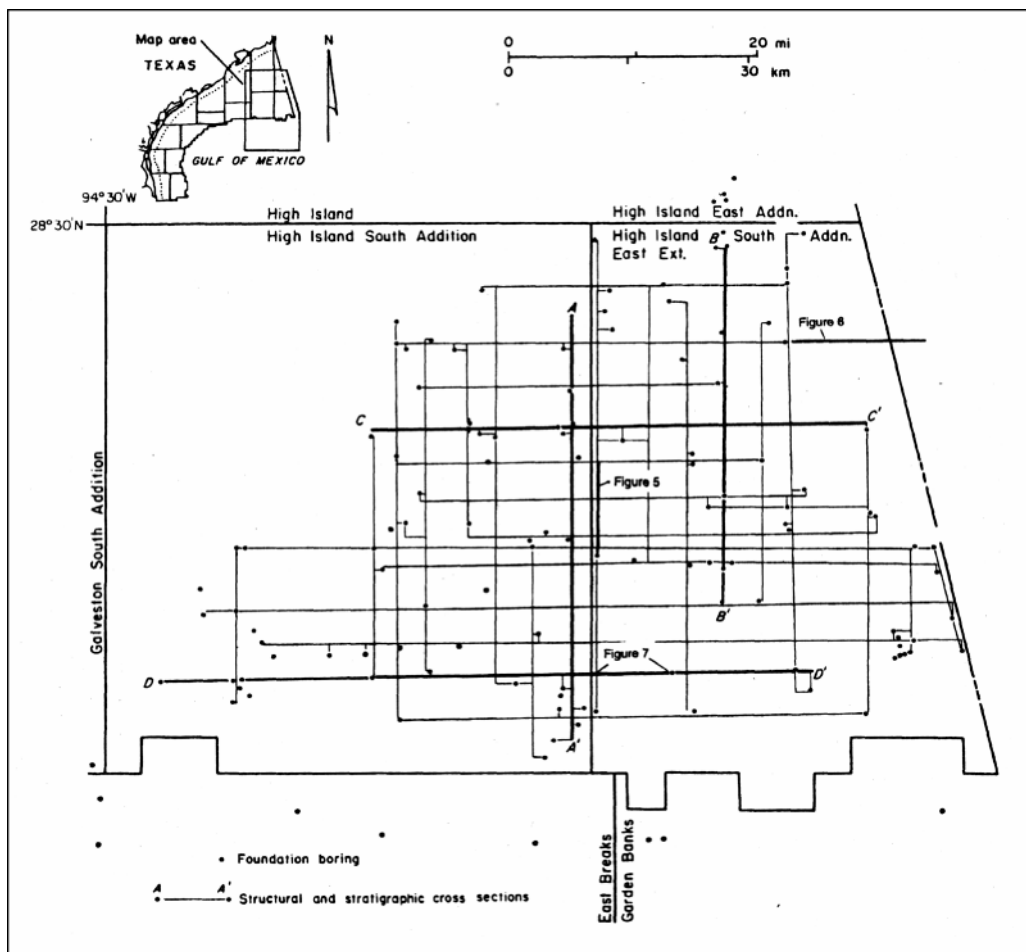
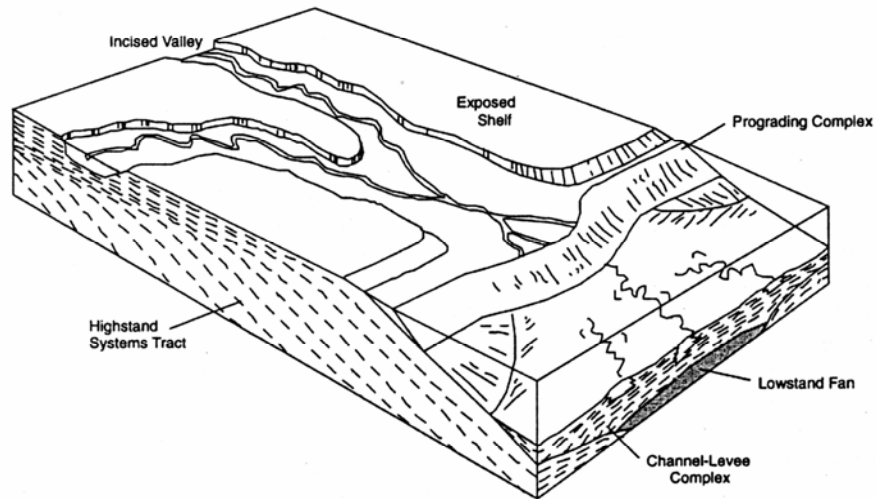


Figure 11. Basemap of Morton and Suter (1996) study area located in the southern High Island lease block area, western Gulf of Mexico. Locations of seismic tracklines as well as structural and stratigraphic cross sections are indicated on the map.

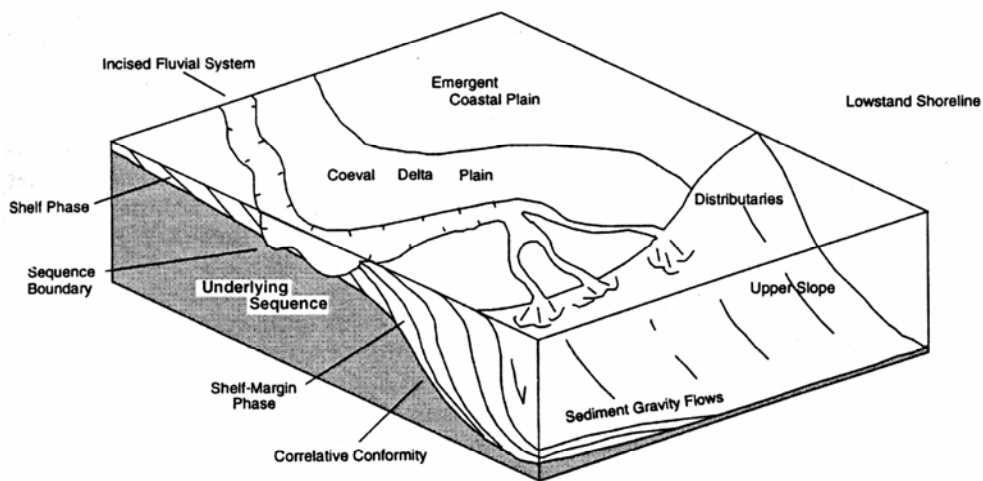
On the basis of their observations, Morton and Suter (1996) suggested a new model for late Quaternary shelf-margin deltaic deposition, called the 'Quaternary Shelf-Margin Delta' model, that has implications for the depositional framework of sedimentary packages linked to small fluvial systems located along the northern Gulf of Mexico (Fig. 12). The standard shelf-margin depositional model (see Vail et al., 1977a) requires that fluvial channels respond to falling sea level by extending their distributary network basinward and incising the exposed shelf as sea level falls below the shelf break. This creates an incised valley complex that is cut into the relic shelf. Deltaic deposition occurs on the outer shelf and upper continental slope as a prograding complex and is linked downslope to a submarine fan. Morton and Suter (1996), however, found no evidence of this pattern of deposition in their study area, instead the formation of extensive fluvial channels were apparently coeval with their shelf-margin deltas. Channels incised the delta complex, and in some examples incision was deep into the delta complex, but incision into the relic shelf was not observed. In their model deltaic deposition occurs on the shelf margin only, with little transport of sediment to the continental slope and no submarine fan formed. Morton and Suter (1996) state that the Quaternary Shelf-Margin Delta model best describes the depositional framework of shelf-margin deltas formed during most recent sea-level lowstands, whereas the Vail et al. (1977a) model only applies to the very large, and therefore anomalous, Mississippi River drainage system.

#### *Central Louisiana Shelf - Mississippi Canyon*

Goodwin and Prior (1989) investigated the most recent depositional history of sediments filling the Mississippi Canyon (Fig. 13). They analyzed high-resolution



**(A) Prograding Complex Model**



**(B) Quaternary Shelf-Margin Delta**

Figure 12. Diagrammatical illustrations of a) the Vail model of fluvial response to a lowering of sea level, and b) the Quaternary shelf-margin delta model proposed by Morton and Suter (1996).



geophysical surveys that were acquired with 3.5-kHz subbottom profilers and medium-penetration seismic reflection profilers. Two borings, taken on the canyon axis and along the canyon rim, provided lithological and paleontological control on units identified in profiles. Carbon-14 dating of selected samples within these cores allowed for age determination.

They identified five seismic units: A, B, C, D, and E. Unit A is stratigraphically located at the bottom of the canyon above a canyon-base unconformity. This unconformity represents the oldest erosional event recorded in this data set; suggested to be approximately 30,000 yr BP in age. Goodwin and Prior (1989) indicate that this event could be older, but 30,000 yr BP was the oldest date that could be obtained using radiocarbon dating methods. Seismically, Unit A is characterized by low amplitude, discontinuous reflectors. A stratigraphically higher, second unconformity separates Unit A from the overlying Unit B. Sediments above this unconformity were dated at 19,000 yr BP in age or younger. Unit B is expressed seismically as high amplitude, parallel, but laterally discontinuous reflectors. Overlying Unit B, Unit C shows chaotic internal seismic reflectors. Radiocarbon dating of this unit indicates deposition took place 19,000 to 15,000 yr BP. Unit D is the thickest unit (375 m) and overlies Unit C. This unit has a chaotic internal seismic reflection character with some parallel reflectors evident. This unit is dated to between 15,000 and 7,500 yr BP. The uppermost unit is Unit E. This unit is a hemipelagic to pelagic clay drape that has a transparent seismic character. Radiocarbon age data indicates the timing of deposition of this unit to be 7,500 yr BP to present.

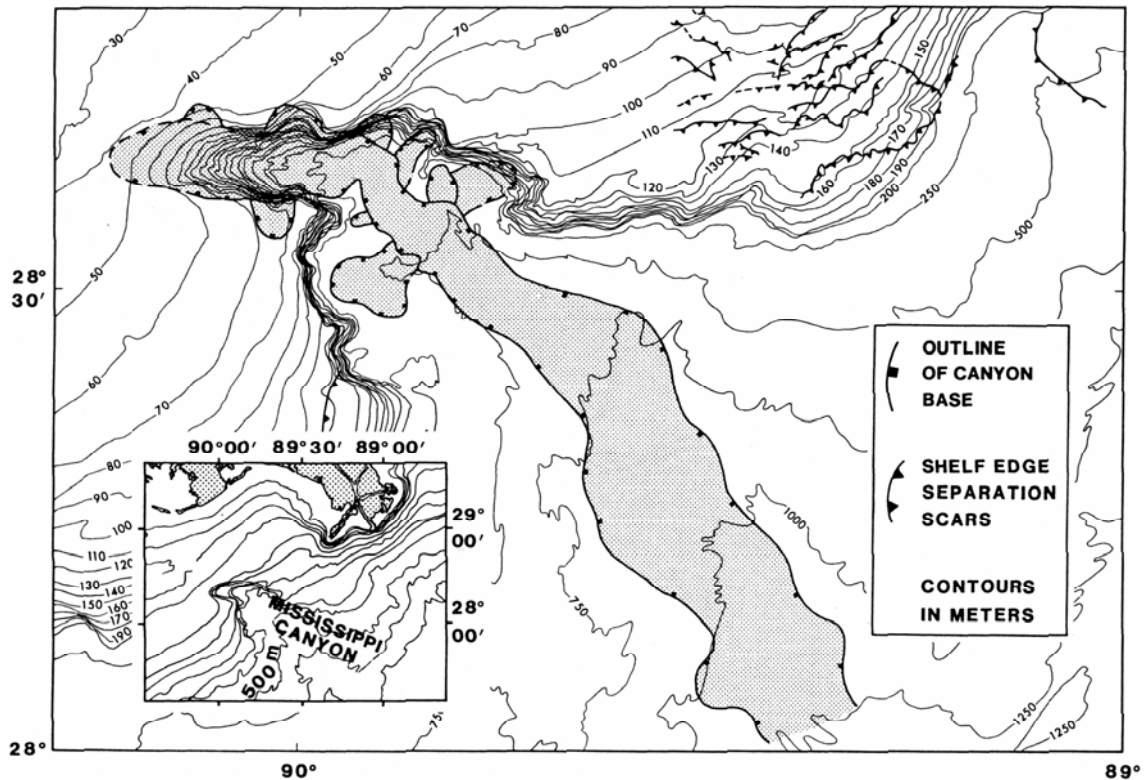


Figure 13. Bathymetric map of Mississippi Canyon area taken from Goodwin and Prior (1989). Shaded area represents extent of canyon base; positions of shelf-margin faults are also provided.

Using these data, Goodwin and Prior (1989) constructed the following depositional history for the Mississippi Canyon. At approximately 30,000 yr BP, or prior to this time, initial canyon incision began. The unconformity surface and stark age contrast between Units A and B indicate that rapid deposition in the form of down-canyon mudflows occurred along the canyon axis at this time, scouring and eroding older sediments. A nearby lowstand delta, hypothesized as the Mississippi River delta, is suggested as the source of the mudflows. Unit C and D are interpreted to be debris flows, mudflows, and prodeltaic sediments deposited as canyon infilling progressed during transgression. As mass-movement processes slowed, prodeltaic sediments became

interbedded with debris flow sediments, contributing to a complex cut-and-fill stratigraphy. By 7,500 yr BP, rising sea level forced a landward shift in the location of the deltaic depocenter that resulted in a marked decrease in prodeltaic sediments transported to the Mississippi Canyon. Most recent sedimentation is comprised of a pelagic drape that has been deposited within the last 7,500 years.

#### *Mississippi-Alabama Shelf*

Kindinger (1988,1989b) researched the depositional framework of a previously unstudied unit that he called the Lagniappe Delta on the outer Mississippi-Alabama shelf east of the St. Bernard and Belize lobes of the Mississippi Deltaic Plain (Fig. 14). A total of 3,200 trackline-km of high-resolution, single-channel seismic reflection profiles were used by Kindinger (1988) to document the extent and geologic framework of the study area.

Kindinger identified a prominent shelf-wide unconformity (Horizon D) at the base of the deltaic package as an early Wisconsin lowstand erosional surface (~ 150,000 yrs BP). Overlying this surface is a thin transgressive package correlated to the mid-Wisconsinan highstand (128,000 – 75,000 yrs BP). An ensuing sea-level fall from 98,000 to 11,000 yrs BP initiated a basinward shift in fluvial-deltaic deposition. Three stages of channel incision into shelf sediments indicate that sea-level fall was not constant but instead occurred in a step-wise manner. The most recent sea-level fall was the Late Wisconsin lowstand that produced a region-wide unconformable surface (Horizon C). A thick package of sediments located on the shelf margin overlies this unconformity. High-angle oblique, sigmoid, and complex sigmoid-oblique internal reflectors are evidence that this package of sediments were deposited by a shelf-margin

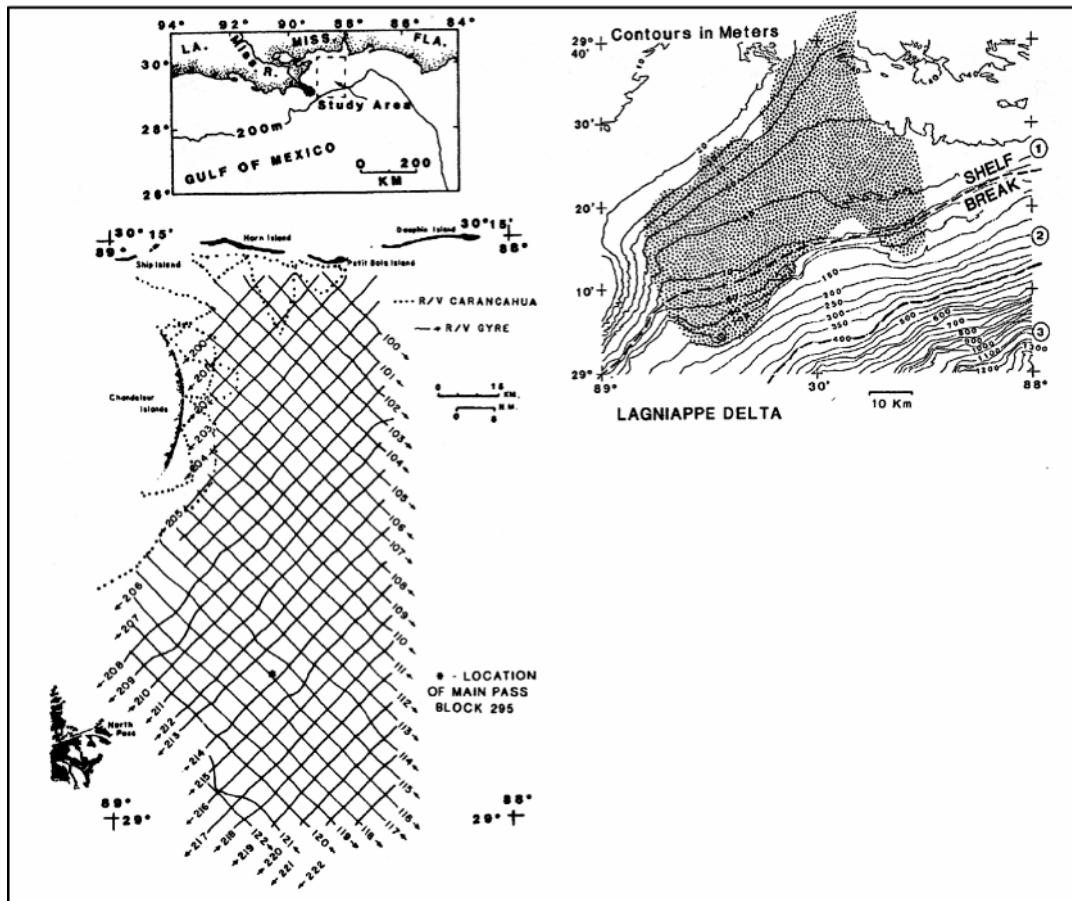


Figure 14. Mosaic of maps showing the location of the Kindinger (1989b) study area, seismic trackline positions, and the extent of the Lagniappe delta on the Mississippi-Alabama shelf margin.

delta. The complex sigmoid-oblique reflectors suggest a fluvially dominated delta that may have undergone delta switching resulting in multiple depositional lobes. Thickness of the deltaic package was controlled by diapirs located on the shelf margin that prevented farther basinward deltaic progradation; resulting in deposition shoreward of the delta front.

A thin transgressive package is located updip of the shelf-margin deltaic package and is stratigraphically younger than those sediments, although it does not directly overlie them. This transgressive package correlates to the Holocene sea-level rise (18,000 to

5,000 yrs BP). An erosional unconformity (Horizon D) overlies and obscures the western extent of these deltaic sediments. This unconformity resulted from sediment reworking accompanying the progradation of the St. Bernard lobe of the modern Mississippi River delta complex (7,000 yrs BP to present). A hiatal surface overlies the St. Bernard lobe depositional package.

A large channel complex is associated with these deltaic sediments (Kindinger 1989b). Kindinger (1989b) did not identify a direct fluvial source but suggested the Pearl and/or Mobil Rivers as possible progenitors. Later studies performed by Roberts et al. (1991) and Sydow et al. (1992) showed the Lagniappe delta linked to a larger delta complex that covers a broad portion of the Mississippi-Alabama shelf. This Mississippi-Alabama delta complex has since been linked to the Mobil River incised-valley system that includes the Mobile and Tombigbee rivers, and may also include the Pascagoula River (Kindinger et al., 1994; Fillon et al., 2004; Roberts et al., 2004).

#### *Louisiana Shelf*

Coleman and Roberts (1988a, 1988b) documented the cyclic sedimentary intervals on the Louisiana shelf. Their data set consisted of 471 offshore geotechnical foundation borings and several hundred thousand kilometers of high-resolution seismic data provided by the hydrocarbon industry (Fig. 15). Cores depths exceed 90 m (295 ft) depth and were semicontinuously sampled.

Summarizing their results, they recognized three complete sea level cycles recorded in the depositional record of the shelf during a 240,000-yr period. Normal deltaic depositional cyclicity combined with sea-level cyclicity during this interval to produce complex sedimentary relationships on the Louisiana shelf.

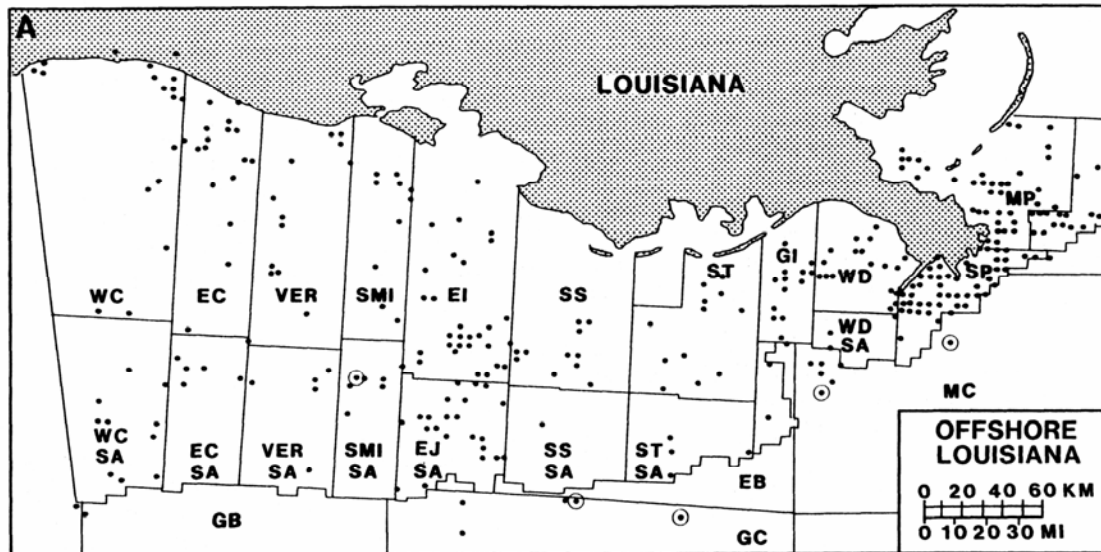


Figure 15. Basemap taken from Coleman and Roberts (1988a) showing location of offshore geotechnical boreholes.

Deltaic sedimentary patterns correlate to specific eustatic conditions (lowstand through highstand). Highstand conditions produce sedimentary packages characterized by the following properties: 1) they are thin, slowly accumulated deposits defined as condensed sections; 2) they are calcareous-rich deposits that include hemipelagics and shell hashes; 3) they possess wide lateral continuity; and 4) they produce a high-amplitude acoustic response. Condensed sections are deposited during periods of rising to highstand sea level. They are easily recognized by specific sedimentological features as well as provide excellent chronostratigraphic markers that are laterally continuous over large areas. Lowstand conditions produce sedimentary sequences that exhibit the following properties: 1) they are variably thick, rapidly accumulated deposits defined as expanded sections; 2) they are coarse-grained clastics, rich in sand and gravel deposits; 3) they are characterized by well-defined depositional trends; and 4) they produce a wide variety of acoustic response. Expanded sections are deposited during lowstand

conditions. They are thick deposits but, in contrast to condensed sections, are limited in areal extent and are not good chronostratigraphic markers.

Coleman and Roberts (1988a) found that sedimentation rates during lowstand conditions were 3 to 15 times higher than sedimentation rates during rising to highstand conditions. The exception to this trend is the fluvially dominated modern Mississippi River delta complex.

Seismic data indicate well-defined, high-amplitude, laterally continuous reflectors correlate well with sedimentary units that were deposited during sea-level highstand. These reflectors immediately overlie erosional unconformity surfaces. Erosional unconformity surfaces are interpreted as sequence boundaries (Vail et al., 1977) and are well defined in seismic records. Variable amplitude, discontinuous reflectors seismically characterize lowstand depositional packages. Moreover, these packages often display scour bases and are thicker than highstand deposits.

Coleman and Roberts (1988a) generally found poor correlation between particular lithofacies identified in cores and a specific acoustic response. Two lithofacies, thin shell beds and laminated sands, did correlate well to an acoustic response; thin shell beds (condensed sections) correlate well with continuous parallel, doublet reflectors. Three reflector types characterize laminated sands: 1) parallel continuous reflectors; 2) discontinuous low-amplitude reflectors; and 3) discontinuous high-amplitude reflectors. All other lithofacies produced acoustic responses that were too variable to use effectively as clear indication of lithology.

### *Summary*

In summary, a generalized late Quaternary shelf-margin deltaic framework model for the northern Gulf of Mexico includes: steeply angled clinoform sets of oblique, sigmoid, and/or complex sigmoid-oblique internal reflectors; channels incised into the underlying shelf sediments; structural control on style of deposition by faulting, salt diapirism, or a combination of both; regionally extensive erosional unconformity surface formed during a fall of relative sea level; thick deltaic packages located on the shelf edge; landward shift of onlapping seismic reflector packages that indicate backstepping of deltaic deposition; transgressive facies overlying deltaic packages; and a thin drape of hemipelagics overlying the transgressive facies. These fundamental features characterize the style of deposition of most shelf-margin deltas in the northern Gulf of Mexico.



## METHODS

The purpose of this section is to define and describe data sets and methodology used in this study. This study incorporates multiple data sets derived from a variety of sources. They are as follows: published, geotechnical foundation borehole data taken from Coleman and Roberts (1988a); two-dimensional, high-resolution seismic profiles from research cruises *Acadiana 86* and *Acadiana 89*; and a Conoco, Inc. lease block engineering survey report from West Delta 96 (Cole, 1983).

### *Data Sets*

#### *Geotechnical foundation borehole data*

Offshore geotechnical foundation borehole data from Coleman and Roberts (1988a) provide lithologic and chronologic information (Fig. 16). Borehole data includes lithofacies type, chronologic data (oxygen isotope and radiocarbon age data), water depth, sample identification, and gamma-ray logs for a limited number of cores. Boreholes were semicontinuously sampled but nonetheless provide critically important information for lithologic and chronostratigraphic control. The upper 20 m of each borehole was continuously sampled using a Shelby push core. Boreholes were noncontinuously sampled at intervals of two to five meters from 20 m below the seafloor to the bottom of the borehole.

Sediment samples are categorized into one of five lithofacies types based on gross lithology. Lithofacies types are: gravel, sand, silt, clay, and carbonate. Lithofacies are determined on percent abundance of sediment and are not homogeneous. A high degree of compositional variability exists in each lithofacies across the sampled area. Sand lithofacies contain mostly sand with zones of interbedded silts and clays. Silt lithofacies

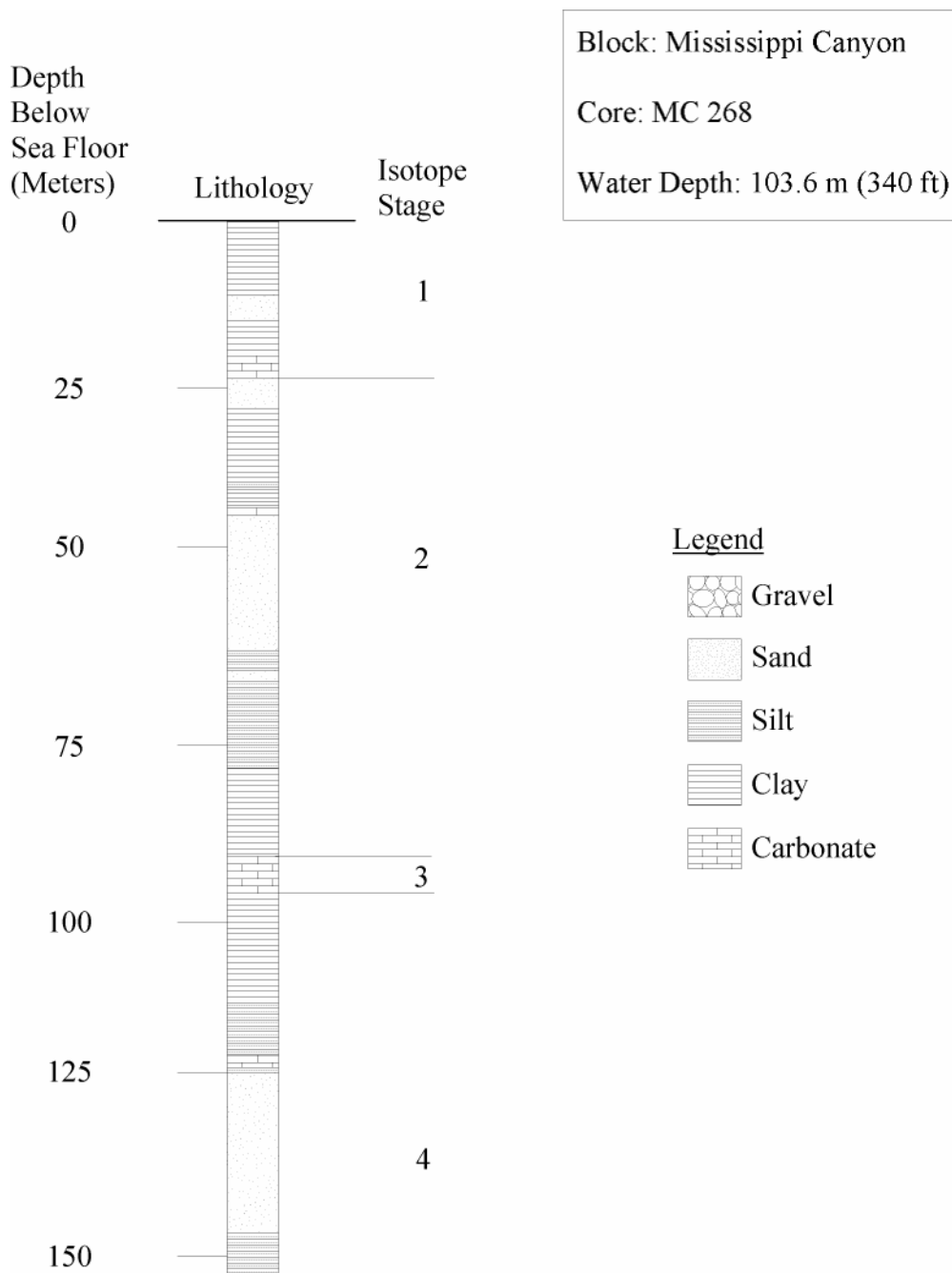


Figure 16. Diagrammatic representation of lithologic data from geotechnical borehole MC 268 (reproduced from Coleman and Roberts, 1988a).

include alternating thin sand, silt, and clay beds. Clay lithofacies possess highly bioturbated clays, thin silt, fine sand laminations, and scattered shell remains. Shell hashes, microfauna-rich hemipelagic clays, and diagenetic carbonate-rich clays are found in the carbonate lithofacies.

Stage	Boundary (yrs BP)	Duration (yrs)
1		12,500
1/2	12,500	
2		11,500
2/3	24,000	
3		35,000
3/4	59,000	
4		12,000
4/5	71,000	
5		57,000
5/6	128,000	
6		58,000
6/7	186,000	
7		59,000
7/8	245,000	

Table 1. Chart showing oxygen isotope stages, stage boundaries, and duration. Stage column lists oxygen isotope stages in descending order from youngest (stage 1) to oldest (stage 7). Stage boundaries are represented as number combinations that list the younger stage first followed by the older stage (e.g., 1/2) (modified from Coleman and Roberts, 1988a).

Oxygen isotope analysis and radiocarbon dating of five boreholes located on the outer shelf and upper continental slope of Louisiana were used to establish chronostratigraphic control. Oxygen isotope analysis measures the ratio of  $^{16}\text{O}$  to  $^{18}\text{O}$  in planktonic foraminifera preserved within sediment samples, which can then be correlated to glacio-eustatic cycles. This allows for organization of the sedimentary record into odd and even numbered 'oxygen isotope stages' (Table 1). Odd numbered stages represent

condensed sections and times of sea-level rise or highstand. Even numbered stages represent deposition during falling or low sea level. Radiocarbon dating techniques supplant oxygen isotope analysis to provide chronostratigraphic control on most recent sedimentation (Late Wisconsin and Holocene). Seismic and lithostratigraphic correlations allow for confidence in chronologies presented by a limited sample set (Coleman and Roberts, 1988a).

#### *High-resolution seismic profile data*

This study incorporates approximately 400 line-kilometers (250 mi) of two-dimensional, high-resolution seismic profiles compiled from two pre-existing data sets, *Acadiana 86* and *Acadiana 89* (Fig 17). Data were acquired on the research vessel R/V *Acadiana*, owned by the Louisiana Marine Consortium (LUMCON) and operated out of the LUMCON facility located in Cocodrie, Louisiana. Data acquisition took place as part of a United States Geological Survey (USGS)/Louisiana Geological Survey (LGS) cooperative research effort during the 1980's. Portions of seismic data used herein are previously unexamined.

*Acadiana 86* seismic profiles are high-resolution, single-channel records gathered using ORE Geopulse boomer instrumentation (500-Hz to 5-kHz filters). Sweep times vary from one-eighth to one-quarter second; fire times range from one-quarter to one-half second in length. This study focuses on Lines 31-33, which were recorded across the axis of the Mississippi Canyon and Louisiana shelf margin.

*Acadiana 89* seismic data are high-resolution, two-channel profiles recorded using ORE 3.5-kHz Subbottom profiler and ORE Geopulse boomer instrumentation. Subbottom profiler data are recorded using sweep and fire times of one-quarter second in

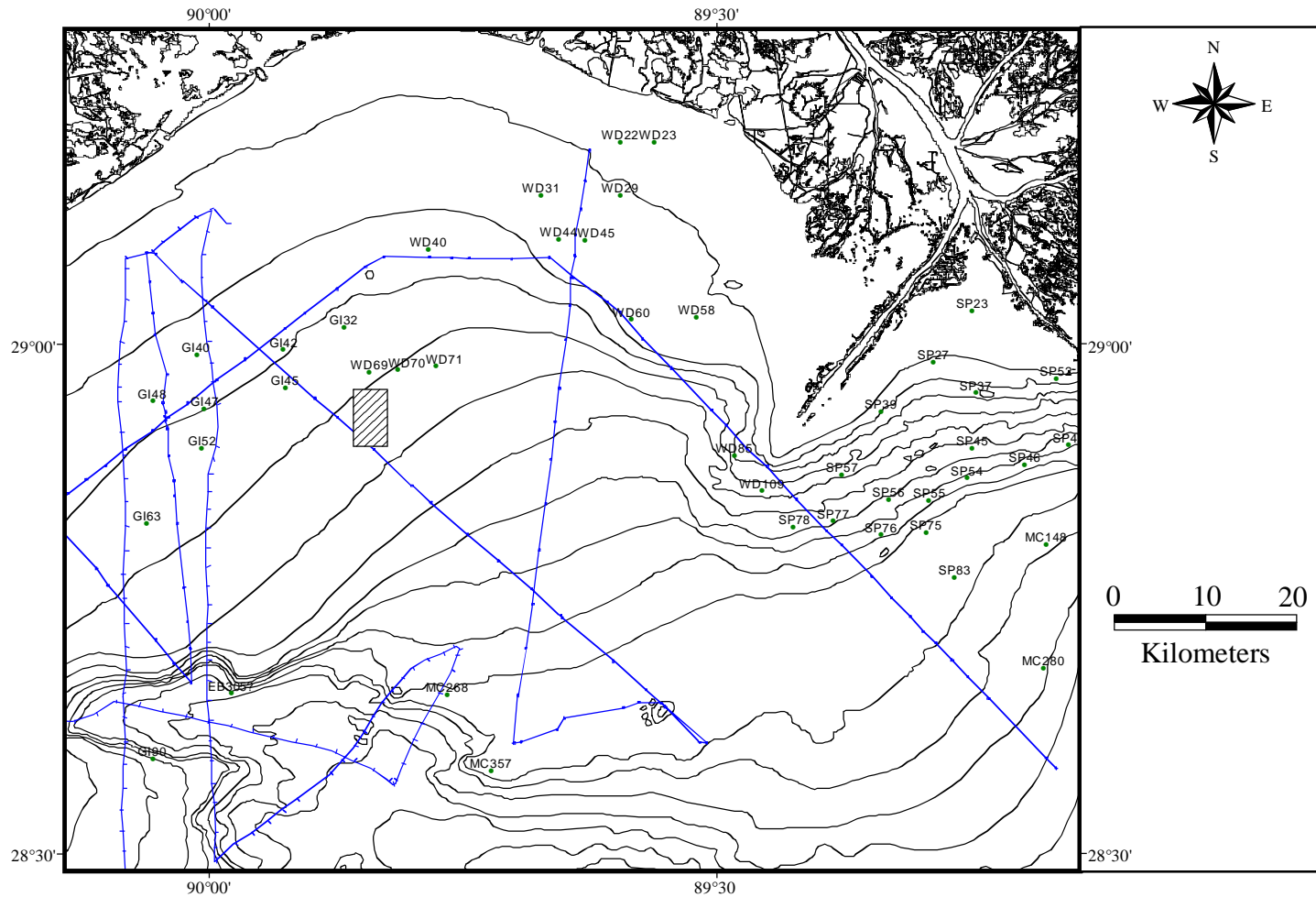


Figure 17. Detailed base map showing the primary features of the study area located on the southeastern Louisiana shelf, north-central Gulf of Mexico. Coleman and Roberts (1988a) geotechnical foundation borings are shown as labeled points. The locations of high-resolution seismic reflection profiles (*Acadiana* cruises 86 and 89) are also shown. Position of the Conoco WD 96 lease block survey report is shown by bold rectangle. The bathymetric contour interval varies on the map, from 10 m to 50 m to 100 m.

length. Boomer data are recorded using 300 to 5000-Hz filters with a one-quarter second sweep time and variable fire time (one-quarter to one-half second).

A two-way travel time of 1500 meters per second (m/sec) is used in time-depth conversions for both seismic data sets. This value is commonly used for shallow seismic stratigraphic analysis (Suter and Berryhill, 1985; Coleman and Roberts, 1988a, 1988b; Kindinger, 1988; Goodwin and Prior, 1989; Kindinger, 1989b; and others).

*West Delta 96 lease block survey report*

A multi-sensor engineering survey of the West Delta 96 lease block was used in this study for lithologic and seismic control (Cole, 1983). This report is the product of an engineering survey contracted to Racal-Decca Survey, Inc. by Conoco, Inc in February 1983. A variety of remote sensing equipment were used to gather data for this report, including a 3.5-kHz subbottom profiler, a 4.2-kilojoule Sparker system, a towed-array side scan sonar, a precision echosounder, and a marine proton magnetometer. Data gathering took place from the M/V *Pacific Seal*. Approximately 84 line-kilometers of survey data were obtained in the West Delta 96 lease block area (Fig 18). Shotpoint intervals were set at 500 feet. A two-way travel time of 1524 m/sec was used in time-depth conversions for this data set. Lithologic data integrated into this report are from a borehole located 1220 m east of the eastern-most boundary line of the West Delta 96 lease block.

Line 4 of the subbottom profiler records will be used in this study. Raw and interpreted portions of the Line 4 profile are included in the lease block survey report (Fig. 19). Interpretations and lithologic correlations are provided courtesy of Thomas

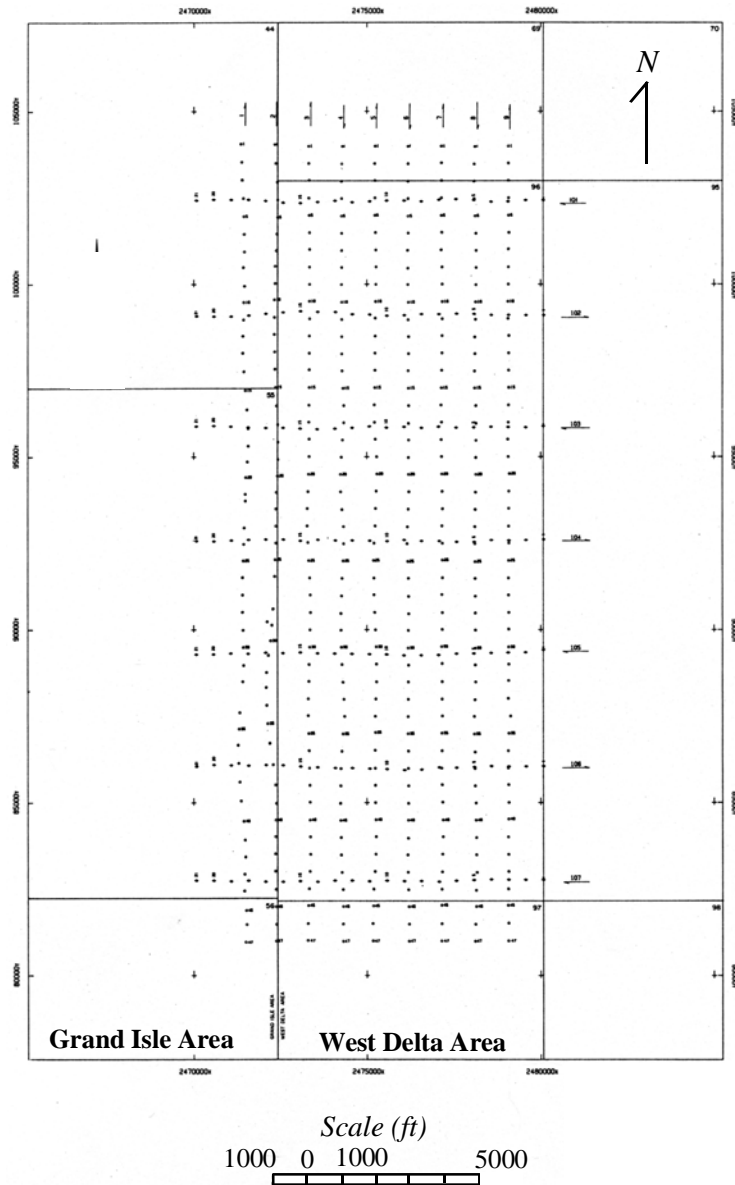


Figure 18. Basemap from Conoco, Inc. West Delta 96 lease block survey report showing locations of shotpoints used to collect seismic profile and side-scan sonar data (modified from Cole, 1983).

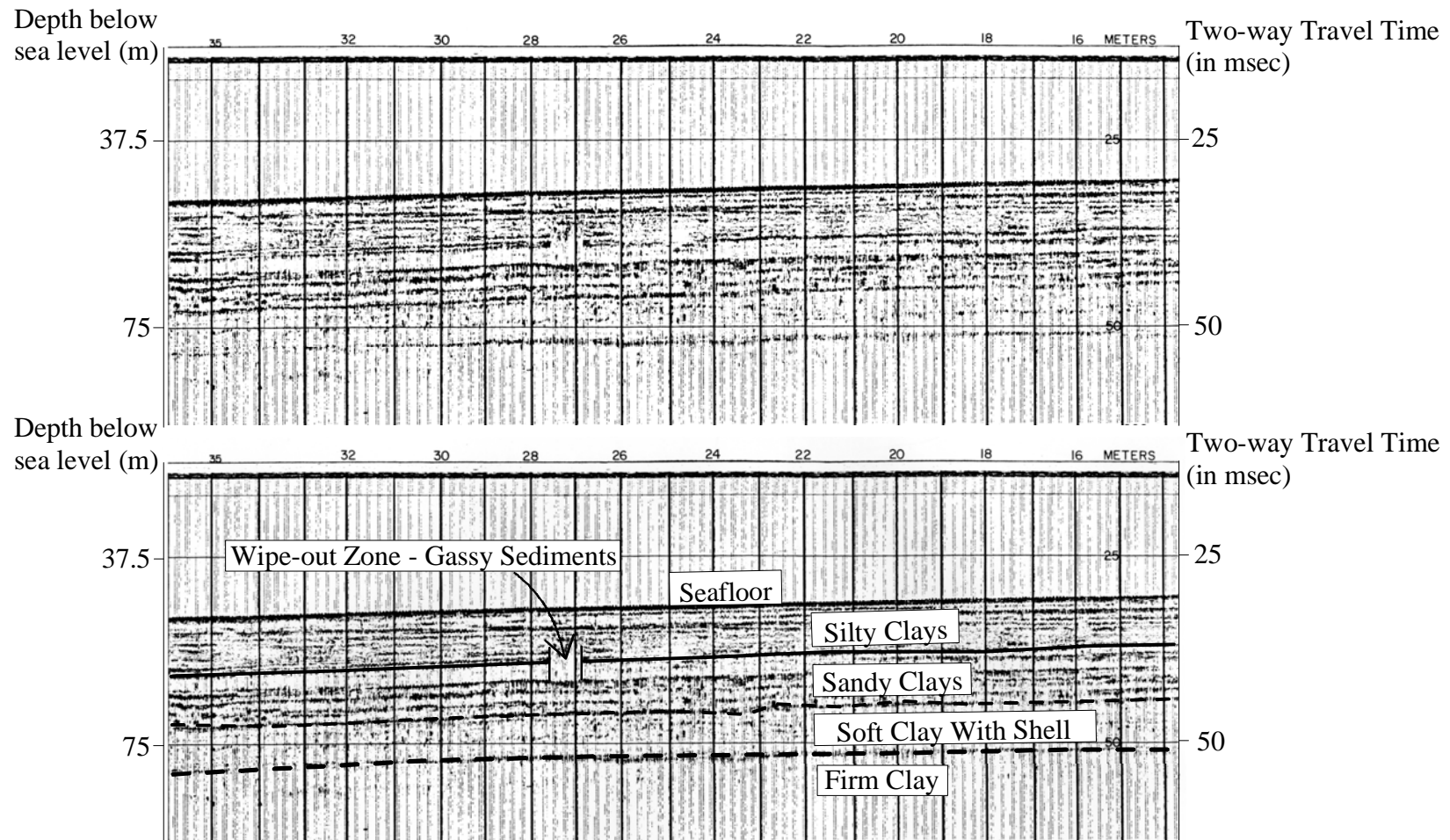


Fig. 19. Raw and interpreted seismic profile from Conoco, Inc. lease block survey of West Delta 96, Line 4. Seismic interpretations and sedimentological correlations made by Thomas Neurauter , Racal-Decca Survey, Inc. (modified from Cole, 1983).



Neurauter of Racal-Decca Survey, Inc. This study will focus on the interpreted portion of Line 4 and lithologic correlations shown.

### *Seismic Sequence Stratigraphy*

This study uses the Exxon seismic sequence stratigraphic methodology ('Vail methodology') pioneered by P. R. Vail and associates at the Exxon Production Research Company in the 1970's (Mitchum et al., 1977a; Mitchum et al., 1977b; Vail and Mitchum, 1977; Vail et al., 1977a; Vail et al., 1977b). Drawing upon the principles of sequence stratigraphy presented in the seminal work of L.L. Sloss (1963), seismic stratigraphy is a 'geologic approach to the stratigraphic interpretation of seismic data' (Vail and Mitchum, 1977). This methodology uses reflection patterns in seismic data to interpret stratal surfaces and unconformities in the rock record. Seismic data is considered to be a "record of the chronostratigraphic (time-stratigraphic) depositional and structural patterns", making chronostratigraphic correlations and postdepositional structural deformation analysis possible (Vail and Mitchum, 1977). One limiting factor to this methodology is that no direct determination of lithofacies can be made from seismic profile data alone (Vail and Mitchum, 1977). Because seismic reflectors are considered expressions of stratal surfaces, the terms stratum and reflector will be used interchangeably in the following discussions.

Seismic stratigraphy allows for several types of stratigraphic interpretations on the basis of seismic reflection geometry and correlation patterns. These interpretations are as follows: relative geologic time correlations, identification and mapping of depositional units, thickness and depositional environment of depositional units, paleobathymetry, burial history, relief and topography on unconformities, and paleogeography and geologic

history when combined with other types of geologic data such as information provided by cores.

Seismic sequence stratigraphy involves a three-step procedure. The three steps are as follows: seismic sequence analysis, seismic facies analysis, and analysis of relative changes in sea level.

#### *Seismic sequence analysis*

Seismic sequence analysis involves identifying depositional sequences on a seismic profile (Mitchum et al., 1977a). A depositional sequence is defined as “stratigraphic units composed of a relatively conformable succession of genetically related strata” (Vail and Mitchum, 1977). Depositional sequences are bounded by unconformities or their correlative conformities (Fig. 20). A seismic sequence is defined as a “relatively conformable succession of reflections on a seismic section...bounded at its top and base by surfaces of discontinuity marked by reflection terminations” (Mitchum et al., 1977b). In seismic sequences, the conformable succession of genetically related reflectors is generally interpreted as genetically related strata; likewise, the reflection terminations that mark bounding discontinuity surfaces in seismic sequences are interpreted as the unconformity surfaces bounding depositional sequences (Mitchum et al., 1977b) (Fig. 21). Seismic sequences are identified on the basis of lateral reflection terminations, which are categorized using the following terminology: baselap, which is subdivided into onlap and downlap; toplap; and truncation (Vail and Mitchum, 1977) (Fig. 22).

Baselap is defined as lapout at the lower boundary of a depositional sequence. Lapout is the “lateral termination of a stratum at its original depositional limit” (Mitchum

et al., 1977a). Onlap is a form of baselap in which initially horizontal reflectors terminate on an initially inclined surface, or initially inclined reflectors terminate updip on a surface of greater initial inclination (Mitchum et al., 1977a) (Fig. 22). Downlap is the downdip equivalent of onlap (Fig. 22). Onlap and downlap indicate nondepositional hiatuses rather than erosional hiatuses (Mitchum et al., 1977a).

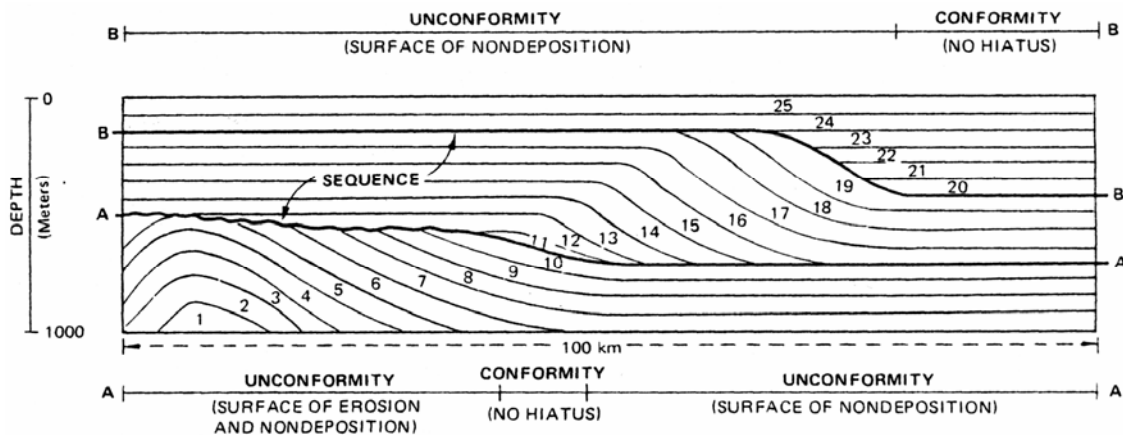


Figure 20. Diagram showing a generalized depositional sequence (numbers 11 through 19) bounded by unconformities and correlative conformities. Numbers indicate episodes of deposition and are labeled in order of oldest to youngest (from Mitchum et al., 1977a).

Toplap is the termination of reflectors at the upper boundary of a depositional sequence (Mitchum et al., 1977a) (Fig. 22). In the updip direction, the spacing between lateral terminations may narrow and approach the upper boundary asymptotically. Toplap is an indicator of nondepositional hiatus, usually with the implication that depositional base level was too low to allow for updip deposition and may indicate that sediment bypass or minor erosion took place (Mitchum et al., 1977a).

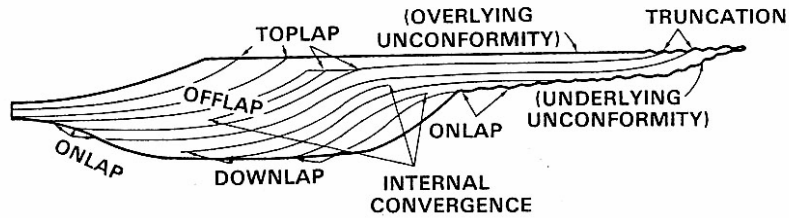


Figure 21. Diagrammatical illustration of an idealized seismic sequence shows relationships of internal seismic reflectors with upper and lower bounding surfaces (from Mitchum et al., 1977b).

There are two types of truncation: erosional truncation and structural truncation.

Erosional truncation is the lateral termination of reflectors by erosion (Mitchum et al., 1977a) (Fig. 22). Erosional truncation occurs at the upper boundary of a depositional sequence. This type of truncation varies in extent; it may cover large areas, such as a subaerially exposed surface, or be confined to small features, such as channels (Mitchum et al., 1977a). Structural truncation is defined as the lateral termination of a stratum by “structural disruption” (Mitchum et al., 1977a). This type of truncation may be a result of faulting, gravity sliding, diapirism, or igneous intrusion. It is most easily recognized when the structure cross-cuts strata.

#### *Seismic facies analysis*

Following identification of seismic sequences, seismic facies analysis involves describing the internal reflection properties of a seismic sequence, such as geometry, continuity, amplitude, frequency, and interval velocity, as well as external form and overall organization of seismic facies units within a depositional sequence framework (Mitchum et al., 1977b). A seismic facies unit is a three-dimensional, mappable group of reflectors that differ in seismic character from those adjacent to it (Mitchum et al., 1977b). Determination of these characteristics allows for interpretation of depositional

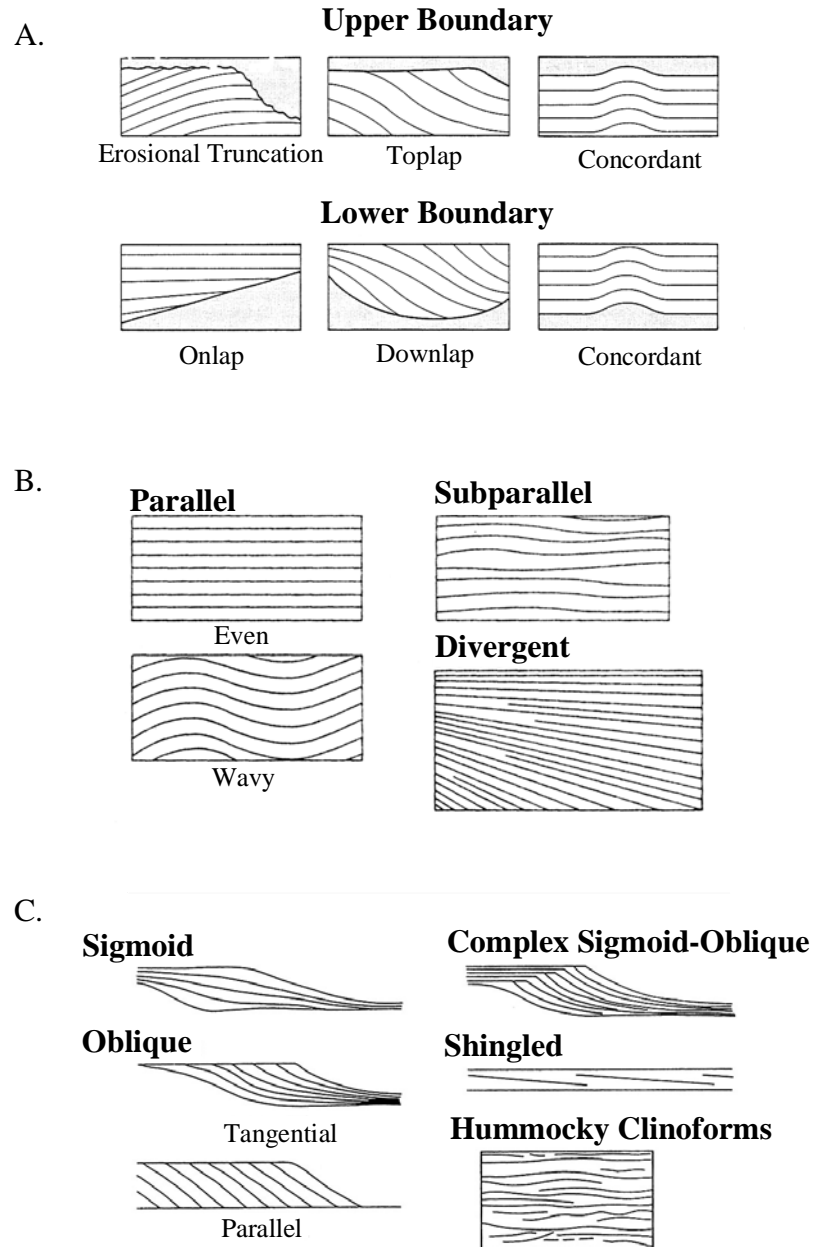


Figure 22. Seismic reflector patterns used to identify and describe seismic sequences. Part A. Types of top-discordant and base-discordant seismic reflector terminations. Part B. Simple varieties of internal seismic facies reflection patterns. Part C. Complex varieties of internal seismic facies reflection patterns, called prograding reflection configurations (from Mitchum et al., 1977a, b).

processes, hence environmental settings, that were active at time of deposition. This information can then be used to predict the lithology of the seismic facies (Vail and Mitchum, 1977).

#### *Internal seismic facies reflection patterns*

Seismic facies analysis interpretations are developed on the basis of seismic reflection patterns. These patterns vary in complexity ranging from simple to complex. Simple varieties include even and wavy parallel reflectors, subparallel, and divergent. More complex patterns are referred to as prograded reflection patterns, and include sigmoid, oblique, complex sigmoid-oblique, shingled, and hummocky. Other patterns of interest include chaotic and reflection-free configurations (Mitchum et al., 1977b).

Parallel and subparallel reflector configurations suggest uniform rates of deposition in a stable basin or across a uniformly subsiding shelf (Mitchum et al., 1977b) (Fig. 22). Divergent reflectors are wedge-shaped and exhibit lateral thickening accompanied by thickening of individual reflection couplets within the seismic facies unit (Mitchum et al., 1977b) (Fig. 22). This pattern suggests lateral variability in depositional rate or tilting of the depositional surface.

Prograded reflection configurations often exhibit more complex reflection patterns, and include the following varieties: sigmoid, oblique, complex sigmoid-oblique, shingled, and hummocky (Fig. 22). These are interpreted as strata deposited during periods of progradation or lateral outbuilding (Mitchum et al., 1977b). The term clinoform, borrowed from Rich (1951), describes a gently sloping surface formed through progressive lateral sediment deposition (Mitchum et al., 1977b). Distinct internal

clinoform patterns characterize the prograded reflection configurations of seismic facies units.

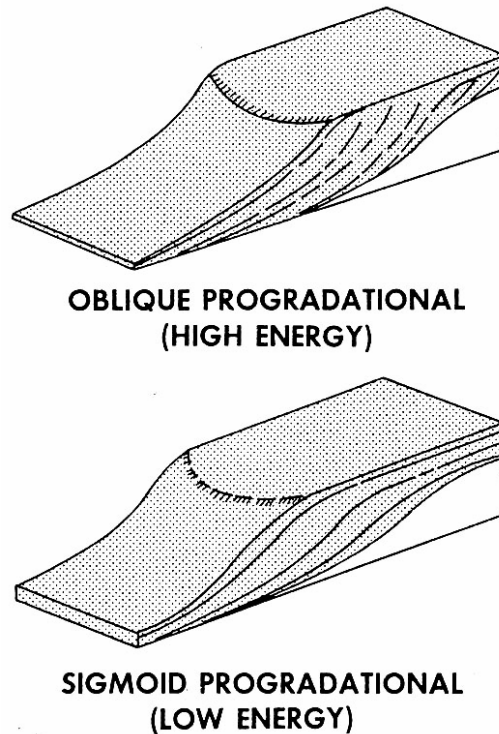


Figure 23. Illustration of oblique and sigmoid progradational reflection configurations. Sigmoid progradational reflection configurations imply low-energy sedimentary regimes due to preservation and aggradation in topsets. Oblique progradational reflection configurations suggest high-energy sedimentary regimes on the basis of topset truncation along a relatively flat-lying surface (from Sangree and Widmier, 1977).

A sigmoid progradational configuration is a prograded clinoform pattern typified by stacked, offset, lens-shaped segments of sigmoid (s-shaped) reflectors (Mitchum et al, 1977b) (Figs. 22, 23). Segments thin in the updip direction, becoming concordant, and reflectors are horizontal. Reflectors in the middle of segments dip at shallow angles, usually less than one degree (Mitchum et al., 1977b). In the downdip direction reflectors downlap or appear to downlap at very low angles onto the basal bounding surface

(Mitchum et al., 1977b). The updip reflection pattern suggests aggradation occurs concomitant with progradation. Preservation of the updip reflector configuration implies low sediment supply, rapid basin subsidence, and/or rapid sea-level rise took place within a relatively low-energy sedimentary regime (Mitchum et al., 1977b) (Fig. 23).

Oblique progradational patterns are composed of a prograded clinoform pattern of relatively steep-dipping reflectors terminating updip by toplap at a flat or nearly flat surface, and terminate downdip by downlap against the basal seismic facies unit boundary (Mitchum et al., 1977b) (Figs. 22, 23). Clinoform stacking patterns indicate lateral outbuilding in the downdip direction by successively younger strata from a constant upper surface characterized by abrupt toplap termination (Mitchum et al., 1977b). Steep depositional dips (approximately 10 degrees) are associated with this progradational pattern. Two subtypes of oblique progradation exist: tangential oblique and parallel oblique. Tangential oblique progradational patterns are characterized by a decrease in dip of the lower portion of the foreset strata, concave-upward stratal orientations in the middle of the clinoform sets, and gently dipping bottomset strata, which terminate in tangential downlap or apparent downlap against the lower seismic facies unit boundary (Mitchum et al., 1977b) (Fig. 22). Parallel oblique progradational patterns are characterized by steeply dipping parallel foresets that downlap onto the lower facies unit boundary at high angles (Mitchum et al., 1977b) (Fig. 22). The oblique progradational pattern suggests high sediment supply conditions in a relatively stable or slowly subsiding basin during sea-level stillstand; this is interpreted as a high-energy depositional regime (Mitchum et al., 1977b).



Variable, alternating sigmoid and oblique progradational configurations within the same seismic facies unit characterize the prograded clinoform pattern of a complex sigmoid-oblique progradational pattern (Mitchum et al., 1977b) (Fig. 22). An alternating pattern of horizontal sigmoid reflections in combination with topset terminations found in oblique progradational topset typifies the topset segment of this progradational pattern. This suggests a depositional history marked by alternating aggradation and sediment bypass in the topset segment within a high-energy sedimentary regime (Mitchum et al., 1977b). This configuration shows reflector termination by toplap internally, rather than at the upper seismic facies unit boundary, suggesting the presence of depositional sequences on a scale smaller than seismic resolution. These smaller depositional sequences are interpreted as discrete lobes of a prograded depositional unit (Mitchum et al., 1977b).

Shingled progradational reflection configurations are typically thin prograded seismic patterns with parallel upper and lower boundaries (Mitchum et al., 1977b) (Fig. 22). Gently dipping parallel oblique reflectors characterize the internal organization of these configurations. Reflectors terminate by toplap and downlap. These configurations are interpreted as forming in shallow water, prograded depositional settings (Mitchum et al., 1977b).

Hummocky clinoform reflection configuration is an apparently random; hummocky pattern recognized by irregular, discontinuous subparallel reflectors and characterized by reflection terminations and splits that are nonsystematic in nature (Mitchum et al., 1977b) (Fig. 22). This reflection pattern is interpreted to form as small, interfingering clinoform lobes prograde into shallow water (Mitchum et al., 1977b).

Chaotic reflection patterns are made of discontinuous and discordant reflectors, suggesting a variable, high-energy depositional environment or heavily deformed strata (Mitchum et al., 1977b). These are commonly associated with cut-and-fill channel complexes, penecontemporaneous slump structures, and zones of folding and/or faulting.

Reflection-free intervals are geologic units that do not express seismic reflection patterns. Large igneous masses, salt bodies, or thick seismically homogeneous shales or sandstones produce these reflection-free areas (Mitchum et al., 1977b).

#### *External seismic facies forms*

Three-dimensional external forms characterize seismic facies units as well as their internal reflection patterns. These external forms include sheets, wedges, banks, lenses, mounds, and fills. Sheet, wedges, and banks are most commonly associated with shelf-edge seismic facies units (Mitchum et al., 1977b) (Fig. 24). Sheet drapes exhibit parallel reflection patterns generally interpreted as strata deposited uniformly over underlying topography in a low-energy depositional environment (deep marine) (Mitchum et al., 1977b) (Fig. 24). Lenses are associated with a variety of seismic facies but are most commonly interpreted as the external form of prograded clinoform seismic facies units (Mitchum et al., 1977b) (Fig. 24). Reflection configurations that appear to rise above the level of the surrounding area are known as mounds. These features are generally restricted in areal extent, and identified by onlap or downlap of overlying strata that fill in around the mounds (Mitchum et al., 1977b) (Fig. 24). Fill reflection patterns define strata that in-fill negative-relief features, such as channels or basins. External form and internal reflection patterns can be used in the identification of fill patterns (Mitchum et al., 1977b) (Fig. 24).

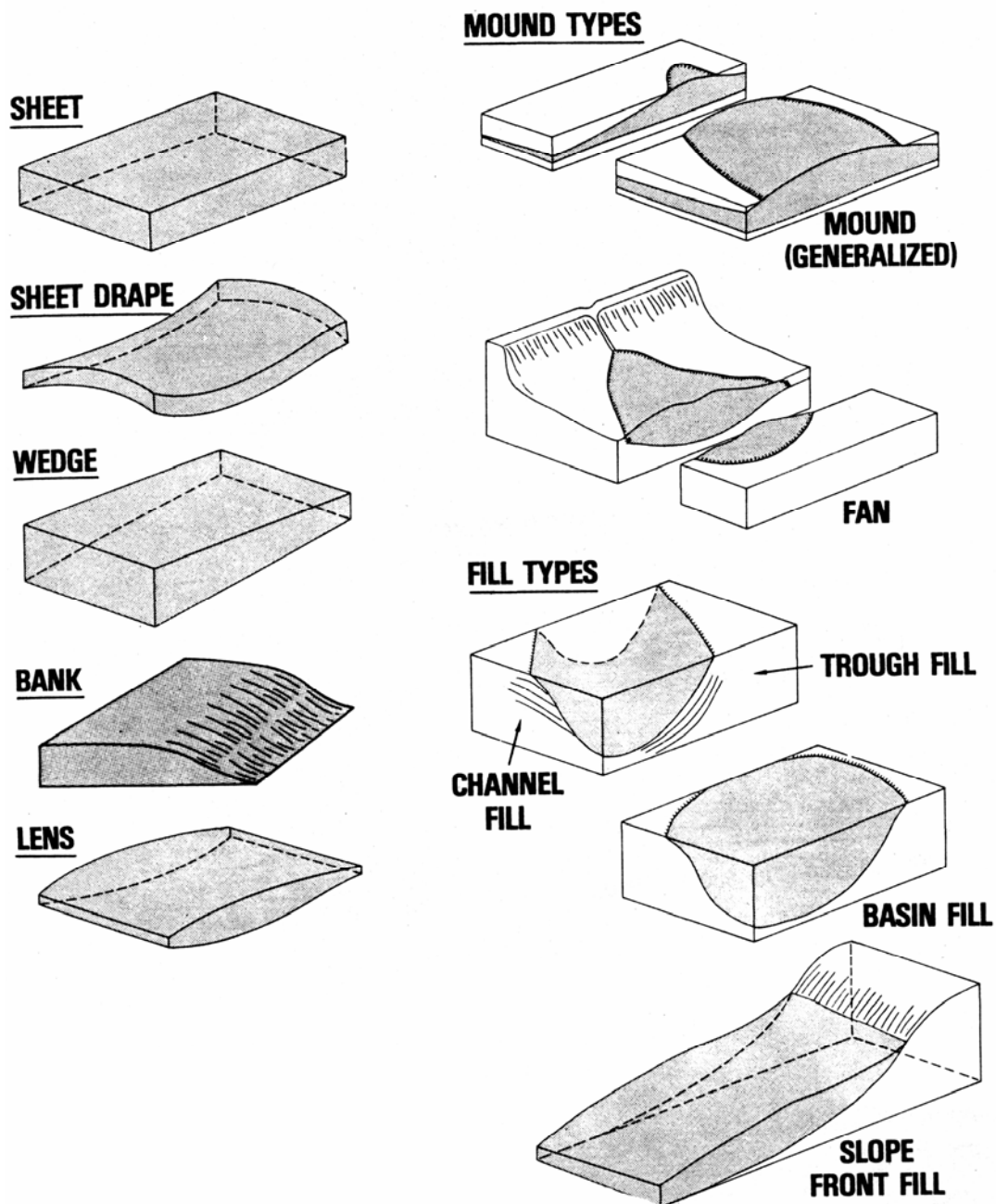


Figure 24. Diagrammatic representation of types of external forms used to describe seismic facies units (from Mitchum et al., 1977b).

#### *Analysis of relative change of sea level*

Once the reflection patterns have been identified seismic sequence analysis focuses on the construction of chronostratigraphic correlation charts and charting cycles

of relative change in sea level on a regional scale for purposes of comparison with global relative sea-level data (Vail and Mitchum, 1977). Depositional limits of onlap and toplap of seismic reflectors are the basis for determining cyclicity of relative change in sea level (Vail et al., 1977a). Relative change in sea level is defined as “an apparent rise or fall of sea level with respect to the land surface” as a result of eustatic (global) fluctuation, the land surface changing elevation (e.g., tectonism), or a combination of these factors (Vail et al., 1977a). Relative sea-level rise is defined as “an apparent sea-level rise with respect to the underlying initial depositional surface and is indicated by coastal onlap”, where coastal onlap defines the “progressive landward onlap of littoral and/or nonmarine coastal deposits” (Vail et al., 1977a). Conversely, relative sea-level fall is defined as an “apparent fall of sea level with respect to the underlying initial depositional surface, indicated by a downward shift of coastal onlap” (Vail et al., 1977a). Relative stillstand of sea level is “an apparently constant position of sea level with respect to the underlying initial surface of deposition”, indicated in this case by coastal toplap. This results from sea level and the underlying surface of initial deposition remaining at a constant elevation, or if sea level and the initial depositional surface rise or fall at the same rate (Vail et al., 1977a).

Changes in relative sea level influence the architecture of coastal deposits. Relative sea-level rise may result in transgression, regression, or a stationary shoreline depending upon the magnitude of sediment supply (Fig. 25). Coastal onlap is observed during transgression, a landward shift in shoreline position, if the rate of sea-level rise exceeds sediment supply (Vail et al., 1977a) (Fig. 25). Regression, or the basinward shift in shoreline position, occurs when terrigenous influx is higher than the rate of sea-level

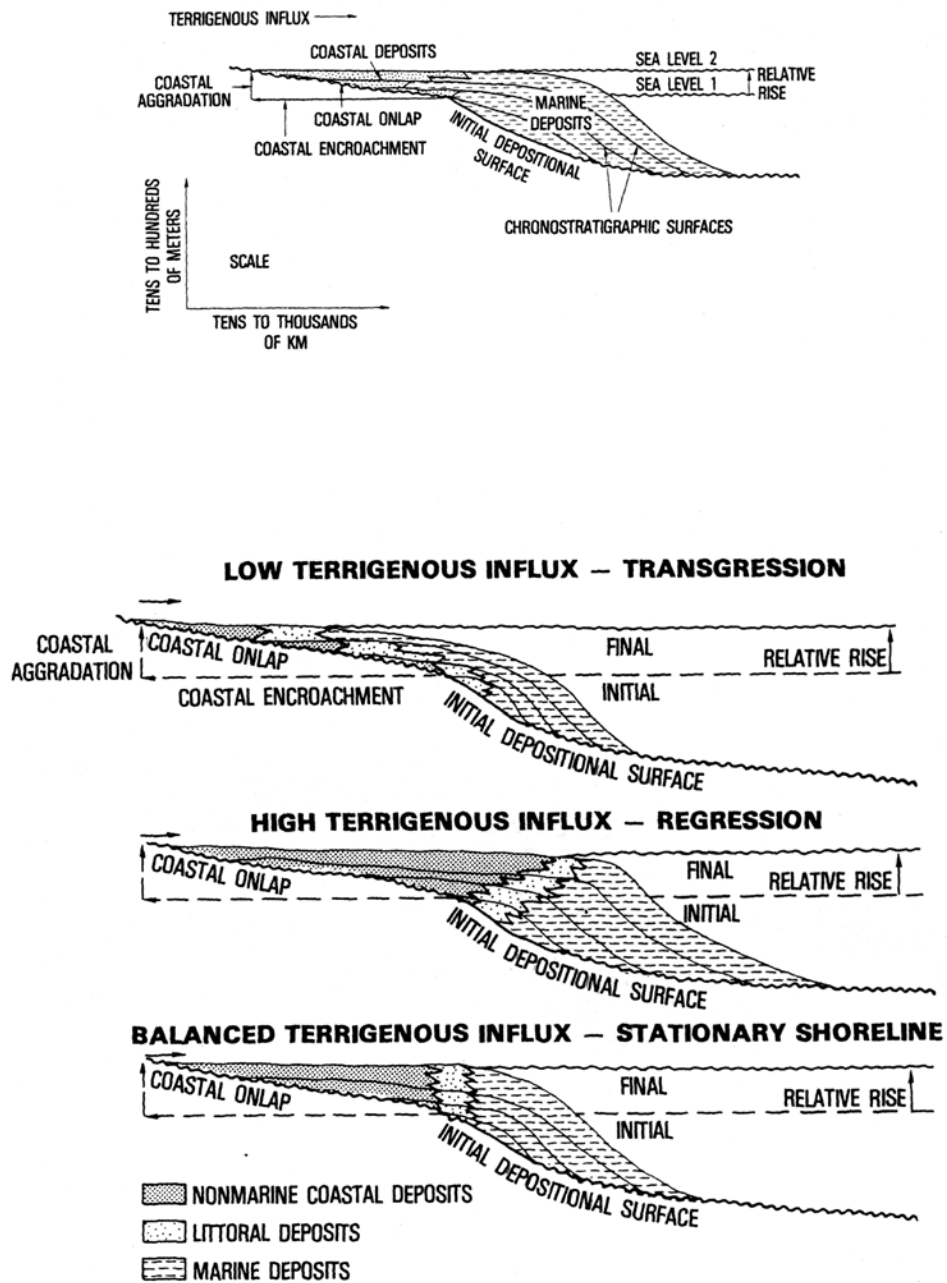


Figure 25. Diagram illustrating styles of deposition possible during relative rise of sea level. Sediment input in combination with relative rise in sea level results in transgression, regression, or a stationary shoreline (Vail et al., 1977a).

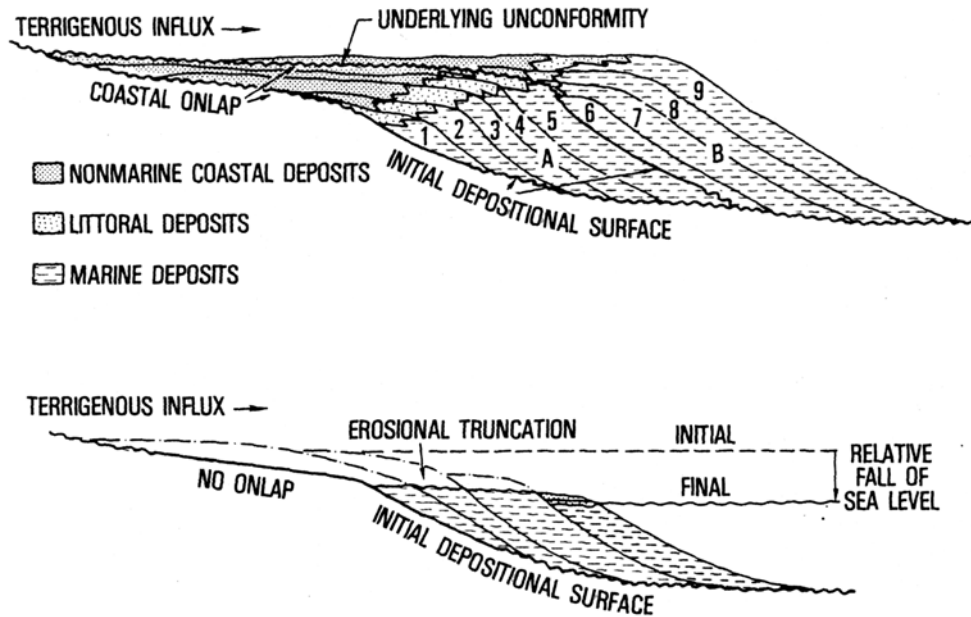
rise; this marks a period of progradational outbuilding of sedimentary facies (Vail et al., 1977a) (Fig. 25). A stationary shoreline setting is achieved when the rate of supply of sediment matches the rate of sea-level rise, resulting in aggradation of depositional sequences (Vail et al., 1977a) (Fig. 25).

Relative sea-level stillstand produces prograding depositional sequences characterized by toplap of the seismic reflector topsets. Toplap is a product of sediment bypass as sediment is transported laterally to the position of depositional base level (Vail et al., 1977a) (Fig. 26).

A relative sea-level fall produces a basinward shift in coastal onlap. During a rapid fall of relative sea level sediment bypass takes place on the shelf and coastal onlap becomes restricted to the apex of a lowstand fan on the basin margin (Vail et al., 1977a) (Fig. 26).

Vail et al. (1977a) present idealized depositional models based on depositional sequence patterns formed in response to sea-level highstand and lowstand (Fig. 27a, b). In the highstand model deposition takes place in the form of clinoform lobes prograding across a shallow shelf; progradation proceeds into deeper water if sediment supply is high (Vail et al., 1977a) (Fig. 27a). This model indicates transport of fine-grained sediments to the toes of clinoforms and deposition of coarse clastic sediments on the shelf. The lowstand model, based on the assumption that sea level falls below the shelf edge, indicates subaerial exposure and sediment bypass taking place on the shelf, and deposition occurring directly on the continental slope in the form of a submarine fan (Vail et al., 1977a) (Fig. 27b). Coastal onlap takes place during the ensuing rise in sea level near the depositional source. Another type of onlap, marine onlap, may be

### Relative Fall In Sea Level



### Relative Stillstand In Sea Level

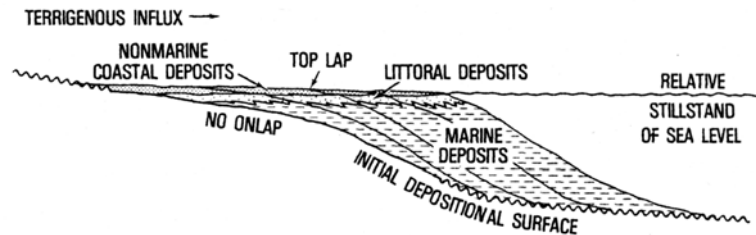


Figure 26. Upper two diagrams are diagrammatical representations of deposition during relative fall to lowstand of sea level. Sediment input in combination with relative fall or lowstand in sea level results in either basinward outbuilding of progradational depositional sequences (high sediment input) or erosional truncation of topsets (low sediment input). Lower diagram is an illustration of clinoform geometries formed during a stillstand in relative sea level. Coastal toplap and sediment bypass characterize deposition during this time (modified from Vail et al., 1977a).

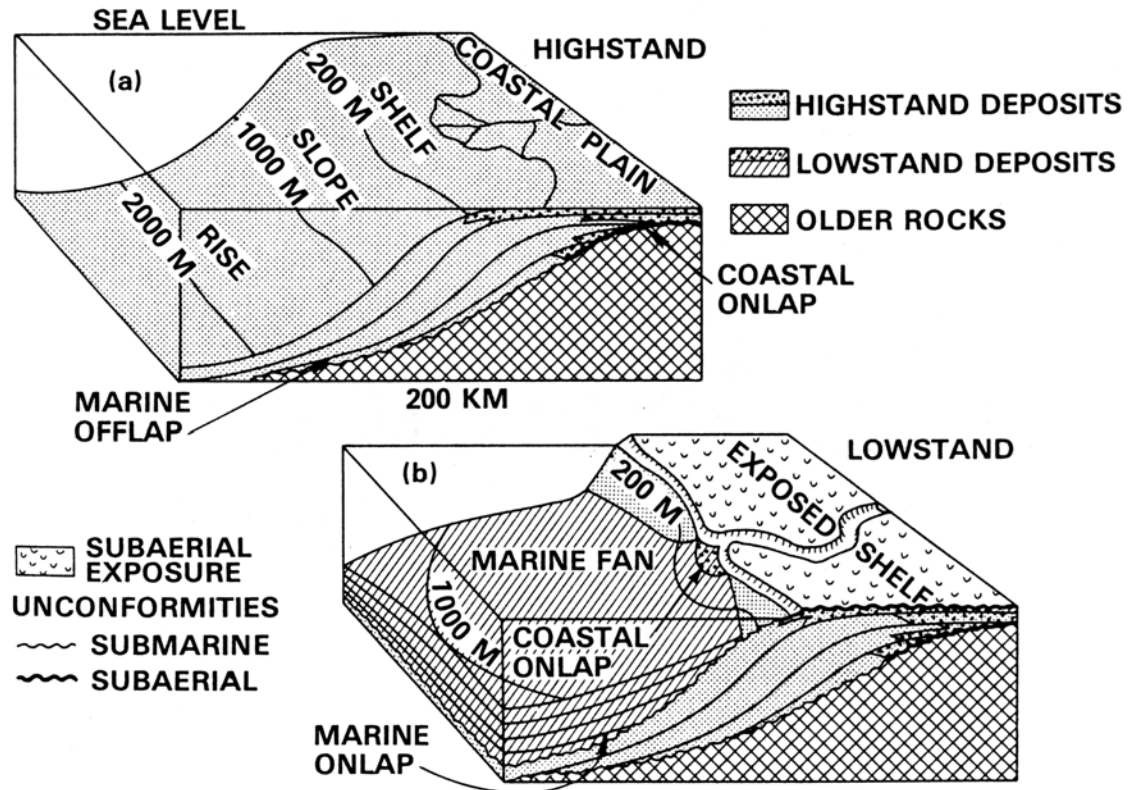


Figure 27. Depositional models proposed by Vail et al. (1977a) for highstand (a) and lowstand (b) of sea level. The highstand depositional model shows that during this time progradation takes place accompanied by coastal plain formation. Basinward progradation may even result in sediments transported to the distal shelf or upper continental slope. Exposure of the shelf occurs during sea-level lowstand as fluvial systems extend across the shelf and incise the shelf edge. Submarine canyons and linked marine fans may form at this time (from Vail et al., 1977a).

produced at this time if sediments are channeled through a submarine canyon (Vail et al., 1977a) (Fig. 27b).

Determining global cycles of sea level is important in the analysis of relative change in sea level step in the seismic sequence stratigraphic methodology. Vail et al. (1977b) present global sea-level curves for Mesozoic and Cenozoic time. Vail and associates construct these curves on the basis of global coastal onlap patterns determined through the application of seismic sequence stratigraphy. The purpose of these curves is



to introduce the element of predictability into stratigraphy, allowing for the prediction of age, lithofacies, paleoenvironments, and timing of unconformities (Vail and Mitchum, 1977).

*Arguments against seismic sequence stratigraphy*

The Vail methodology has received much attention from the scientific community since its introduction in the late 1970's. Many researchers utilize this methodology in regional depositional framework studies (Suter and Berryhill, 1985; Suter et al., 1987; Coleman and Roberts, 1988a,b; Kindinger, 1988; Goodwin and Prior, 1989; Kindinger et al., 1994; Sydow and Roberts, 1994; Morton and Suter, 1996; Winn et al., 1998; Anderson et al., 2004; and many others).

Others offer critical analysis of seismic sequence stratigraphy. Miall (1986) questions the importance that Vail et al. (1977b) place on the global sea-level curves they present as well as the accuracy of these curves. Miall (1986) cites the lack of supporting data offered by Vail et al. (1977b) and effects of localized tectonism on the stratigraphic record as reasons for taking a more cautious approach toward the seismic sequence stratigraphic methodology.

Galloway (1989a,b) presents an alternative to seismic sequence stratigraphy with genetic sequence stratigraphy. The genetic sequence stratigraphic method organizes strata into genetic stratigraphic sequences bounded by marine flooding surfaces. Genetic stratigraphic sequences are packages of genetically related sediments that record significant depositional outbuilding and infilling events within a basin (Galloway, 1989a). The genetic stratigraphic sequence boundary is defined as a "sedimentary veneer or surface that records the depositional hiatus that occurs over much of the transgressed

shelf and adjacent slope during maximum marine flooding” (Galloway, 1989a). This method places emphasis on thin, shelf-wide hiatal surfaces or deposits (condensed sections) rather than subaerially formed erosional unconformities and their down-dip correlative conformities, as in Vail et al. (1977a). Galloway (1989a) states that marine flooding surfaces are more easily recognized and preserved in the stratigraphic record of basin margins than unconformity surfaces. This methodology also differs from the seismic sequence stratigraphic approach by placing equal emphasis on the roles of tectonism, sediment supply, and eustatic change (Galloway, 1989a).

*In defense of seismic sequence stratigraphy*

This study defends the use of the seismic sequence stratigraphic approach with the following statements:

- 1) Arguments critical of the Vail methodology chiefly center on the lack of data used to support the global sea-level curves presented in Vail et al. (1977b). This study incorporates the sea level curve of Fairbanks (1989), an effective sea level curve for the Gulf of Mexico basin determined from age-elevation analysis of coral reef samples from Barbados. This curve correlates well with global sea level curves derived from similar studies in the Pacific Ocean basin (Chappell and Shackleton, 1986), and sea level curves obtained through stratigraphic analyses of northern Gulf of Mexico shelf-margin deposits. Consequently this study does not rely upon the strongly criticized global sea level curves presented in Vail et al. (1977b).
- 2) Seismic sequence stratigraphy relies on the identification of subaerially exposed unconformity surfaces and their correlative conformities to bound

seismic sequences. Galloway (1989a) cites this as a fundamental flaw in methodology on the basis that subaerially exposed unconformity surfaces can be restricted in extent and therefore do not make for good sequence bounding surfaces. This study focuses on the stratigraphic architecture of sediments deposited on the northern Gulf of Mexico at the time of Late Wisconsin sea-level lowstand. Numerous studies undertaken on the northern Gulf of Mexico shelf have recognized a regionally extensive unconformity surface, formed during the Late Wisconsin lowstand, that is readily visible in seismic profile data. There is no debate about the presence of a regional, subaerially exposed erosional unconformity surface; therefore the application of the Vail methodology is valid in this study.

## RESULTS

### *Modern Bathymetry*

Bathymetry of the southeastern Louisiana shelf within the study area indicates that the shelf strikes east-northeast and dips to the south-southeast. Bathymetric data show the presence of two major geomorphologic features linked to Mississippi River deposition during the last cycle of eustatic change, the modern Balize delta and the Mississippi Canyon (Fig. 28). The Balize delta of the Mississippi River deltaic plain is the dominant geomorphic feature along the eastern margin of the study area. Closely spaced isobath intervals show the presence of a steep delta front. Also noteworthy is the presence of Southwest Pass, an elongate distributary channel oriented to the southwest that lies near *Acadiana* 89 Line 1, as shown by basinward expansion of shallow isobaths. The upper portion of the Mississippi Canyon lies in the southwest corner of the study area. The canyon axis is elongate to the northwest. Canyon walls are visible as closely spaced isobaths.

Sackett Bank is a bathymetric expression created by diapirism that lies in the south-central portion of the study area near the shelf break (Fig. 28). This feature is distinctive due to its ‘bear paw’ morphology – a single, large diapiric structure flanked by four smaller structures in a configuration similar to that of an animal track. Note that *Acadiana* 89 Lines 19 and 20 transect the larger structure as well as one of the smaller structures (Fig. 28).

### *Structural Features*

Analysis of the seismic datasets indicates the presence of two salt structures and a series of small, normal faults within the study area (Fig. 29). The larger of the two salt

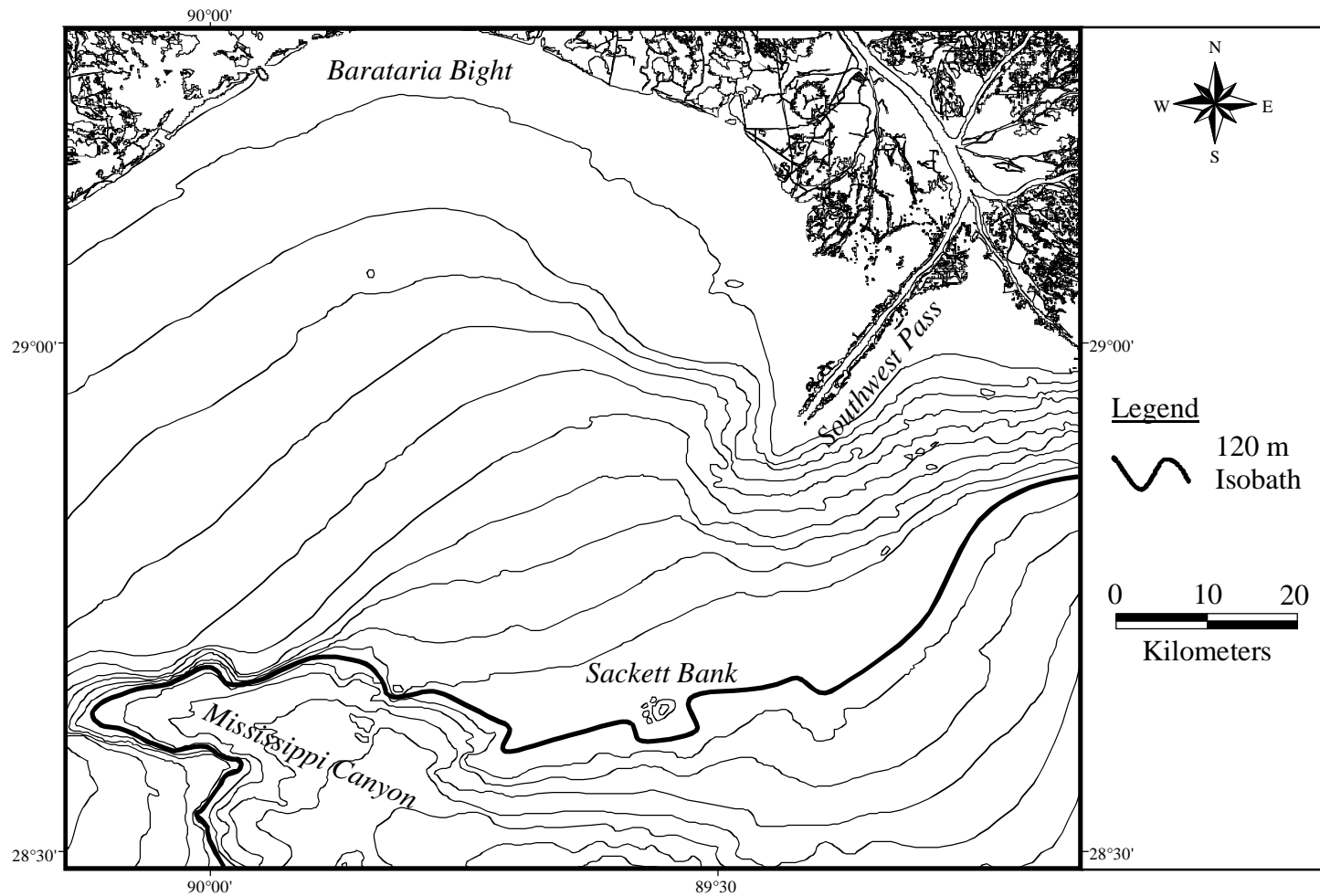


Figure 28. Bathymetric map of the study area is labeled with major geomorphologic and bathymetric features. The Mississippi Canyon forms the southwestern boundary for the study area, while the Barataria Bight and Balize delta lobe bound the area to the north and northeast respectively. The bold line marks the location of the 120 m isobath, the approximate location of sea level at the time of maximum sea-level lowstand.

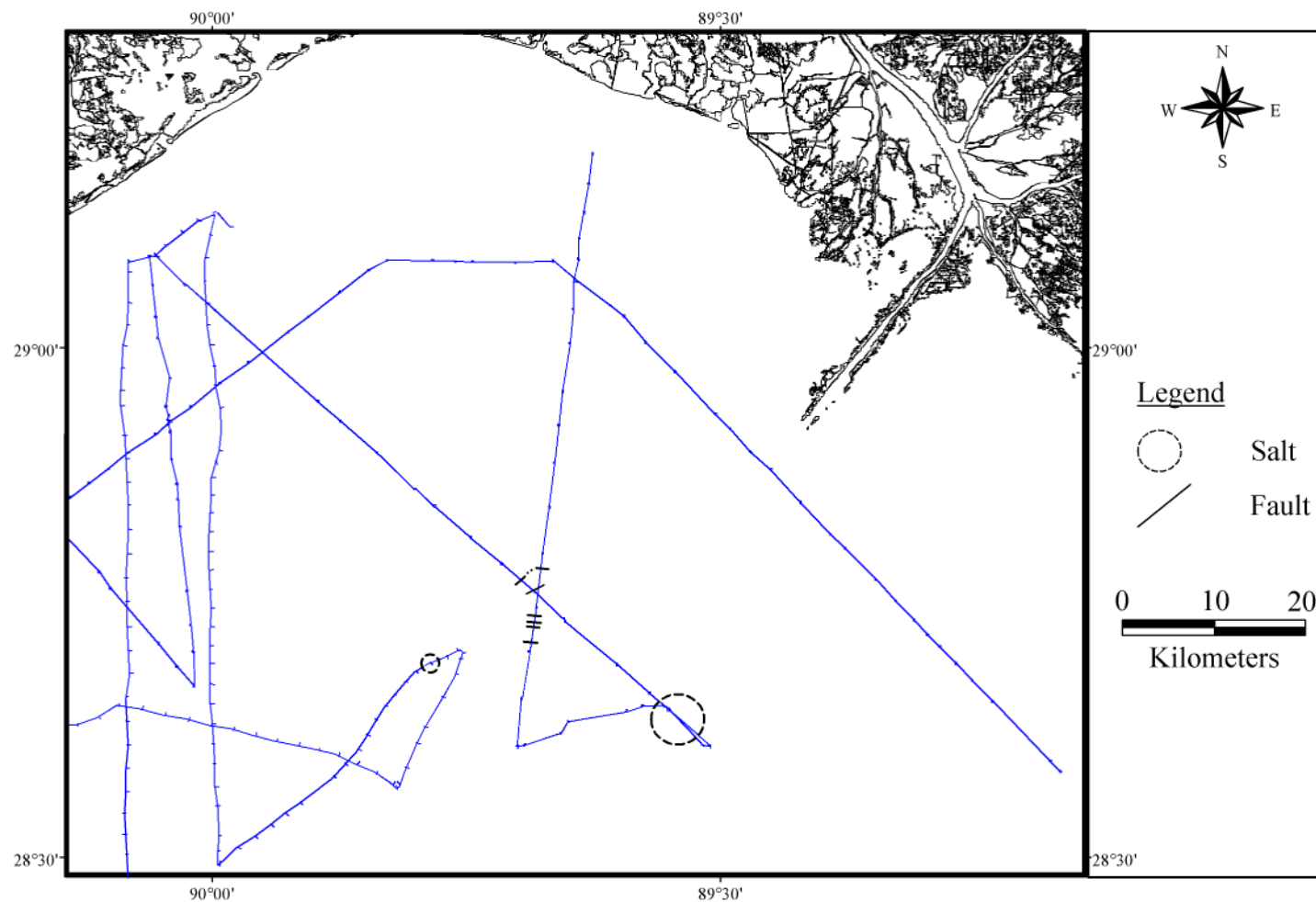


Figure 29. Structural map of study area indicates position of salt bodies and down-to-the-south faults in relation to seismic trackline positions. More heavily stippled trackline are from the *Acadiana 86* data set; smoother trackline are from the *Acadiana 89* data set.

structures is associated with Sackett Bank and appears in seismic records as a broad zone of acoustic wipeout bounded by onlapping reflectors (Fig. 30). The smaller diapir appears on *Acadiana 86* Line 33 as a zone of acoustic wipeout flanked by onlapping reflectors to the north and to the south by the Mississippi Canyon (Fig. 31). In contrast to Sackett Bank, this smaller salt structure is confined to the subsurface and is not expressed in the bathymetry.

Six small down-to-the-south faults are observed in seismic profile data across the study area (Fig. 29). The faults are confined to an area between the 80 and 100 m isobaths. Offset along these faults range from two to seven milliseconds (1.5 – 5.25 m). Faults occur in the shallow subsurface at depths of 137 to 148 milliseconds (102.7 – 111 m below sea level), but no fault planes penetrate the seafloor.

#### *Seismic Sequence Analysis*

Seismic sequence stratigraphic analysis of the *Acadiana 86* and *Acadiana 89* seismic data sets resulted in the identification of four bounding unconformable surfaces, referred to here as ‘horizons’, and five seismic facies units, referred to here as ‘packages’. The term package is substituted for the term ‘sequence’ to avoid confusion with the depositional sequence of Vail et al. (1977a) and is used only to signify a grouping of apparently related seismic reflectors. Four horizons have been identified in this study. They are: Horizon A, Horizon B, Horizon C, Horizon D, and Horizon E; Horizon A is stratigraphically the lowest horizon and Horizon E is stratigraphically the highest. Five packages have been identified in this study; they are: Basal Package, Package 1, Package 2, Package 3, and Package 4. The Basal Package is stratigraphically the lowest and Package 4 is stratigraphically the highest.

## *Horizons*

### *Horizon A*

Horizon A is observed as a continuous, medium to high-amplitude reflector visible throughout much of the seismic profile data set (Figs. 30, 32, 33, 34, 35). Horizon A is not continuous along the flanks of the Sackett Bank salt dome, except, where it terminates by toplap against an overlying group of high-amplitude reflector couplets (Fig. 30). Overlying reflectors exhibit baselap on this surface; onlap is commonly observed in the updip direction and downlap in downdip areas. The relationship of overlying reflectors to Horizon A transitions from gradual downlap to subparallel or parallel near the Sackett Bank salt dome (Fig. 34). This concordant configuration shifts to downlap in the immediate vicinity of the Sackett Bank salt dome; direction of downlap is opposite that observed in updip directions (Fig. 34).

Reflectors from the underlying basal package terminate by toplap on Horizon A in updip sections (Figs. 32, 35). This relationship gradually shifts to parallel to subparallel concordance in the downdip direction. On the flanks of diapirs, direction of toplap changes to opposite that of the direction observed in updip sections (Fig. 30).

Several down-to-the-south faults crosscut Horizon A, as seen in seismic reflection profiles (Figs. 32, 35).

A time-structure map of Horizon A shows several key features (Fig. 36). Contours indicate basinward deepening of Horizon A, illustrated by more widely spaced contours in updip sections and closely spaced contours near the shelf break in a fashion similar to that of modern bathymetry. Horizon A becomes shallower in the immediate



vicinity of the Sackett Bank salt dome, expressed as the concentric patterns of the 190, 200, and 210 msec contours.

Horizon A correlates well with the boundary between the oxygen isotope stages 1 and 2 in the Coleman and Roberts (1988a) data set (Fig. 33). This correlation allows for additional contouring of this surface in areas that lack seismic coverage. In the area between *Acadiana* 89 Lines 1 and 22 Horizon A deepens in an updip direction as seen by the patterns for the 110 through 150 msec contours. This appears to be a valley-shaped feature with a south-trending axis that terminates updip of the Sackett Bank salt dome.

Structural patterns of Horizon A indicate a depression in the area adjacent to the Sackett Bank salt dome and along the axis of the valley-like feature.

#### *Horizon B*

Horizon B is a locally confined surface visible in seismic profiles as a medium to high-amplitude reflector that terminates by toplap against Horizon E on the flank of the Sackett Bank salt dome in the downdip direction and laps out against Horizon A in the updip direction (Figs. 30, 34, 35). Underlying reflectors terminate against this surface by toplap, although in some areas underlying reflectors are parallel to subparallel to Horizon B (Fig. 34). Overlying reflectors are generally parallel to subparallel to Horizon B (Figs. 30, 34). On the flank of the Sackett Bank salt dome underlying reflectors steeply toplap against Horizon B, while overlying reflectors maintain concordance with Horizon B (Fig. 30).

A time-structure map of Horizon B shows the limited extent of this surface, terminating just updip of the 150 msec contour and around the Sackett Bank salt dome (Fig. 37). Contour line spacing shortens in the downdip direction except around the

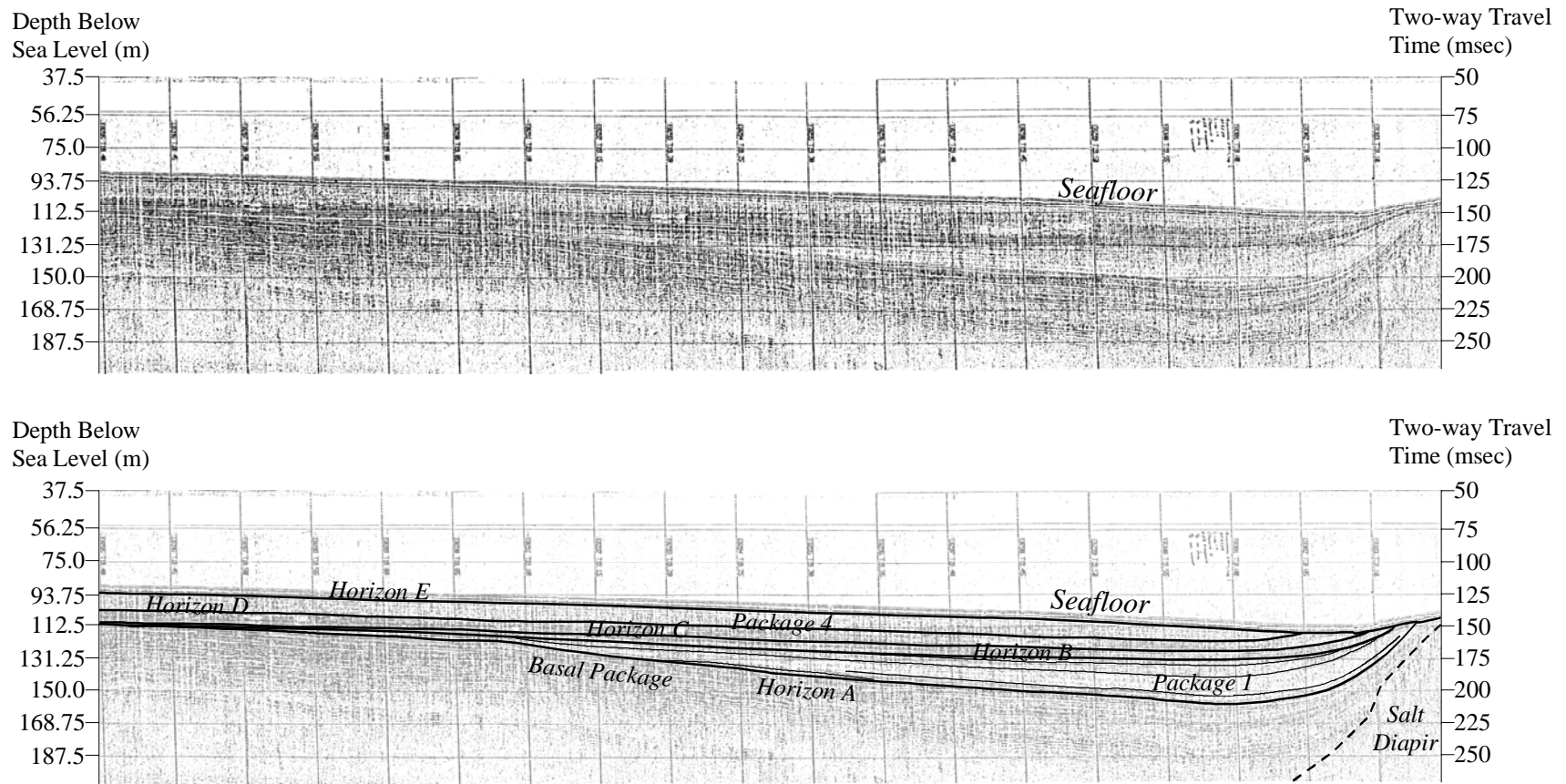


Figure 30. Seismic profile of *Acadiana* 89 Line 19, taken along depositional dip, shows the downdip portion of this line. Seismic packages deform upward and terminate against the flanks of the salt diapir, which appears on the seismic record as a zone of acoustic washout. Lowermost packages terminate updip by way of onlap against Horizon A.

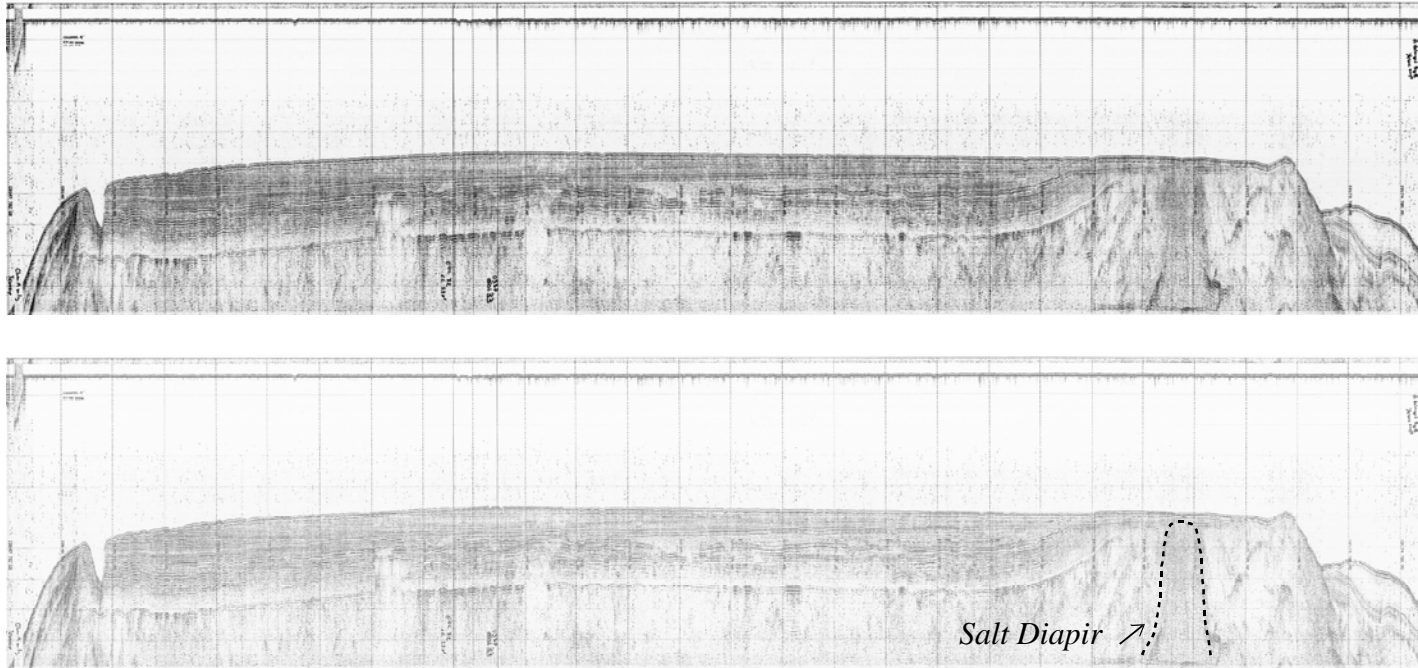


Figure 31. *Acadiana* 86 Lines 31-33 seismic profile showing the presence of a small salt diapir. Due to unresolved complications with time-depth conversions, this profile could not be accurately measured, effectively eliminating it from further use in this study.

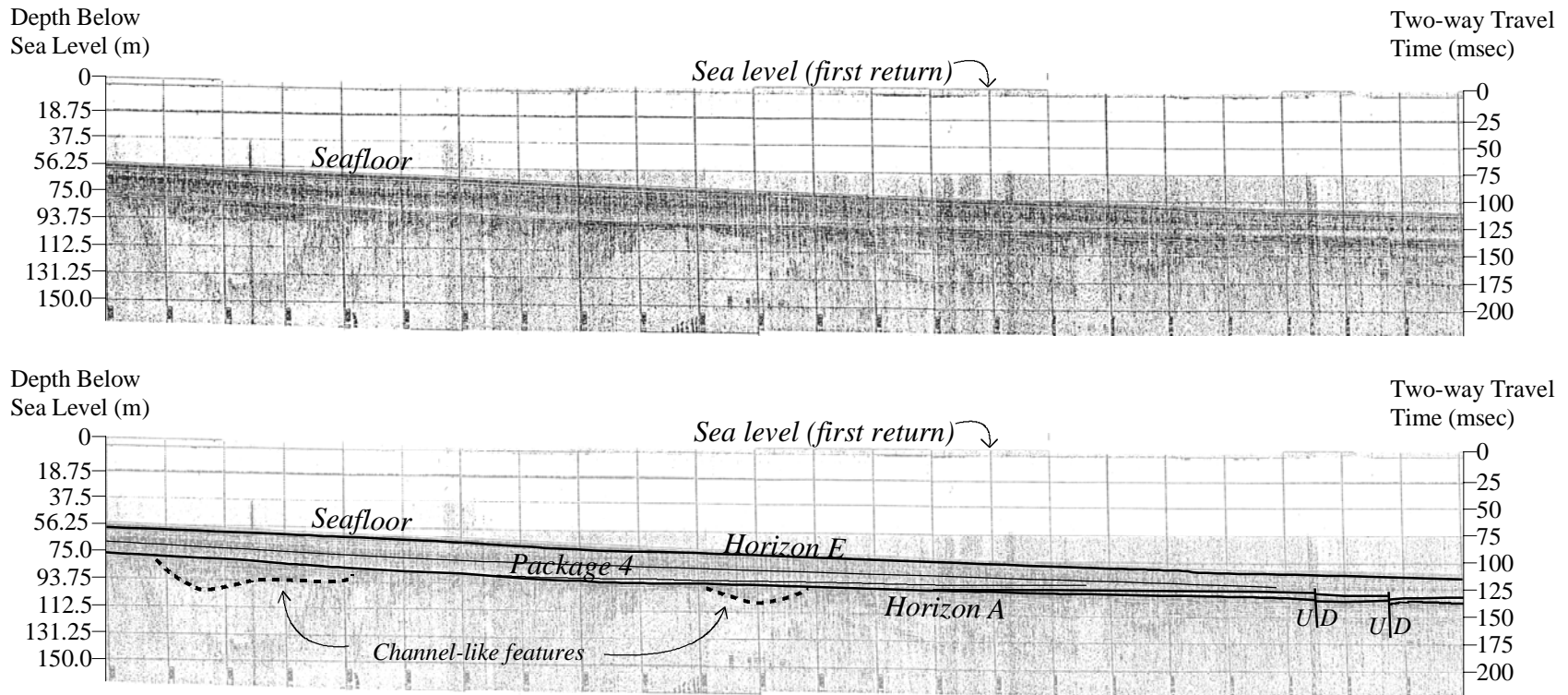


Figure 32. Seismic profile of *Acadiana* 89 Line 19, taken along depositional dip, shows the updip portion of this line. To the right of the figure, Package 3 thins and laps out against Horizon A. Two small down-to-the-south faults locally affect package thickness. Note also the presence of two channel-like features located within the top of the Basal Package immediately below Horizon A.

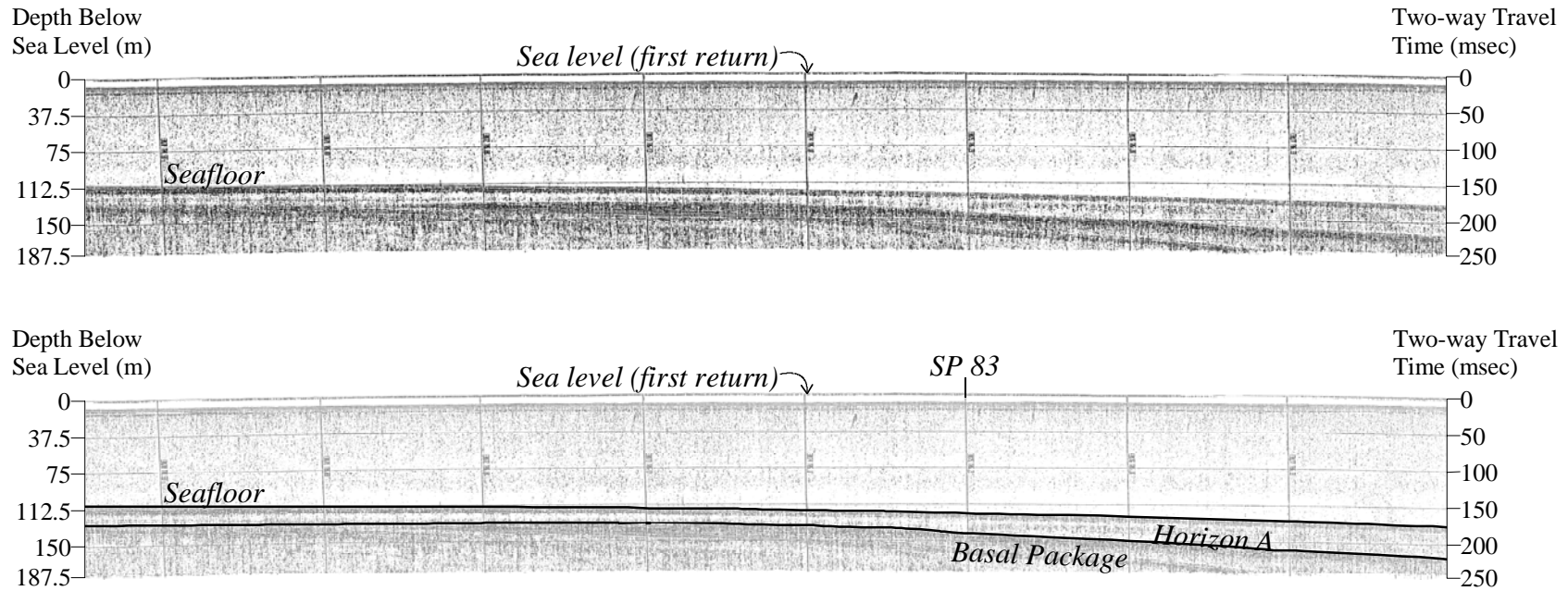


Figure 33. Seismic profile of *Acadiana* 89 Line 1 displays the continuous high-amplitude reflector characteristic of Horizon A. Geotechnical borehole SP 83 position indicated at time marker 05:23; this borehole, in part, allows for correlating seismic profile data to geotechnical borehole data. Note that this segment of seismic profile lies near the shelf margin, as shown by the downward curvature of the seafloor on the right side of the figure.

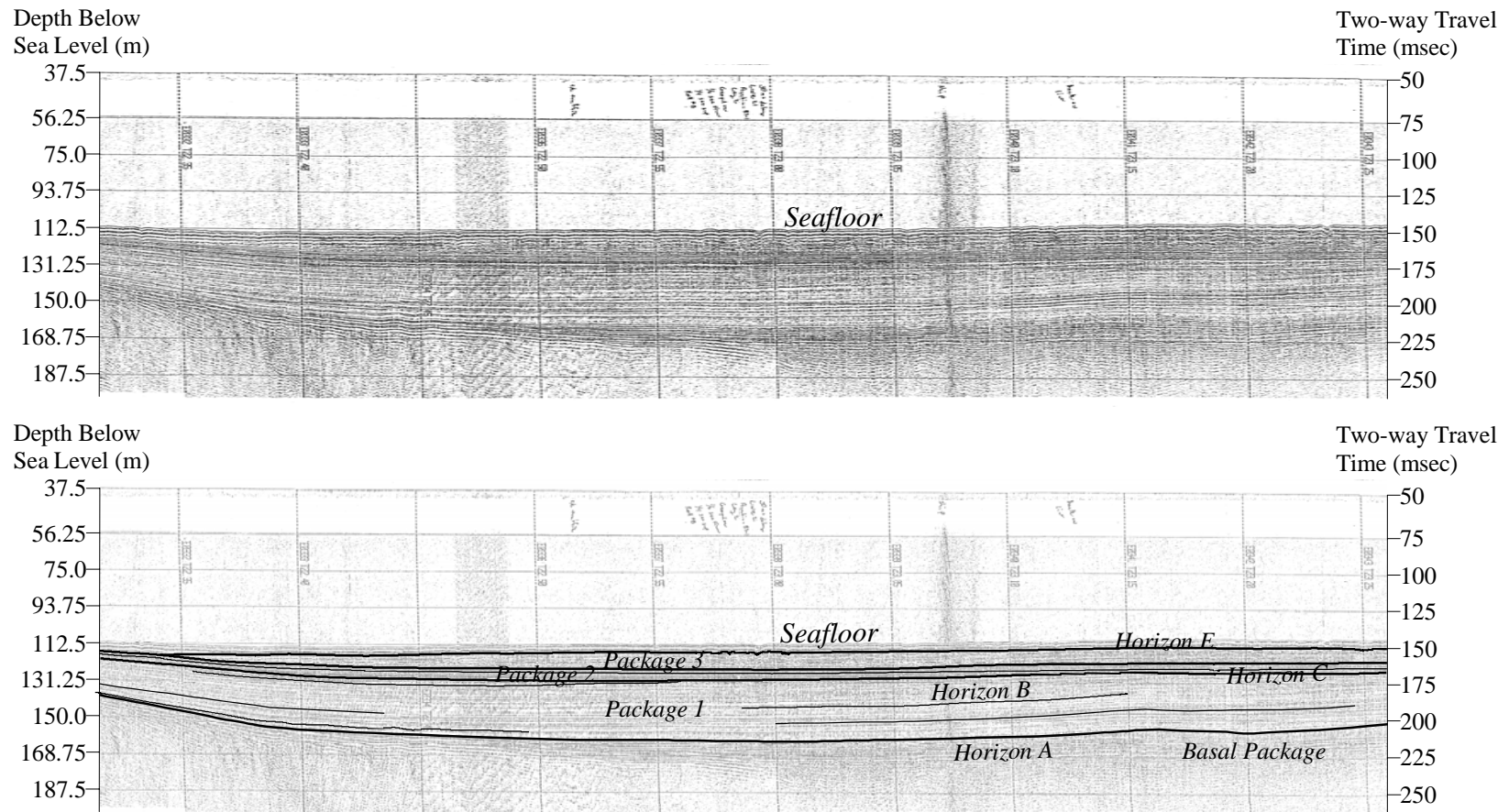


Figure 34. Seismic profile of *Acadiana* 89 Line 21, taken along depositional strike, shows the downdip portion of this line. At this location, Horizon A and the overlying reflectors of Package 1 are conformable to the right and middle of the figure, and to the left of the figure near the salt diapir they become convergent, with basal reflectors terminating by toplap against Horizon A. Hummocky reflectors in Package 3 are visible at this location.

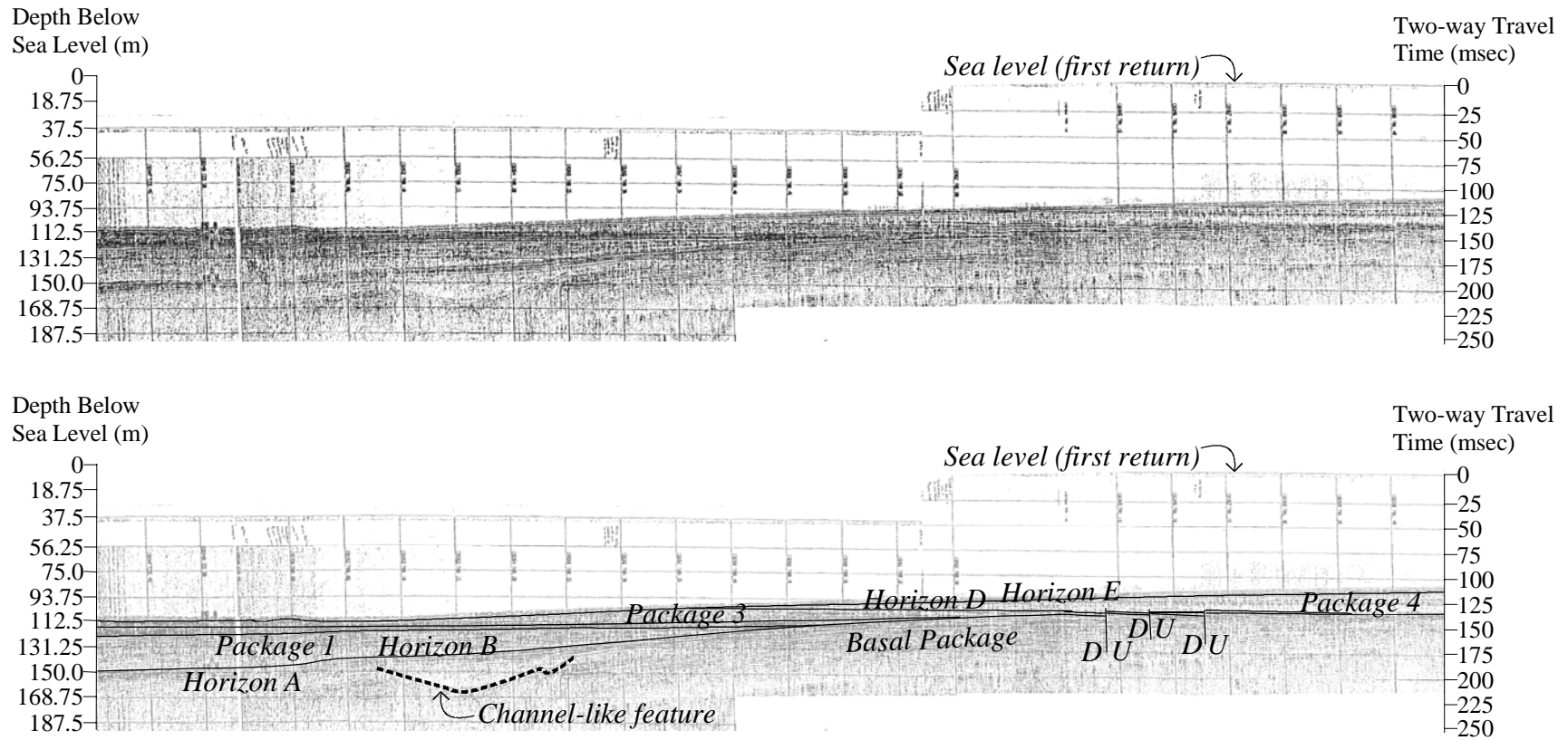


Figure 35. Seismic profile of *Acadiana* 89 Line 22, oriented along depositional dip, shows the updip relationships of packages and horizons. Packages 1, 2, and 3 terminate by onlap in the updip direction against the Basal Package. Package 4 thickens landward. Note the presence of three small down-to-the-south faults, and a large channel-like feature visible in the basal package.

Sackett Bank salt dome, where spacing increases between the 170 and 180 msec contours. Horizon B shallows around the Sackett Bank salt dome. Structural trends show a depression adjacent to the Sackett Bank salt dome and in the updip direction between the 150 and 160 msec contours (Fig. 37).

#### *Horizon C*

Horizon C is a regionally confined surface expressed seismically as a medium-amplitude reflector (Figs. 30, 34, 35). This surface terminates updip against Horizon A and downdip by toplap against Horizon E along the flanks of the Sackett Bank salt dome (Fig. 30). Underlying and overlying reflectors are generally concordant with this surface.

A time-structure map of Horizon C shows the updip extent of this surface as well as the downdip relationship of this surface with the Sackett Bank salt dome (Fig. 38). Wide spacing between the 145 and 150 msec contours indicate the updip presence of accommodation, while in the downdip area accommodation is seen around the flanks of the Sackett Bank salt dome, as expressed by the 160 and 165 msec contours (Fig. 38).

#### *Horizon D*

Horizon D is expressed seismically as a medium to high-amplitude reflector that terminates in the updip direction by onlap against Horizon A (Figs. 32, 35). Underlying and overlying reflectors share a concordant relationship with Horizon D. Horizon D can be identified in downdip areas as the bounding surface between an underlying, high-amplitude seismic facies package and an overlying, low-amplitude seismic facies package (Figs. 30, 34). Down-to-the-south faults offset this surface (Fig. 35).



A time-structure map of this surface shows a deepening of the surface in the downdip direction (Fig. 39). Accommodation occurs near the Sackett Bank salt dome. Contours are more widely spaced in the updip direction.

#### *Horizon E*

This surface is expressed seismically as a regionally extensive, continuous, high-amplitude reflector or reflector couplet (Figs. 30, 32, 34, 35). Horizon E delineates the underlying low to medium-amplitude seismic facies package from several overlying high-amplitude reflector couplets, or ‘reflector train’, created by ringing of the acoustic signal off the sea floor that obscures the true reflection patterns of the uppermost subsurface strata (see Kindinger, 1988; and, Goodwin and Prior, 1989). Horizon E does not represent a true bounding surface, but rather serves as the upper limit of seismic resolution in this study.

A time-structure map of Horizon E shows that it closely matches modern bathymetric contours (Fig. 40).

#### *Seismic facies units*

##### *Basal package*

This is the lowermost package identified in this study (Figs. 30, 32, 33, 34, 35). This package is poorly constrained, as limited seismic penetration does not allow for determination of the lowermost boundary and external seismic form of this package. The Basal Package is, therefore, defined only by its uppermost boundary, Horizon A, and does not constitute a true seismic facies unit. The internal seismic character of this package varies from chaotic to parallel (Fig. 30, 32, 34, and 35). Several channel-like

features are visible in this package; channels are confined to the uppermost portion of the basal package and terminate laterally against Horizon A (Figs. 32, 35).

#### *Package 1*

Package 1 overlies the basal package with Horizon A and Horizon B forming the lower and upper bounding surfaces, respectively (Figs. 30, 34, 35). The internal seismic organization of this package is characterized by dipping clinoform sets that terminate updip by toplap against Horizon B, and downdip convergence into parallel to subparallel concordant toe sets (Fig. 30). Package 1 exhibits an oblique tangential internal configuration, as well as a lens-shaped external form.

An isochron map of this package shows that it has a maximum thickness of 40 msec in the area of the Sackett Bank salt dome (Fig. 41). This correlates well to the time-structure map of Horizon A, which indicates this area as the location of the most accommodation. Package 1 thins in the updip direction, as seen in seismic (Fig. 41) and in the isochron map (Fig. 41), pinching out in the updip direction against the basal package. The downdip extent is limited by the Sackett Bank salt dome.

#### *Package 2*

Package 2 is located stratigraphically above Package 1. Horizons A and B form the lowermost bounding surface and Horizon C is the uppermost bounding surface of this package (Figs. 30, 34, 35). This package pinches out in the updip direction onto Horizon A, while the Sackett Bank salt dome controls the downdip extent. The internal seismic character consists mostly of high-amplitude continuous parallel to subparallel reflectors (Figs. 30, 34). A sheet drape external form best characterizes this package.

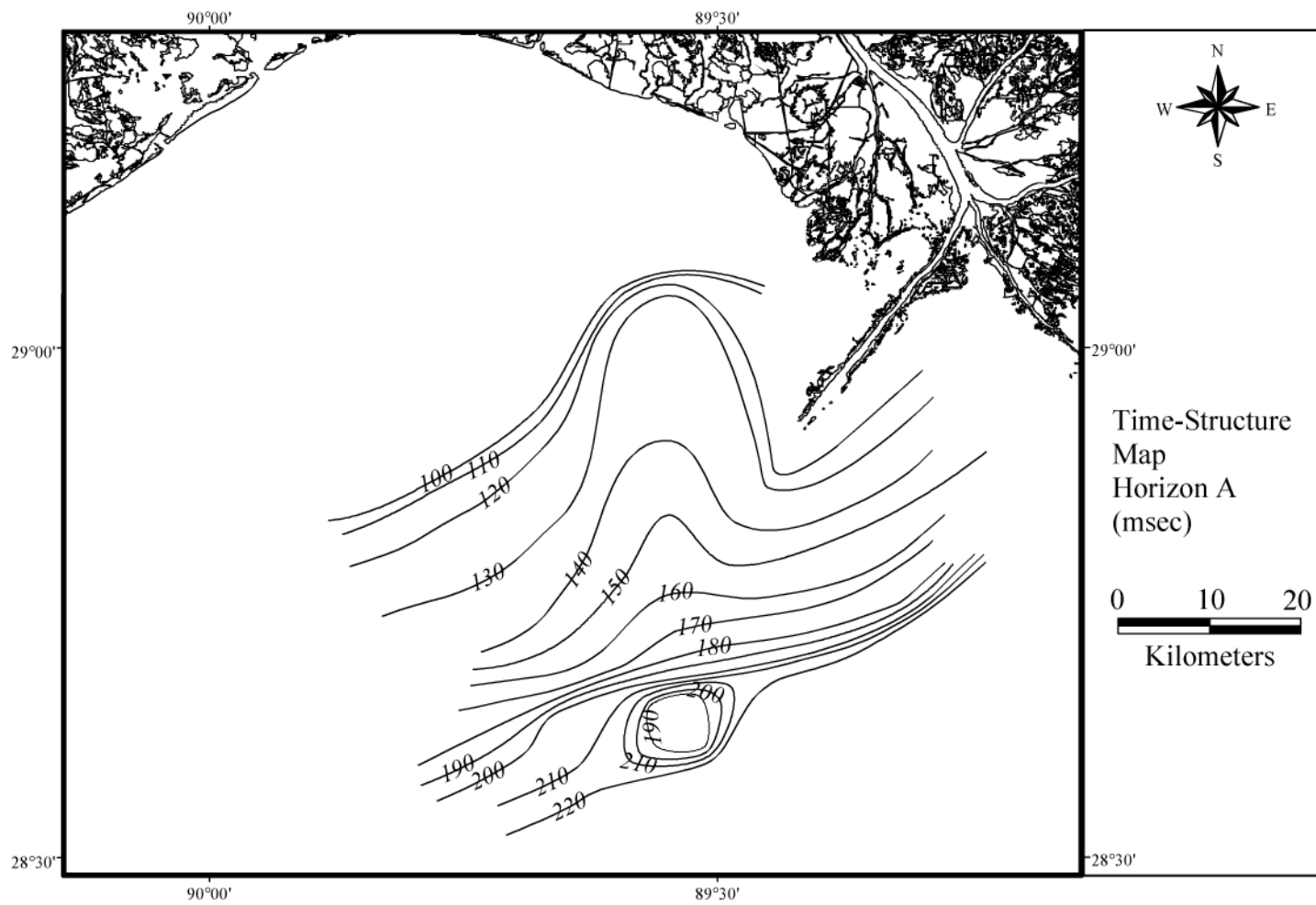


Figure 36. The time-structure map (in msec) of Horizon A combines data measured from seismic profiles and Coleman and Roberts (1988a) oxygen isotope age data in order to better contour those areas not covered by seismic tracklines. Two important features are evident: 1) a deepening of Horizon A in the immediate vicinity of the salt dome located to the south of the map, and 2) the valley-like structure with a south-trending axis located in the middle of the map.

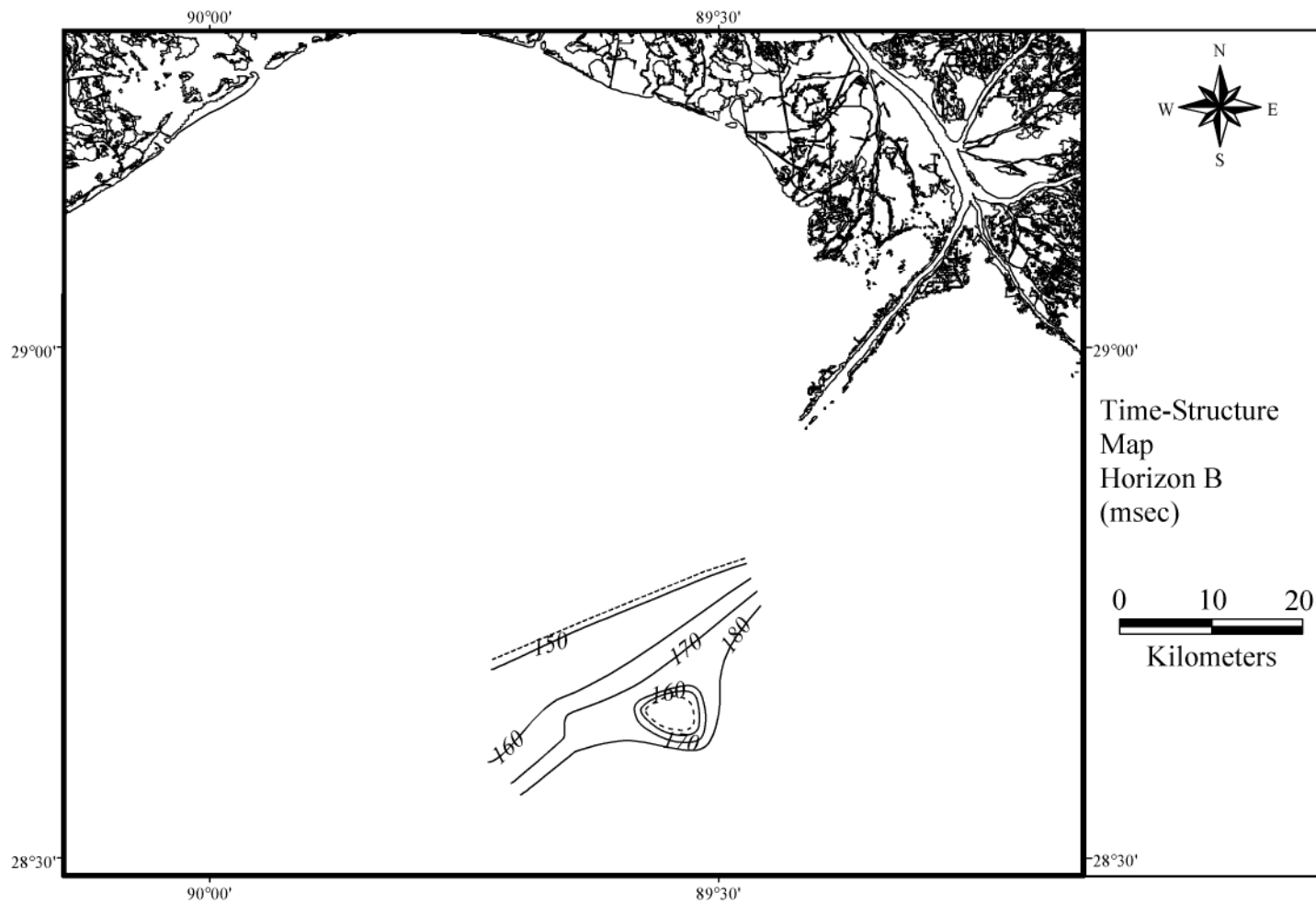


Figure 37. A time-structure map (in msec) of Horizon B indicates the presence of accommodation to the west of the salt dome. This horizon shallows around the flanks of the salt dome, and terminates updip of the 150 msec contour line.

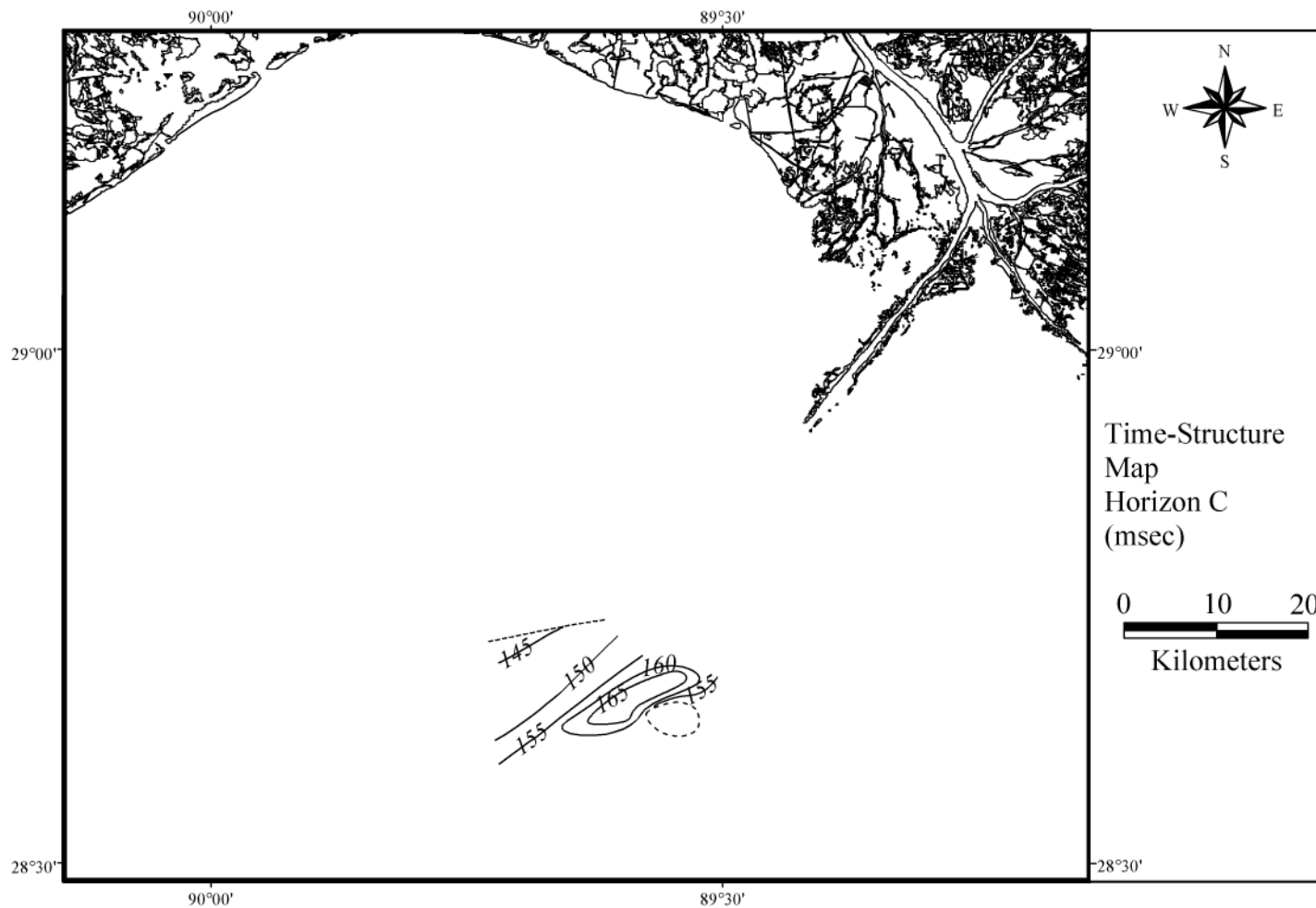


Figure 38. A time-structure map (in msec) of Horizon C indicates the presence of accommodation on the north-northwest flank of the salt dome. This horizon shallows around the flanks of the salt dome and terminates updip.

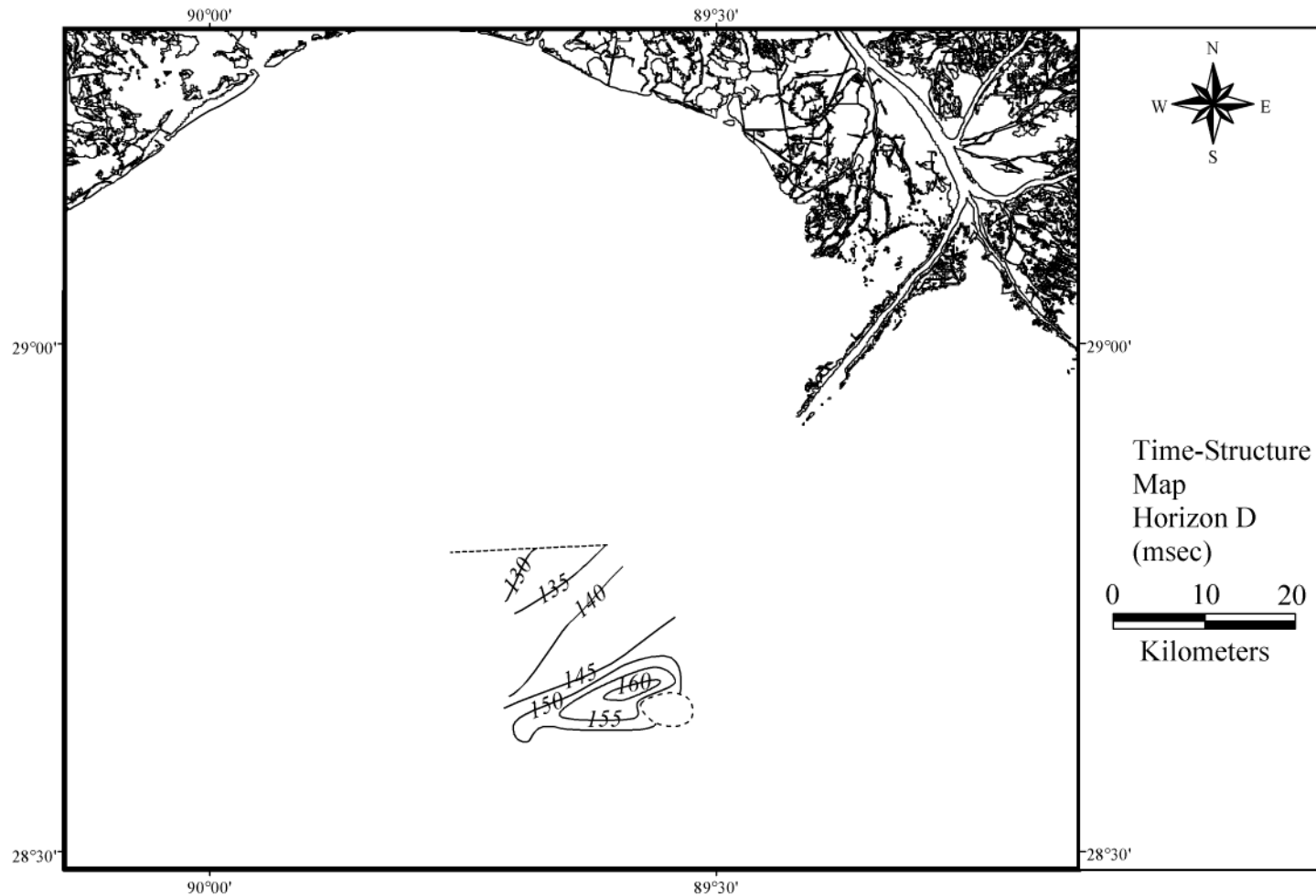


Figure 39. A time-structure map (in msec) of Horizon D indicates the presence of accommodation on the north-northwest flank of the salt dome and to the west of the salt dome. This horizon gradually shallows updip as contour lines terminate against Horizon A. The overall strike of contours begins to mirror that of modern isobaths.

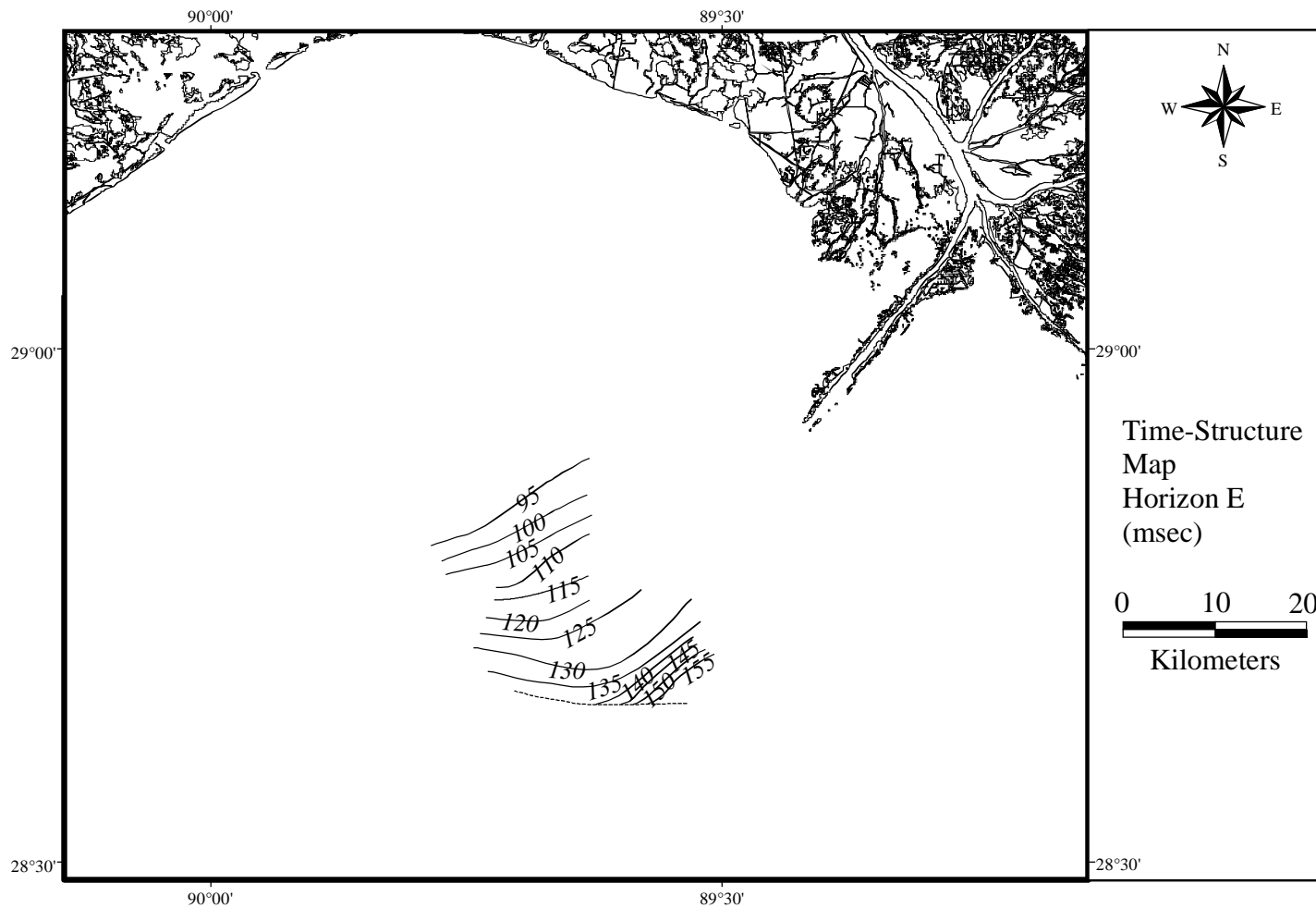


Figure 40. A time-structure map (in msec) of Horizon E shows that contour line patterns for this surface closely mirror those of modern bathymetry. This horizon deepens in the downdip areas near the salt dome and gradually shallows in the updip direction.

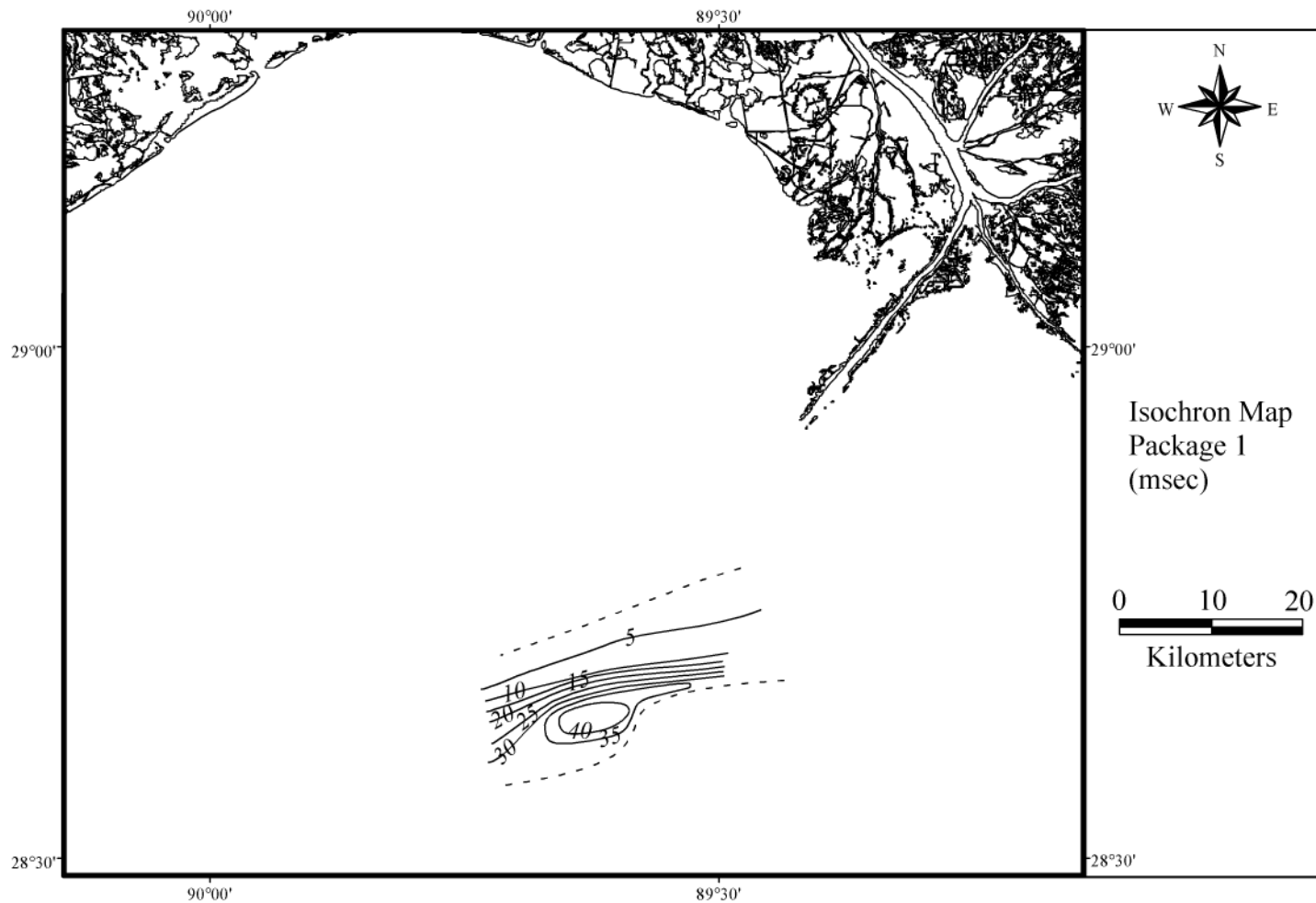


Figure 41. The isochron map of Package 1 (in msec) is constructed from seismic profile data. This package is thickest in the area immediately west of the Sackett Bank salt dome and thins in the updip direction. Dashed lines indicate extent of Package 1.



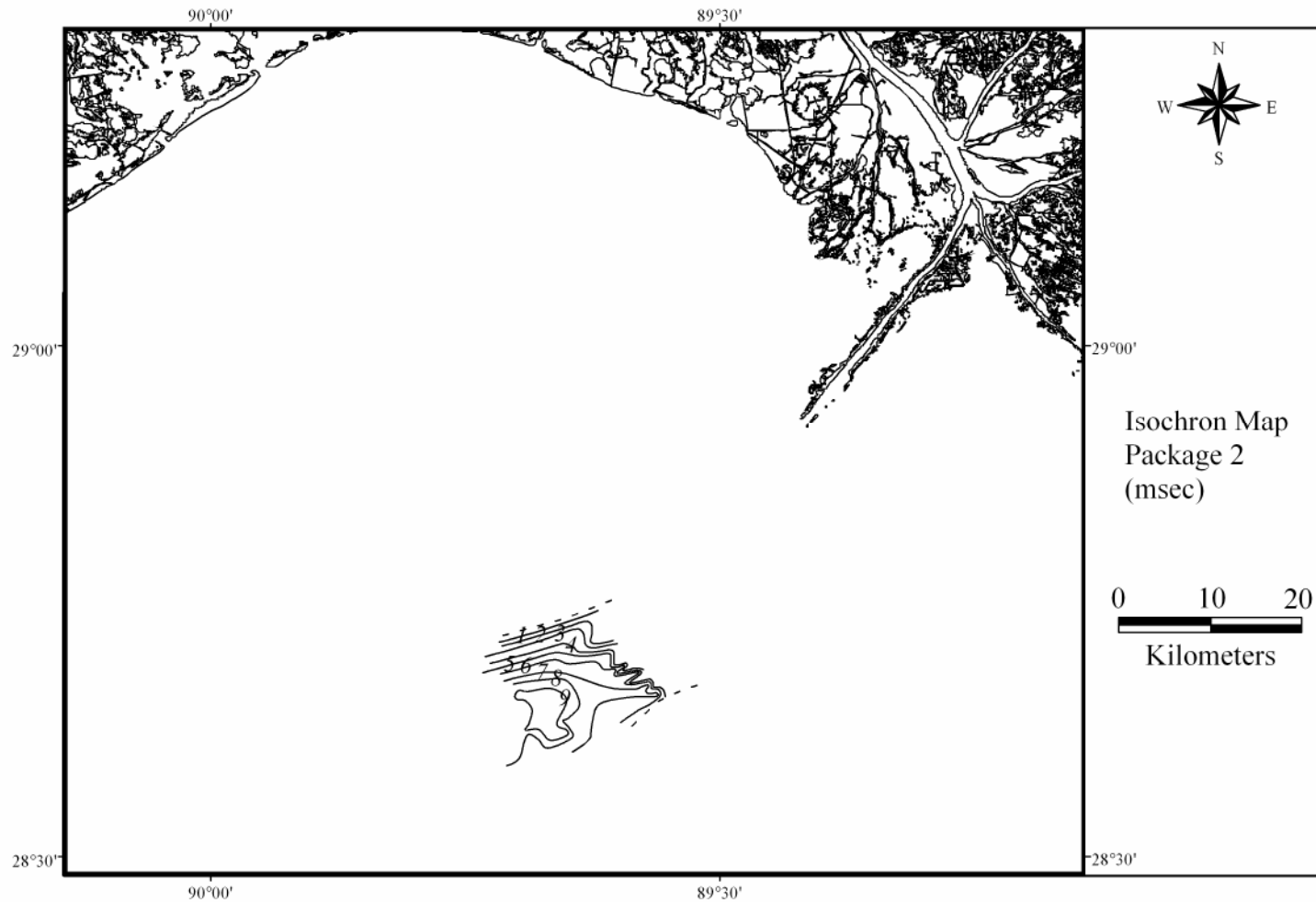


Figure 42. The isochron map of Package 2 (in msec) is constructed from seismic profile data. This package is thickest in an area further west than the depocenter of Package 1. Package 2 terminates further updip than Package 1, indicating a change in the style of deposition from progradational to backstepping.

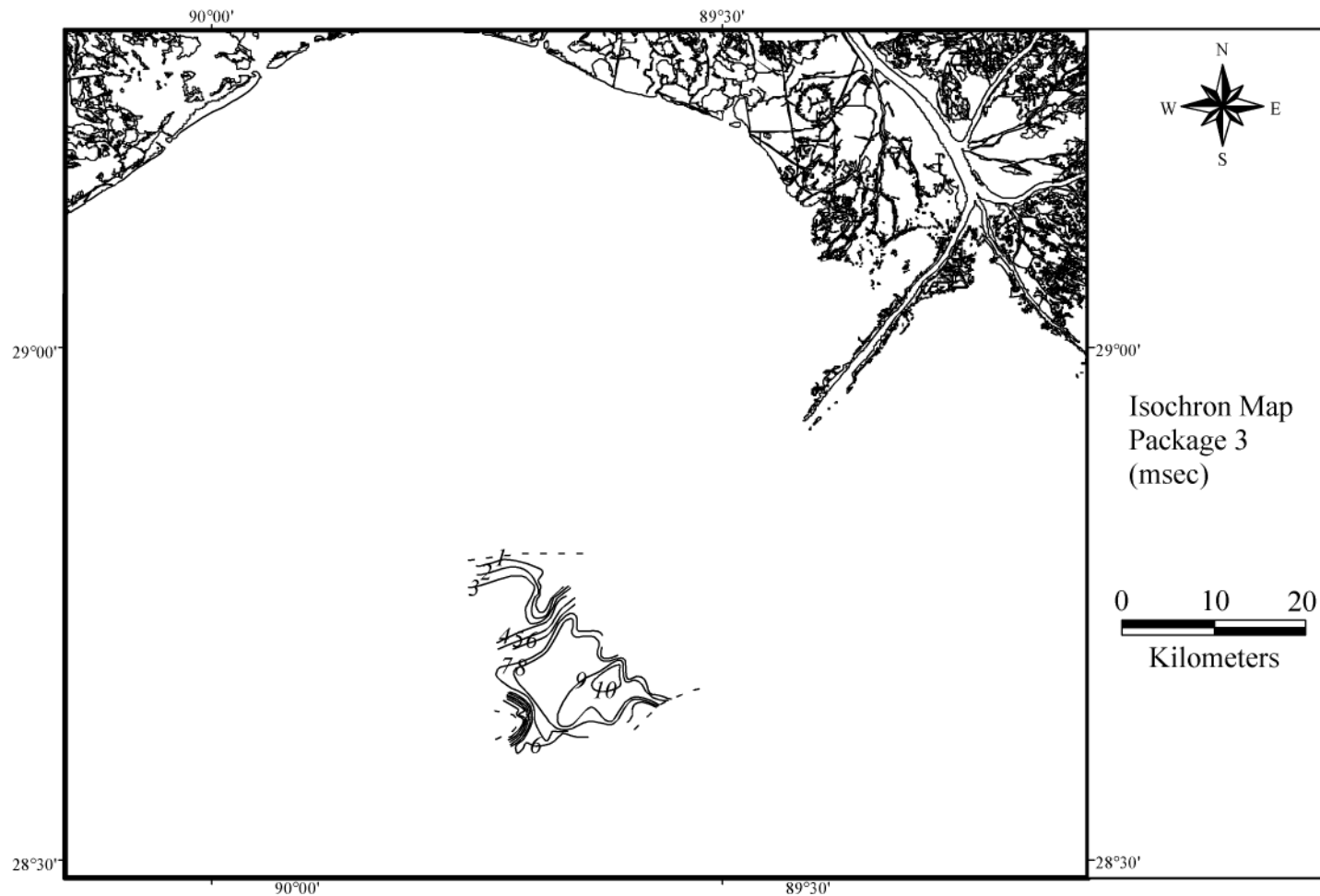


Figure 43. The isochron map of Package 3 (in msec) is constructed from seismic profile data. This package is thickest in on the north-northwest flank of the salt dome. Thickness distribution patterns indicate that Package 3 filled in the available downdip accommodation before backstepping initiated. Small down-to-the-south faults locally control package thickness in the updip direction.

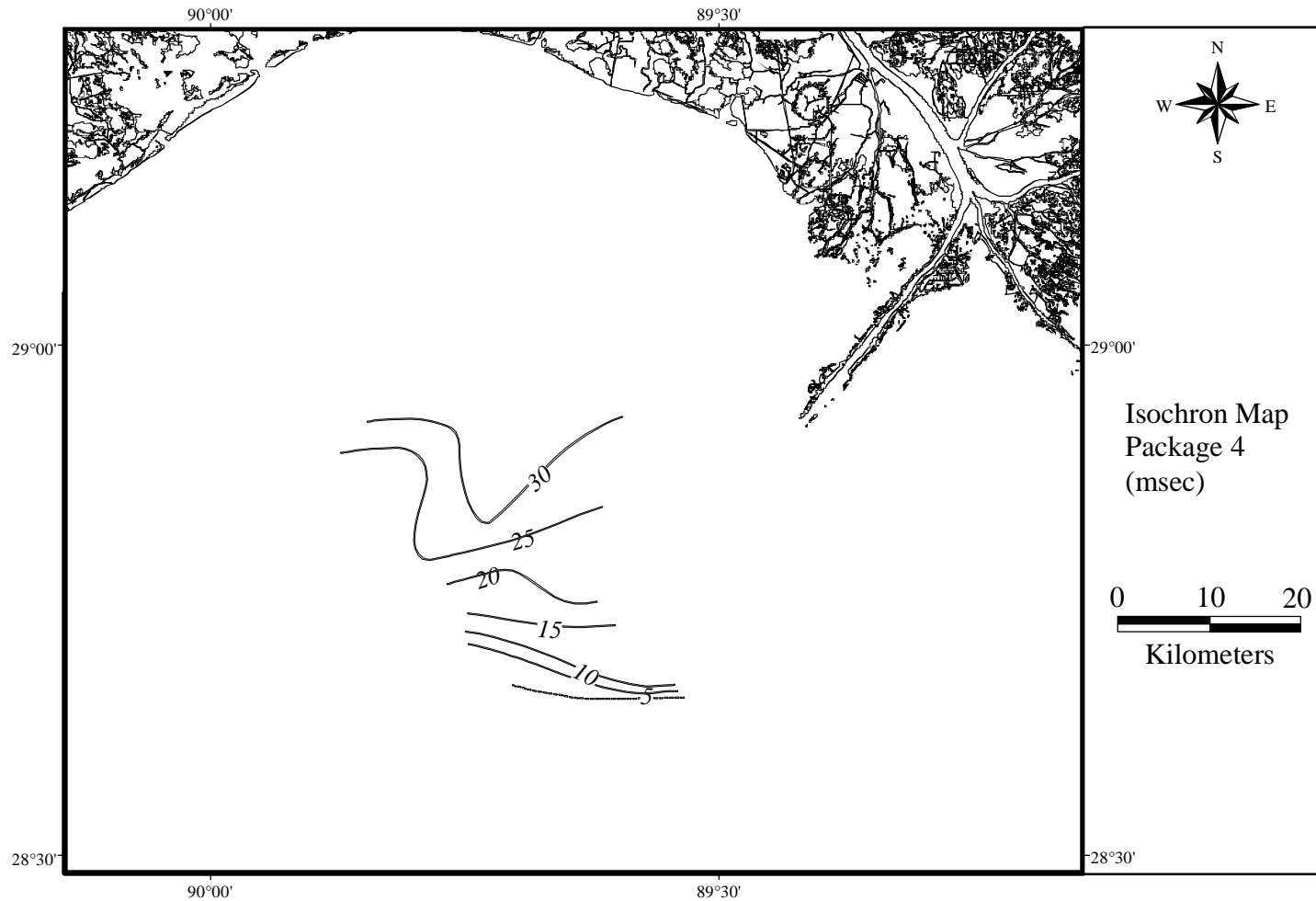


Figure 44. The isochron map of Package 4 (in msec) is constructed from seismic profile data. This package thickens in the updip direction; the updip limit of this package has not been determined due to poor seismic resolution in the updip direction. This package correlates well with a late Pleistocene-early Holocene transgressive facies.

An isochron map of this package indicates it is a thin layer with a maximum thickness of 9 msec, located west of the Sackett Bank salt dome (Fig. 42). The package thins away from the 9 msec isopach contour to the north and east directions. The unusual isochron contour line pattern observed at the eastern limit of the package, seen as sharply curved, closely spaced contour lines, may result from limited data or human error.

### *Package 3*

Package 3 overlies Package 2, bounded by Horizons C and A on the bottom and Horizon D on the top (Figs. 30, 34, 35). This package extends further in the updip direction than Package 2, pinching out against Horizon A; in the downdip direction it terminates on the flanks of the Sackett Bank salt dome and pinches out to the west of the salt body (Figs. 30, 32, 34, 35). The internal seismic character of this package varies from medium-amplitude parallel to subparallel reflectors to medium to high-amplitude hummocky reflectors (Fig. 34). The external form of this package most closely resembles a sheet drape.

An isochron map of Package 3 reveals it is thickest on the flank of the Sackett Bank salt dome (Fig. 43). It thins to the west, as seen by the closely spaced contour lines. Thinning is more gradual in the updip direction. It is important to note that the thickness of this package is controlled by both the structure of Package 2, the basal package, as well as by faulting.

### *Package 4*

Package 4 is the uppermost package identified, and overlies Package 3. Horizons D and A form the lowermost bounding surface; Horizon E forms the uppermost bounding surface (Figs. 30, 32, 35). This package terminates downdip on the flanks of the Sackett

Bank salt dome to the south and pinches out to the west, and extends updip beyond the limit of seismic resolution. Continuous parallel low to medium-amplitude onlapping reflectors characterize the internal seismic pattern of this package (Fig. 30, 35). A wedge or bank best describes the external form of this package.

The isochron map of Package 4 illustrates this external form, showing that Package 4 thins in the downdip direction and thickens in the updip direction (Fig. 44).

#### *Late Wisconsin unconformity*

Seismic data analysis allows for the identification of several bounding surfaces. Wide areal extent, prominent reflector terminations against it, and underlying channel-like features distinguish Horizon A from other surfaces identified in this study. A correlation of the seismic analysis in this study with Coleman and Roberts (1988a) geotechnical foundation borehole data, Conoco West Delta 96 lease block survey data (Cole, 1983), and data from existing literature allows for further determination of the stratigraphic significance of Horizon A.

Subsurface elevations of Horizon A in the vicinity of key geotechnical boreholes taken from the Coleman and Roberts (1988a) data set closely match those of the oxygen isotope stage boundary 1/2 (Fig. 45). This boundary is at a depth equivalent to 169 msec in the MC 268 borehole. Extrapolating the 160 and 170 msec isochrons on the Horizon A time-structure map to the location of the MC 268 borehole shows that the depth of the oxygen isotope stage boundary 1/2 correlates well with the seismically derived isochron contours of Horizon A. The subsurface depth of oxygen isotope stage boundary 1/2 in geotechnical borehole SP 83, located near *Acadiana* 89 Line 1 time marker 05:23, is approximately 190 msec, which correlates well to the depth of Horizon A at that location

(Fig. 33). The implications of this correlation are that: 1) oxygen isotope stage boundary 1/2 depths are equivalent to the depth of Horizon A, and, therefore, the Coleman and Roberts (1988a) borehole analysis can be used to map the extent of Horizon A outside the coverage of seismic data (Fig. 36); and 2) the minimum age of Horizon A is 12,500 yrs BP. This age determination suggests the Horizon A developed during late Pleistocene to early Holocene time. These relationships provide the basis for further correlation.

Analysis of the West Delta 96 lease block survey report corehole data (Cole, 1983) shows that a distinct change in lithofacies correlates to a high-amplitude seismic reflector (Fig. 45). Lithofacies overlying this reflector are described as soft clays with shell fragments; a stiff clay layer 'with significantly higher shear strengths than the overlying sediments' underlies the high-amplitude reflector. The subbottom depth of this reflector (68 feet) converts to approximately 85 msec in depth, which correlates well to the 88 msec depth of Horizon A at time marker 15:15 on *Acadiana 89* Line 19. This evidence suggests that Horizon A is the acoustic expression of a change in lithofacies from soft clays to stiff clay.

The next step in this investigation centers on correlating these results to other data for purposes of establishing a regional depositional framework and testing the accuracy of these results. Stanley et al. (1996) and Kulp et al. (2002) investigated the late Quaternary stratigraphic relationships of the area of Louisiana shelf within the vicinity of the Plaquemines-Balize delta lobe area of the modern Mississippi River deltaic plain. Stanley et al. (1996) focused on two lithofacies - a late Pleistocene facies and a late

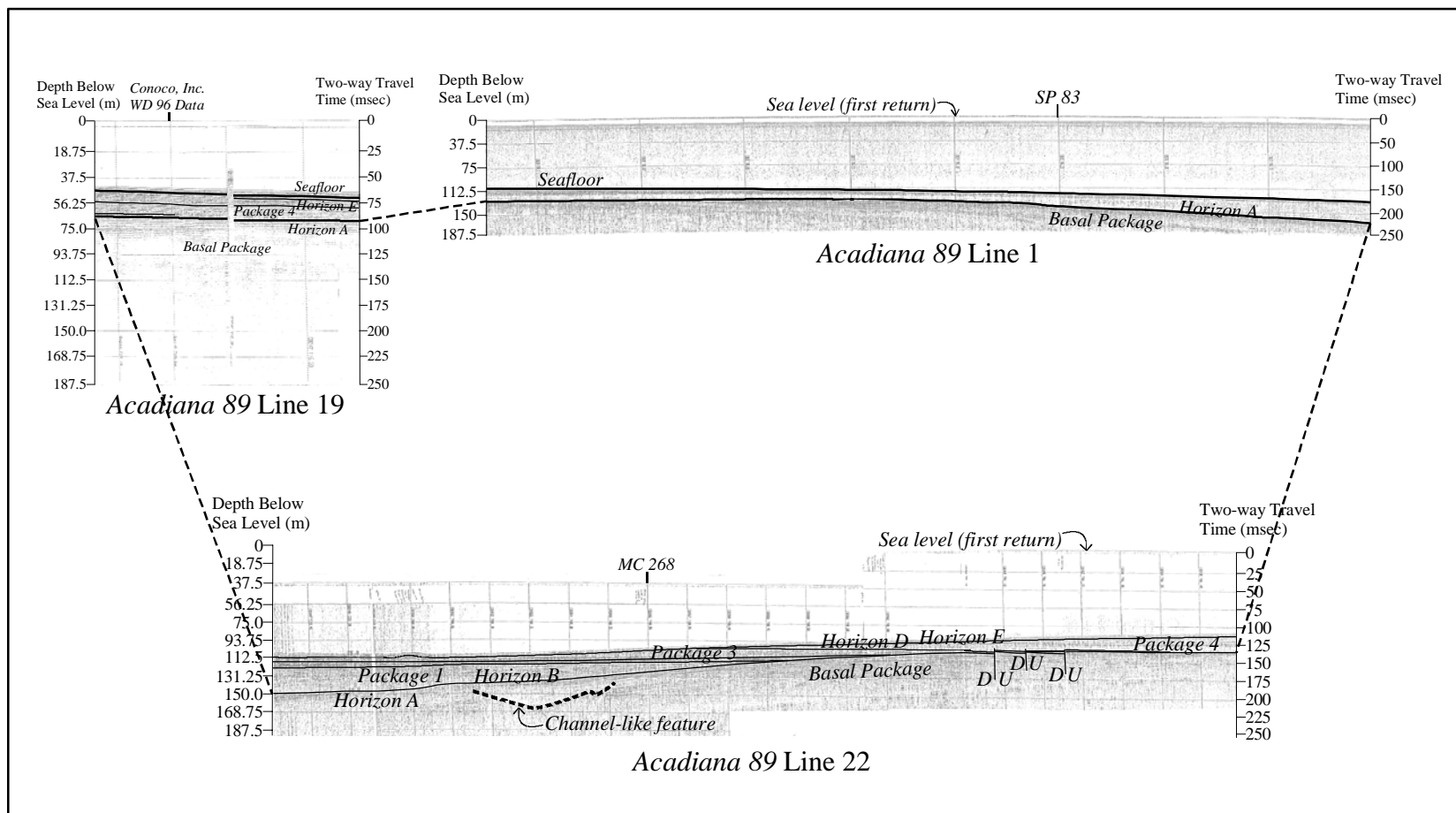


Figure 45. This figure illustrates the correlation of Horizon A across the study area with data taken from Coleman and Roberts (1988a) and the West Delta 96 lease block survey report (Cole, 1983). The Basal Package and Package 4 in *Acadiana 89 Line 19* seismic profile correlate well with lithologies of WD 96. Horizon A is found at depths matching those of the oxygen isotope stage boundary 1/2 in cores MC 268 and SP 83.

Pleistocene-early Holocene transgressive facies – and the late Wisconsin unconformity (LWU) that separates these two units. The Late Pleistocene facies is described as “compact silty mud and muddy silt” that may appear as mottled in color, and contain concretions, shells, and wood fragments (Stanley et al., 1996). Low water content and high shear strength characterizes this lithofacies. The late Pleistocene-early Holocene transgressive facies is a ‘shell-rich sandy and silty marine unit’ characterized by abundant shell material, the presence of light tan to gray sand and grey-green silt and clay. These lithofacies descriptions closely match those presented in the Conoco West Delta 96 lease block survey report (Cole, 1983). The late Pleistocene facies very closely resembles the stiff clay that underlies Horizon A. Kulp et al. (2002) correlated multiple data sets, including U.S. Army Corps of Engineers onshore-borehole data and Coleman and Roberts (1988a) offshore geotechnical borehole data to reach similar conclusions about the sedimentology of the LWU and overlying transgressive facies. Also, structural contours of the late Wisconsin unconformity in the vicinity of *Acadiana* 89 Line 1 show a strong correlation to those constructed from seismic data in this study. Kulp et al. (2002) mapped the LWU using. In their study, they mapped the structure of the base of the Holocene transgressive and highstand sedimentary package (topstratum), which is equivalent to mapping the structure of the LWU, and produced results unique from, but not dissimilar to, those presented by Stanley et al. (1996). The time-structure map of Horizon A in this study compares more favorably with the structure map of Kulp et al. (2002) than that of Stanley et al. (1996). While the structural maps presented by Stanley et al. (1996) and Kulp et al. (2002) differ from the structural map in this study



and each other, there are sufficient similarities shared among them to place confidence in these correlations.

These correlations allow for the following conclusions:

- 1) Sediments located below Horizon A - the Basal Package - are late Pleistocene in age.
- 2) Horizon A represents the late Wisconsin unconformity formed during subaerial exposure of the Pleistocene shelf during the falling to lowstand of sea level.
- 3) Sediments overlying Horizon A in the Conoco West Delta 96 lease block survey area - Package 4 – represent a late Pleistocene to early Holocene transgressive facies.

#### *Summary*

Seismic profile data analysis identifies five seismic facies units, referred here as packages, and five bounding surfaces, or horizons. Correlation of these results to other data sets allow for lithologies to be assigned to specific packages and identification of a major unconformity surface.

The basal package is variable in acoustic character, and cannot be fully analyzed due to shallow seismic penetration. Package 1 is the thickest seismic facies unit; it is limited in extent and confined to areas near the shelfbreak. Internal seismic character is oblique tangential. Packages 2 and 3 overlie Package 1, are both relatively thin, and exhibit similar external seismic form. These two packages terminate updip by onlap against Horizon A. Package 4, the uppermost package, thickens updip and is composed of continuous parallel onlapping reflectors.

Horizon A is prevalent throughout the study area as a prominent surface of reflector termination underlain by channel-like features. Horizons B, C, and D separate seismic packages, are limited in extent, and terminate in the updip direction by way of onlap against Horizon A and in the downdip direction either by pinch out or termination on the flanks of the Sackett Bank salt dome. Horizon E is also regionally extensive; however, this horizon delineates a series of high-amplitude reflectors, created by acoustic ringing off the sea floor, from the underlying seismic signal and is not a true stratigraphic surface.

Correlation of seismic results to other data sets allows for the determination of Horizon A as the late Wisconsin unconformity (*sensu* Stanley et al., 1996), a regionally extensive hiatal surface, which also correlates well to oxygen isotope stage boundary 1/2 from Coleman and Roberts (1988a). This correlation also shows the basal package to be late Pleistocene shelf sediments composed of stiff, weathered clay. Package 4 can be correlated to late Pleistocene-early Holocene transgressive facies deposits.

## DISCUSSIONS

### *Late Quaternary Shelf-Margin Delta*

This section presents the results from this study as evidence for the existence of a previously unstudied shelf-margin delta along the south-central Louisiana shelf.

Discussions of paleodrainage patterns and evidence presented in existing literature support the idea that the Pearl River is the fluvial source for this deltaic complex. This conclusion derives from multiple factors, which are discussed in detail in this section.

### *Seismic characteristics*

The characteristics of seismic facies identified in this study suggest shelf deltaic deposition in response to changing elevation of relative sea level. The Basal Package contains channel-like features that indicate the presence of an entrenched fluvial drainage network (Fig. 46). Similar features are associated with deltaic complexes across the northern Gulf of Mexico continental shelf margin (Fisk and McFarlan, 1955; Suter and Berryhill, 1985; Kindinger, 1988, 1989b; Kindinger et al., 1994; Sydow and Roberts, 1994; Anderson et al., 2004; and many others) (Figs. 47, 48). The structure map of Horizon A indicates the presence of an entrenched fluvial valley (Fig. 36). Package 1 possesses an oblique tangential internal reflector configuration. This configuration in conjunction with lithologic control from boreholes suggests a prograded deltaic system (Mitchum et al., 1977b). Packages 2 and 3 consist mainly of medium to high-amplitude, subparallel to parallel internal reflectors that terminate in onlap, which suggests marine processes, rather than deltaic processes, were dominant at the time of deposition (Vail et al., 1977a). Package 4 is composed of medium-amplitude, continuous parallel reflectors, also indicating that marine processes controlled the style of deposition. The seismic

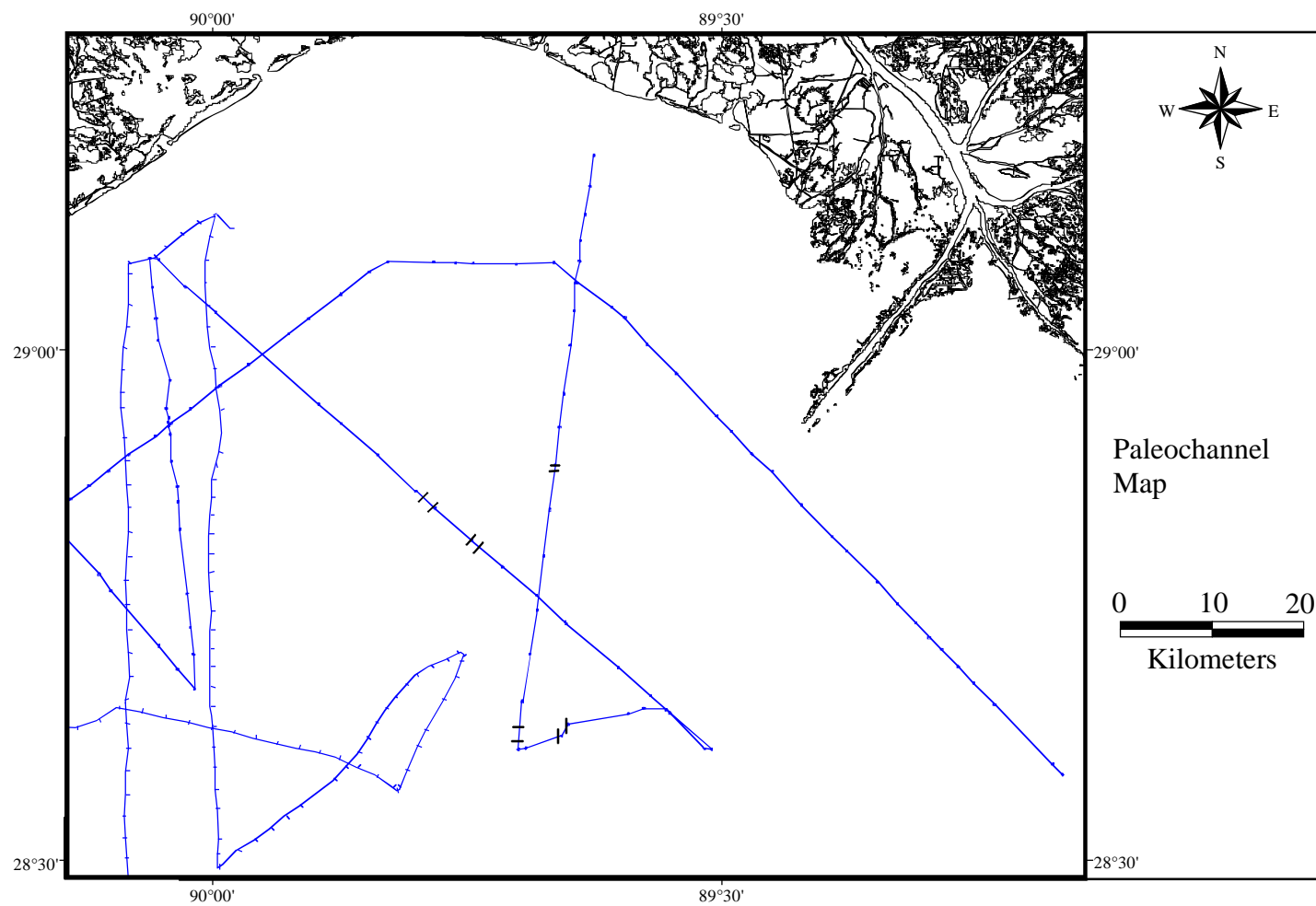


Figure 46. Dark lines mark the position of channel-like features observed in seismic profile data. These features are located in the Basal Package and underlie Horizon A.

character of Packages 2, 3, and 4 suggests that the rate of transgression exceeded the rate of sediment supply.

### *Depositional History*

The Basal Package existed prior to deposition of the shelf-margin delta on the basis of several key points of evidence. The presence of channel-like features in seismic profile records indicates fluvial incision took place on the uppermost boundary of this package. This package correlates to the late Wisconsin facies of Fisk (1944) and Stanley et al. (1996), a stiff clay of varying colors that exhibits many signs of subaerial weathering, and that also has a high shear strength; this correlation is confirmed by sedimentological and seismic data provided by the Conoco West Delta 96 lease block survey report. Therefore, the Basal Package most likely represents relic shelfal sediments exposed during the last lowstand of sea level.

Package 1 represents sediments deposited as a result of deltaic progradation during lowstand or subsequent rise of sea level. This conclusion is based on the stratigraphic stacking order and reflector relationships visible in seismic profile records as well as oxygen isotope data from boreholes. Style of deposition was in part controlled by the nearby Sackett Bank salt dome. Internal reflector patterns of this package on the flanks of the salt dome indicate that diapiric rise took place coincident with deposition. Faulting may have occurred at this time along the small down-to-the-south faults observed in the study area. Outbuilding and thickening of Package 1 increased the isostatic load carried by the shelf margin. A hingeline of small down-to-the-south faults formed in response to deformation associated with increased loading and subsequent downwarping of outer shelf sediments.

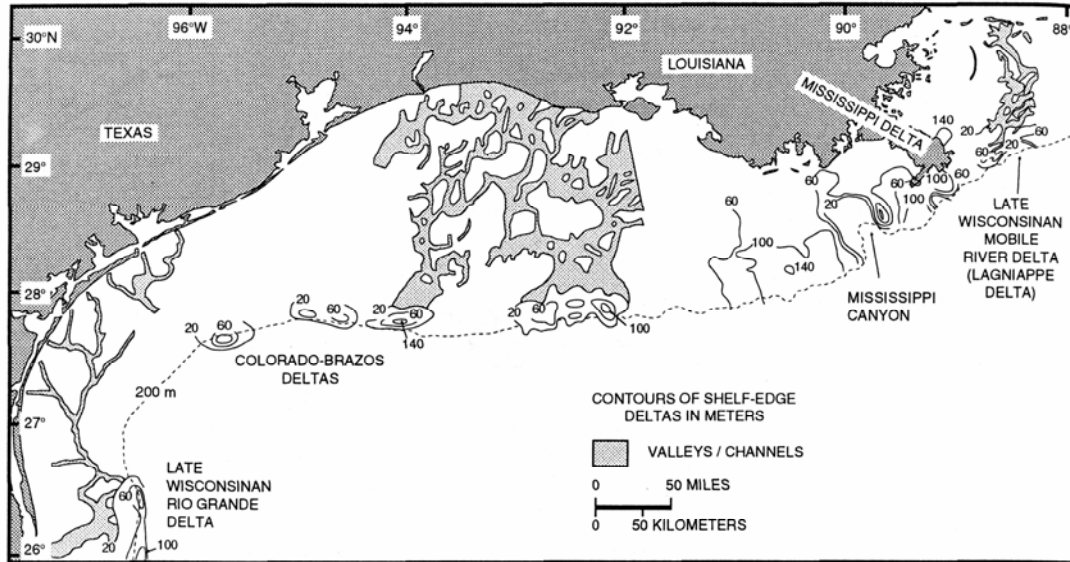


Figure 47. Paleogeographic map showing the distribution of late Pleistocene fluvial channels and their linked shelf-margin deltas on the Texas to Louisiana shelf. These systems formed during the Late Wisconsin sea level lowstand and glacial maximum, incising the underlying strata and extending to the shelf edge. Isopach contours on the shelf margin deltas show the overall position of shelf-margin deltas. Western Louisiana and Texas shelf data taken from Suter and Berryhill (1985); Lagniappe Delta data from Kindinger (1988) (modified from Winn et al., 1995).

Packages 2 and 3 were deposited following deltaic progradation. The predominantly landward onlapping internal reflector configurations in combination with sheet drape external seismic forms, as well as the overall thickness of each package, suggest that these packages suggest that the deltaic complex began backstepping in response to initial sea-level rise. During this time, infilling of the incised valley would have occurred.

Onlapping internal seismic reflector configurations and landward thickening indicate that marine processes deposited Package 4. Package 4 represents the late Pleistocene-early Holocene transgressive facies of Stanley et al. (1996) on the basis that this facies directly overlies the LWU on the eastern side of the study area, and this

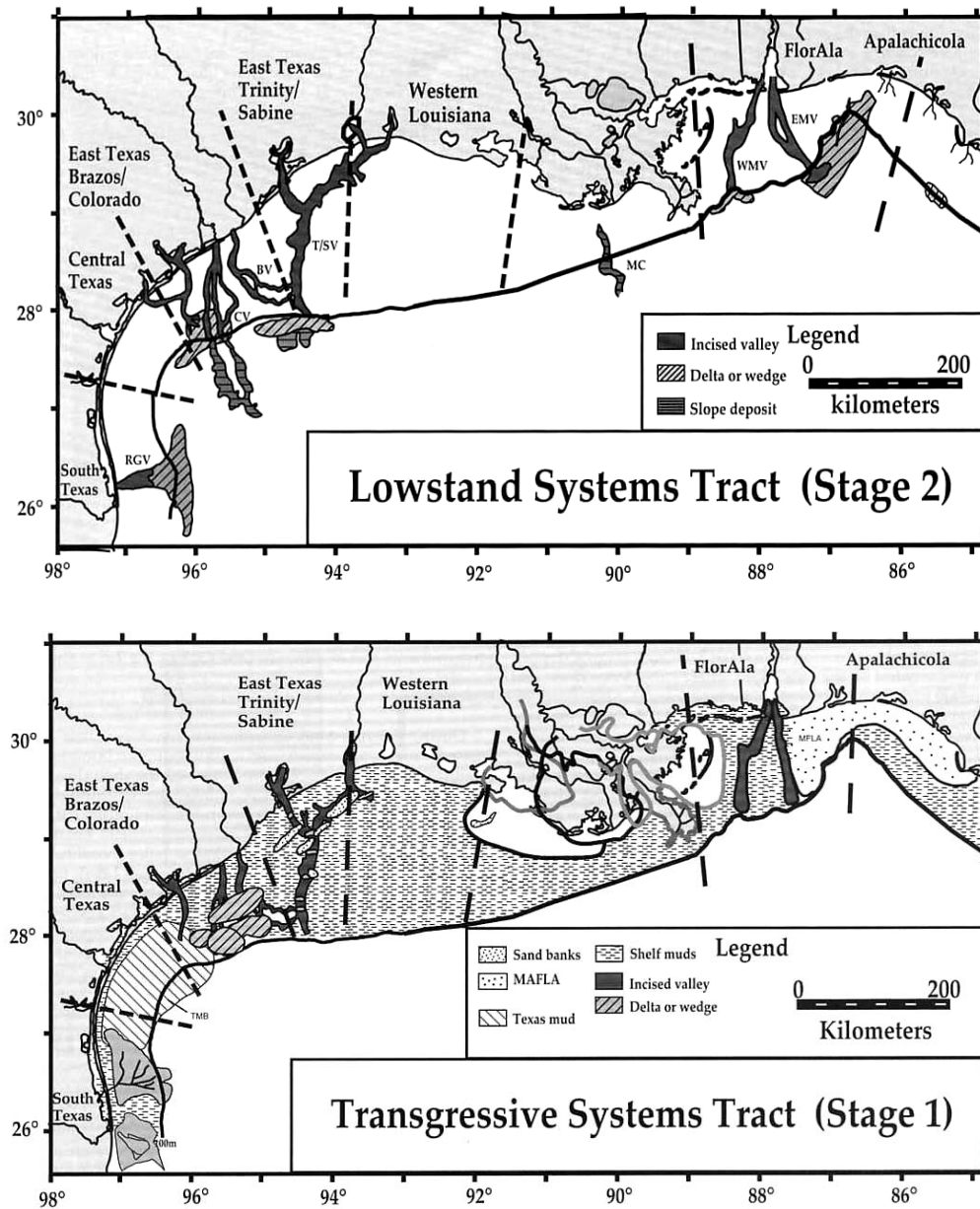


Figure 48. Maps showing distribution of entrenched fluvial drainage systems and their linked shelf-margin or slope depositional packages at the time of maximum sea-level lowstand (top image), and distribution of transgressive facies deposited during sea-level rise following maximum lowstand conditions (bottom image) (modified from Anderson et al., 2004).

stratigraphic relationship is repeated in the seismic and sedimentological data provided in the Conoco West Delta 96 lease block survey report.

The correlation of Horizon A to the late Wisconsin unconformity and oxygen isotope stage boundary 1/2 implies that deposition of this shelf-margin delta occurred between the time of maximum lowstand conditions, approximately 18,000 yrs BP (Fairbanks, 1989), and the youngest age of oxygen isotope stage boundary 1/2, approximately 12,500 yrs BP (Coleman and Roberts, 1988a). More data are needed to more discretely constrain the timing of deposition.

#### *Comparison to Regional Studies*

The framework of the shelf-margin delta presented in this study compares favorably with the overall style and timing of deposition observed in other shelf-margin deltas identified along the northern Gulf of Mexico shelf margin.

Diapiric control on the style of deposition is common among other shelf margin deltas (Suter and Berryhill, 1985; Kindinger, 1988, 1989b; Coleman and Roberts, 1988a,b; Kindinger et al., 1994; Sydow and Roberts, 1994; Morton and Suter, 1996; Anderson et al., 2004). The Sackett Bank salt dome in part controlled the style of deposition of this shelf-margin delta.

Most other regional studies, with the exception of Morton and Suter (1996), show fluvial incision across the exposed shelf during sea-level fall to lowstand. Such was the case with this shelf-margin delta. Structural contouring of Horizon A (LWU) shows the presence of an entrenched fluvial valley, and seismic profile records reveal channel-like features underlie this surface, indicating fluvial incision occurred across the late Pleistocene shelf (Basal Package).



The timing of deposition matches that of other regional shelf-margin deltas. Suter and Berryhill (1985) used radiocarbon dating techniques to determine that deposition of five shelf-margin deltas located on the Texas shelf-margin occurred between 18,000 and 10,500 yrs BP. Goodwin and Prior (1989) suggest the Mississippi River deposited sediments into the Mississippi Canyon between 30,000 and 7,500 yrs BP. Kindinger (1988, 1989b) does not suggest a discrete interval of time for deposition of the Lagniappe delta but does suggest that deposition occurred between the late Pleistocene fall of sea level and subsequent late Pleistocene to early Holocene transgression. These studies indicate that the most recent shelf-margin delta was deposited above a region-wide unconformity surface created by the late Wisconsin sea-level lowstand (LWU), and that a transgressive package, correlating to early Holocene sea-level rise, lies updip of the shelf-edge deltaic sediments. These findings are consistent with the results of this study. Coleman and Roberts (1988a) recognized an organized stratigraphic record of condensed and expanded lithostratigraphic intervals that were also tied to oxygen isotope stages rather than quantifying the nature and timing of specific shelf-margin deltas. Correlation of their oxygen isotope stage boundary 1/2 to the late Wisconsin unconformity suggests that sediments stratigraphically younger than this surface must fall within oxygen isotope stage 1, and thus are approximately 12,500 yrs BP or younger. This age range is consistent with most other studies of the Gulf coast shelf edge systems and seems to apply well to Packages 2 through 4. Package 1 may be older than this time frame indicates; Package 1 and Horizon A are conformable in downdip areas, suggesting deposition of Package 1 was concomitant with formation of Horizon A.

Overall, the style and timing of deposition observed in the shelf-margin delta of this study closely matches that of other regional shelf-margin delta investigations.

### *Paleodrainage Patterns*

The next phase in this investigation is to determine a source for the shelf-margin delta identified in this study. Understanding fluvial drainage patterns during the last sea-level lowstand provides the context within which to consider the source of the shelf-margin delta identified herein.

Vail's lowstand deposition model requires that fluvial systems extend across the exposed shelf during lowstand conditions, forming entrenched valleys and incised channel complexes. This type of drainage pattern is typical of shelf-margin deltas on the northern Gulf of Mexico (Fisk and McFarlan, 1955; Suter and Berryhill, 1985; Kindinger, 1988; Kindinger, 1989b; Sydow and Roberts, 1994; Anderson et al., 2004; and many others).

Figure 48 (Anderson et al., 2004) shows the paleodrainage patterns for some of the fluvial systems draining into the northern Gulf of Mexico during the last lowstand of sea level. The overall direction of drainage was north-to-south. Individual fluvial drainage systems extended basinward to feed into discrete shelf-margin delta complexes. The Mississippi River drainage system differed from other fluvial drainage systems in the Gulf of Mexico due to the large volume of water and sediment it discharged during the most recent deglaciation. As a result, the Mississippi River deeply incised the shelf creating the Mississippi Canyon, which is linked downslope to a large submarine fan.

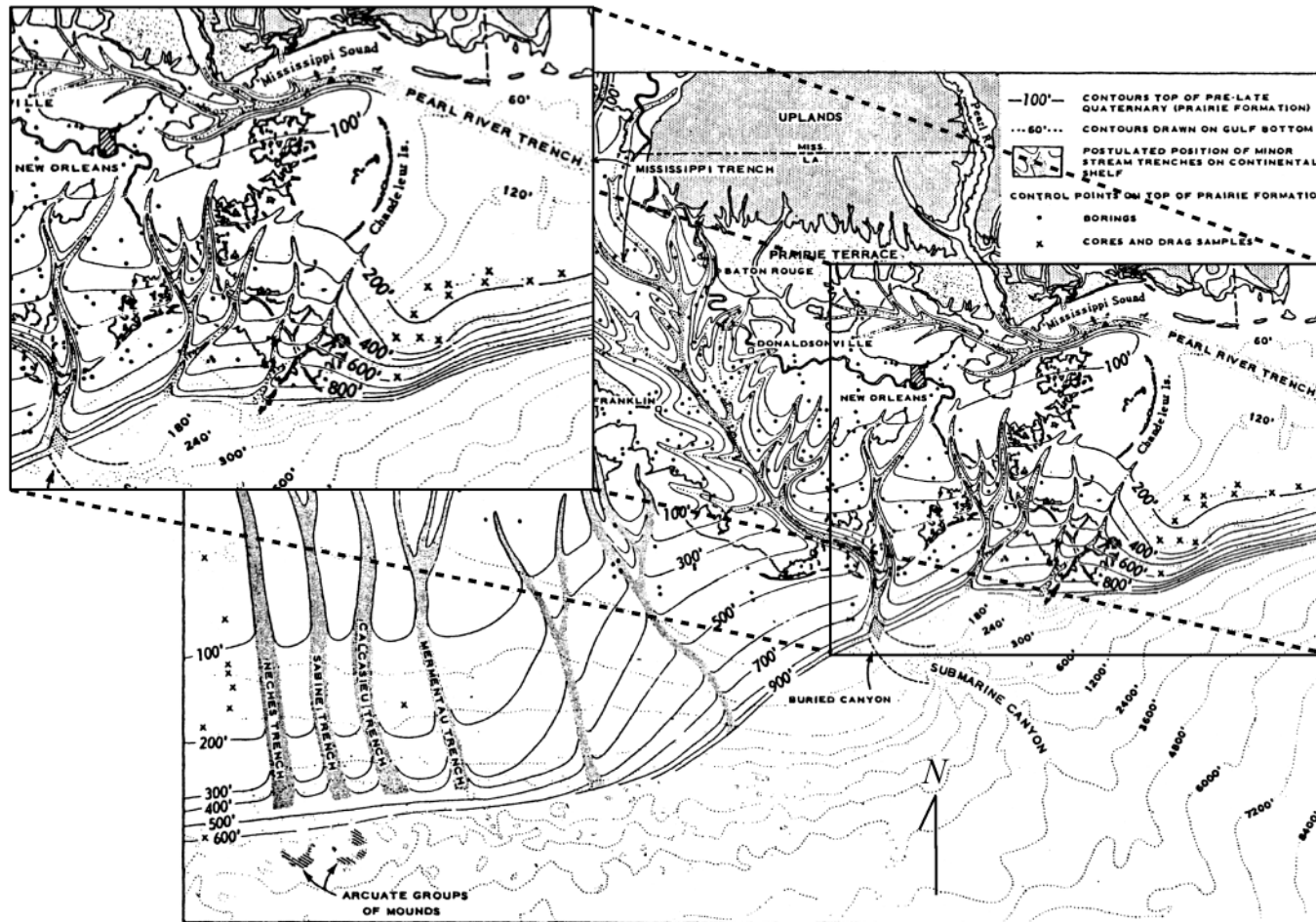


Figure 49. Fluvial paleodrainage systems became elongated across and entrenched into the exposed shelf during the most recent maximum sea-level lowstand, as seen here. The large map shows the Louisiana shelf paleodrainage network; inset map shows location of study area. Note the two small drainage systems located near the modern Balize delta lobe. Also of interest is the Pearl River paleodrainage network (from Fisk and McFarlan, 1955).

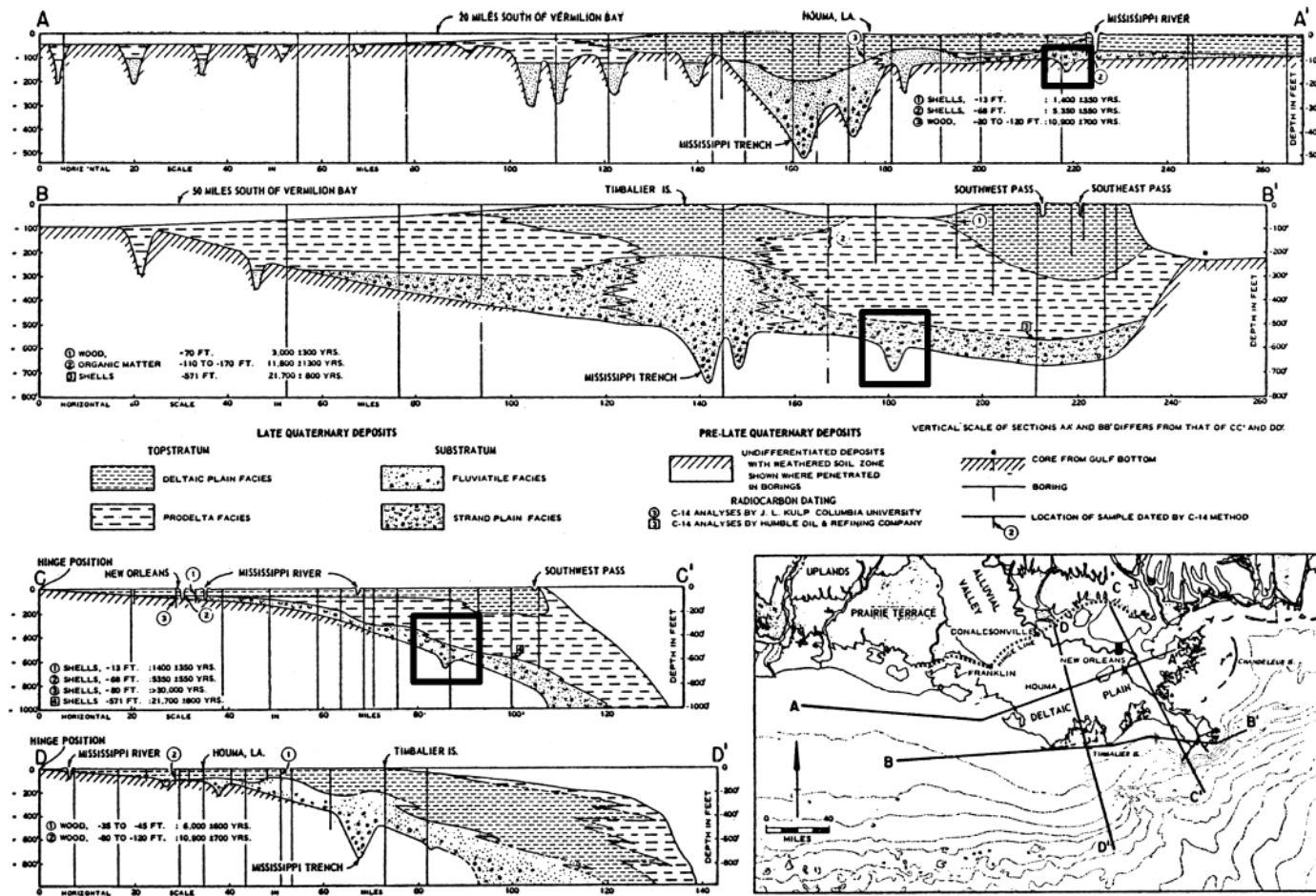


Figure 50. Cross-sectional diagrams of the Mississippi River deltaic plain show stratigraphic relationships of most recent deltaic sedimentary packages. Highlighted boxes indicate positions of small, incised valleys that possibly correlate to entrenched fluvial valley discovered in the study area. See small inset map for locations of each cross-sectional transect (modified from Fisk and McFarlan, 1955).

Other fluvial systems located on the Louisiana shelf extended across the shelf during the last lowstand of sea level, entrenching their distributary networks into the exposed shelf and depositing sediments along the shelf margin. A paleodrainage map shows the location of fluvial systems entrenched into the Louisiana shelf during the last lowstand of sea level (Fisk and McFarlan, 1955) (Fig 49). They identified the Mississippi Canyon, labeled as ‘Submarine Canyon’, and correlated it to a large entrenched fluvial network. Similar distributary networks are shown linked downslope to submarine trenches, including the Pearl River drainage system. The inset picture shows the approximate location of the study area. Fisk and McFarlan identify two entrenched systems in the northeastern portion of the study area. Each system drains roughly north-northwest to south-southwest. The Pearl River drainage system, also visible in the inset, curiously drains west-to-east in a manner contrary to other drainage systems shown. Fisk and McFarlan offer no explanation of the nature of these small systems in the text, nor do they address the anomalous drainage pattern of the Pearl River.

These two smaller paleodrainage systems may possibly be linked to the entrenched fluvial valley observed in this study. Figure 50 shows several cross-sectional diagrams constructed along strike and dip-parallel transects across the Mississippi River deltaic plain (Fisk and McFarlan, 1955). These cross-sections indicate the presence of small valleys incised into the late Wisconsin shelf, visible on cross-sections A-A’, B-B’, and C-C’. The authors do not address these features. However, they correlate well to the entrenched fluvial valley observed in the findings of this study and may represent the updip equivalent of that feature.

### *Pearl River Scenario*

The most plausible choice as fluvial source for the shelf-margin delta presented in this study is the Pearl River.

The entrenched valley evident in the structural map of Horizon A/LWU (Fig. 36) suggests a source lies north-to-northwest of the study area. If, as widely suggested, the Mississippi River occupied the Mississippi Canyon at the time the shelf-margin delta presented in this study formed and knowing that the Mississippi Canyon lies westward of the study area, then the Mississippi River cannot be the source of this shelf-margin delta. The source must, therefore, lie eastwardly of the Mississippi River. There are several fluvial systems to the east of the Mississippi River: the Pearl, Pascagoula, and Mobile rivers. Kindinger et al. (1994) suggests that the Pascagoula and Mobile Rivers source the Lagniappe delta and associated Mississippi-Alabama shelf-margin delta complex, a claim supported by Fillon et al. (2004) and Roberts et al. (2004). The source for this shelf-margin delta must, therefore, lie between the Mississippi and Pascagoula Rivers. The Pearl River remains the only logical choice.

The drainage patterns presented by Fisk and McFarlan (1955) indicate the Pearl River drained west-to-east in a configuration unlike other fluvial systems in the northern Gulf of Mexico. They provide no supporting arguments in their text for this trend. Furthermore, their cross-sections show the presence of small fluvial channels incising the late Pleistocene shelf in a north-to-south orientation that closely matches the orientation of the entrenched fluvial valley observed in the findings of this study (Fig. 50).

This paper suggests that the Pearl River is the fluvial source for the shelf-margin delta described herein. A re-interpretation of the paleodrainage map of Fisk and

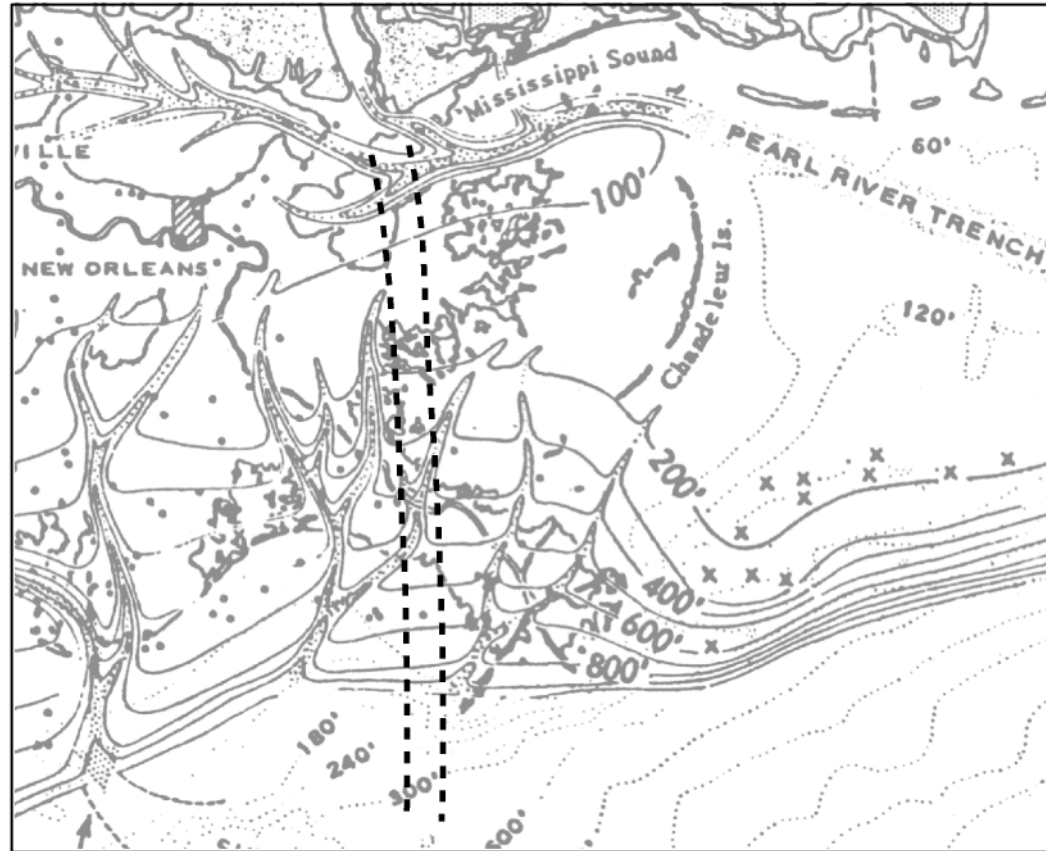


Figure 51. Magnified image of paleodrainage map (seen in Figure 49) illustrates a re-interpreted paleodrainage network for the Pearl River during the last maximum sea-level lowstand. Bold dashed lines indicate the relative position of the Pearl River distributary channel as re-interpreted in this study. This configuration is more consistent with the orientation of other fluvial drainage patterns observed on the northern Gulf of Mexico continental shelf (after Fisk and McFarlan, 1955).

McFarlan (1955) is presented in Figure 51. A north-to-south axis is offered in place of the west-to-east orientation of the axis of the Pearl River entrenched valley. This more logically explains the presence of the shelf-margin delta and the entrenched fluvial valley observed in the study area, and reconfigures the Pearl River drainage system in a manner more consistent with drainage patterns observed across the northern Gulf of Mexico continental shelf.



## **CONCLUSIONS**

This study has identified a previously unknown shelf-margin delta located on the southeastern Louisiana shelf in the north-central Gulf of Mexico. The style and timing of deposition of this shelf-margin delta is consistent with other shelf-margin deltas located on the northern Gulf of Mexico shelf margin. The Pearl River is the most likely fluvial source of the shelf-margin delta.

Future research of this shelf-margin delta should focus on identifying lithofacies relationships, better constraining timing of deposition, and correlating known contacts and packages in the updip direction.

## REFERENCES

- Anderson, J. B., Rodriguez, A., Abdulah, K. C., Fillon, R. H., Banfield, L. A., McKeown, H. A., Wellner, J. S., 2004, Late Quaternary stratigraphic evolution of the northern Gulf of Mexico margin: a synthesis, *in* Anderson, J. B., and Fillon, R. H., eds., Society of Economic Paleontologists and Mineralogists Special Publication 79, p. 1-25.
- Ballard, R. D., and Uchupi, E., 1970, Morphology and Quaternary history of the continental shelf of the Gulf coast of the United States. Woods Hole Oceanographic Institution Contribution, no. 2399, 13 p.
- Buffler, R. T., and Thomas, W. A., 1994, Crustal structure and evolution of the southeastern margin of North America and the Gulf of Mexico basin, *in* Speed, R.C., ed., Phanerozoic evolution of North American continent-ocean transitions: Boulder, Colorado, Geological Society of America, The Geology of North America, v. CTV-1, p. 219-264.
- Chappell, J. and Shackleton, N. J., 1986, Oxygen isotopes and sea level: *Nature*, v. 324, p. 137-140.
- Cole, J. F., 1983, A multi-sensor engineering survey of West Delta block 96 for Conoco Inc., C.A.G.C. Marine Region, Racal-Decca Survey, Inc., Houston, TX, 19 p.
- Coleman, J. M., and Roberts, H. H., 1988, Sedimentary development of the Louisiana continental shelf related to sea-level cycles: Part I – Sedimentary sequences: *Geo-Marine Letters*, v. 8, p. 63-108.
- Coleman, J. M., and Roberts, H. H., 1988, Sedimentary development of the Louisiana continental shelf related to sea-level cycles: Part II – Seismic response: *Geo-Marine Letters*, v. 8, p. 109-119.
- Coleman, J. M., Roberts, H. H., and Bryant, W. R., 1991, Late Quaternary sedimentation, *in* Salvador, A., ed., The Gulf of Mexico Basin: Geological Society of America, The Geology of North America, v. J. p. 325-352.
- Curry, J. R., 1960, Sediments and history of Holocene transgression, continental shelf, northwest Gulf of Mexico, *in* Shepard, F. P., Phleger, F. B., and Van Andel, T. H. ed., Recent Sediments, Northwestern Gulf of Mexico: American Association of Petroleum Geologists, p. 221-236.
- Ewing, T. E., 1991, Structural Framework, *in* Salvador, A., ed., The Gulf of Mexico Basin: Boulder, Colorado, Geological Society of America, The Geology of North America, v. J, p. 31- 52.

- Fairbanks, R. G., 1989, A 17,000-year glacio-eustatic sea level record: influence of glacial melting rates on the Younger Dryas event and deep-ocean circulation: *Nature*, v. 342, p. 637-642.
- Fillon, R. H., Kohl, B., and Roberts, H. H., 2004, Late Quaternary deposition and paleobathymetry at the shelf-slope transition, ancestral Mobile River delta complex, northeastern Gulf of Mexico, *in* Anderson, J. B., and Fillon, R. H., eds., *Society of Economic Paleontologists and Mineralogists Special Publication 79*, p. 111-141.
- Fisk, H. N., 1944, Geologic investigations of the alluvial valley of the lower Mississippi River: Vicksburg, Mississippi, U. S. Army Corp of Engineers, Mississippi River Commission, 78 p.
- Fisk, H. N., 1947, Fine grained alluvial deposits and their effects on Mississippi River activity: Vicksburg, Mississippi, U. S. Army Corp of Engineers Waterways Experiment Station, 78 p.
- Fisk, H. N., and McFarlan, E. Jr., 1955, Late Quaternary deltaic deposits of the Mississippi River: Geological Society of America, Special Paper 62, p. 279-302.
- Frazier, D. E., 1967, Recent deltaic deposits of the Mississippi River: their development and chronology: *Gulf Coast Association of Geological Societies Transactions*, v. 27, p. 287-315.
- Frazier, D. E., 1974, Depositional episodes: Their relationship to the Quaternary stratigraphic framework in the northwestern portion of the Gulf basin: Austin, Texas Bureau of Economic Geology Circular 74-1, 28 p.
- Galloway, W. E., 1989a, Genetic stratigraphic sequences in basin analysis I: Architecture and genesis of flooding-surface bounded depositional units: *American Association of Petroleum Geologists Bulletin*, v. 73, no. 2, p. 125-142.
- Galloway, W. E., 1989a, Genetic stratigraphic sequences in basin analysis II: Application to northwest Gulf of Mexico Cenozoic Basin: *American Association of Petroleum Geologists Bulletin*, v. 73, no. 2, p. 143-154.
- Goodwin, R. H., and Prior, D. B., 1989, Geometry and depositional sequences of the Mississippi Canyon, Gulf of Mexico: *Journal of Sedimentary Petrology*, v. 59, p. 318-329.
- Imbrie, J., Hays, J. D., Martinson, D. G., McIntyre, A., Mix, A. C., Morley, J. J., Pisias, N. G., Prell, W. L., and Shackleton, N. J., 1984, The orbital theory of Pleistocene climate: support from a revised chronology of the marine oxygen-18 record, *in*, Berger, A. L., et al., eds., *Milankovitch and Climate, Part I*, p. 269-305.

- Kindinger, J. L., 1988, Seismic stratigraphy of the Mississippi-Alabama shelf and upper continental slope: *Marine Geology*, v. 83, p. 79-94.
- Kindinger, J. L., 1989, Depositional history of the Lagniappe delta, northern Gulf of Mexico: *Geo-Marine Letters*, v. 9, p. 59-66.
- Kindinger, J. L., Balson, P. S., and Flocks, J. G., 1994, Stratigraphy of the Mississippi-Alabama shelf and the Mobile River incised-valley system, *in* Dalrymple, R. W., Boyd, R., and Zaitlin, B. A., eds., *Society of Economic Paleontologists and Mineralogists Special Publication 51*, p. 83-95.
- Kolb, C. R., and Van Lopik, J. R., 1958, Geology of the Mississippi River deltaic plain, southeastern Louisiana: Vicksburg, Mississippi, U. S. Army Corp of Engineers Waterways Experimental Station, Technical Report 3-483, 120 p.
- Kulp, M. A., Howell, P., Adiau, S., Penland, S., Kindinger, J., and Williams, S. J., 2002, Latest Quaternary stratigraphic framework of the Mississippi River delta region, Gulf Coast Association of Geological Societies Transactions, v. 52, p. 573-582.
- Lopez, J. A., 1990, Structural styles of growth faults in the U.S., Gulf coast basin, *in* Brooks, J. ed., *Classic Petroleum Provinces: Geological Society Special Publication 50*, p. 203-219.
- Martinson, D. G., Pisias, N. G., Hayes, J. D., Imbrie, J., Moore, T.C., and Shackleton, N. J., 1987, Age dating and the orbital theory of the ice ages—development of a high resolution 0 to 300,000 year chronostratigraphy: *Quaternary Research*, v. 27, p. 1-29.
- Miall, A. D., 1986, Eustatic sea level changes interpreted from seismic stratigraphy: a critique of the methodology with particular reference to the North Sea Jurassic record: *American Association of Petroleum Geologists Bulletin*, v. 70, no. 2, p. 131-137.
- Mitchum, R. M., Jr., Vail, P. R., and Thompson, S., III, 1977a, Seismic stratigraphy and global changes of sea level, Part II, *in* Payton, C.E., ed., *Seismic Stratigraphy—Applications to hydrocarbon exploration: American Association of Petroleum Geologists Memoir*, 26, p. 53-62.
- Mitchum, R. M., Jr., Vail, P. R., and Sangree, J. B., 1977b, Seismic stratigraphy and global changes of sea level, Part VI, *in* Payton, C.E., ed., *Seismic Stratigraphy—Applications to hydrocarbon exploration: American Association of Petroleum Geologists Memoir*, 26, p. 53-62.
- Morton, R. A., and Suter, J. R., 1996, Sequence stratigraphy and composition of late Quaternary shelf-margin deltas, northern Gulf of Mexico: *American Association of Petroleum Geologists Bulletin*, v. 80, p. 505-530.

- Nelson, T. H., 1991, Salt tectonics and listric-normal faulting, *in* Salvador, A. ed., The Gulf of Mexico Basin: Boulder, Colorado, Geological Society of America, The Geology of North America, v. J., p. 73-89.
- Nelson, H. F., and Bray, E. E., 1970, Stratigraphy and history of the Holocene sediments in the Sabine-High Island area, Gulf of Mexico, *in* Morgan, J. P., (ed.), Delta Sedimentation, Modern and Ancient: Society of Economic Paleontologist and Mineralogists Special Publication, no. 15, p. 48-77.
- Penland, S., McBride, R. A., Williams, S. J., Boyd, R., and Suter, J. R., 1991, Effects of sea level rise on the Mississippi River delta plain, *in* Kraus, N. C., Gingerich, K. J., and Kriebel, D. L., eds., Coastal sediments '91: New York, American Society of Civil Engineers, p. 1248-1264.
- Rich, J. L., 1951, Three critical environments of deposition, and criteria for recognition of rocks deposited in each of them: Geological Society of America Bulletin, v. 62, p. 1-20.
- Roberts, H. H., Fillon, R. H., Kohl, B., Robalin, J. M., and Sydow, J. C., 2004, Depositional architecture of the Lagniappe delta: sediment characteristics, timing of depositional events, and temporal relationship with adjacent shelf-edge deltas, *in* Anderson, J. B., and Fillon, R. H., eds., Society of Economic Paleontologists and Mineralogists Special Publication 79, p. 143-188.
- Salvador, A., 1991b, Origin and development of the Gulf of Mexico basin, *in* Salvador, A., ed., The Gulf of Mexico Basin: Boulder, Colorado, Geological Society of America, The Geology of North America, v. J. p. 389-444.
- Sloss, L. L., 1963, Sequences in the cratonic interior of North America: Geological Society of America Bulletin, v. 74, p. 93-114.
- Stanley, D. J., Warne, A. G., and Dunbar, J. B., 1996, Eastern Mississippi delta: late Wisconsin unconformity, overlying transgressive facies, sea level and subsidence: Engineering Geology, v. 45, p. 359-381.
- Suter, J. R., and Berryhill, H. L., Jr., 1985, Late Quaternary shelf-margin deltas, northwest Gulf of Mexico: American Association of Petroleum Geologists, v. 69, p. 77-91.
- Suter, J. R., Berryhill, H. L., Jr., and Penland, S., 1987, Late Quaternary sea-level fluctuations and depositional sequences, southwest Louisiana continental shelf, *in* Nummedal, D., Pilkey, O. H., and Howard, J. D., eds., Sea-level fluctuation and coastal evolution: Society of Economic Paleontologists and Mineralogists Special Publication 41, p. 199- 219.
- Swift, D. J. P., 1975, Barrier island genesis: evidence from the central Atlantic shelf, eastern U.S.A.: Sedimentary Geology, v. 14, p. 1-43.

- Sydow, J., Roberts, H. H., Bouma, A. H., and Winn, R., 1992, Constructional subcomponents of a shelf-edge delta, northeast Gulf of Mexico: Gulf Coast Association of Geological Societies Transactions, v. 42, p. 717-726.
- Sydow, J., and Roberts, H. H., 1996, Stratigraphic framework of a Late Pleistocene shelf-edge delta, northeast Gulf of Mexico: American Association of Petroleum Geologists, v. 78, no. 8, p. 1276-1312.
- Törnqvist, T. E., González, J. L., Newsom, L. A., Van der Borg, K., De Jong, A. F. M., Kurnik, C. W., 2004, Deciphering Holocene sea-level history on the U. S. Gulf Coast: A high-resolution record from the Mississippi Delta: Geological Society of America Bulletin, v. 116, p. 1026-1039.
- Vail, P. R., and Mitchum, R. M., Jr., 1977, Seismic stratigraphy and global changes of sea level, Part I, *in* Payton, C.E., ed., Seismic Stratigraphy—Applications to hydrocarbon exploration: American Association of Petroleum Geologists Memoir, 26, p. 51-52.
- Vail, P. R., Mitchum, R. M., Jr., and Thompson, S., III, 1977a, Seismic stratigraphy and global changes of sea level, Part III, *in* Payton, C.E., ed., Seismic Stratigraphy—Applications to hydrocarbon exploration: American Association of Petroleum Geologists Memoir, 26, p. 63-81.
- Vail, P. R., Mitchum, R. M., Jr., and Thompson, S., III, 1977b, Seismic stratigraphy and global changes of sea level, Part IV, *in* Payton, C.E., ed., Seismic Stratigraphy—Applications to hydrocarbon exploration: American Association of Petroleum Geologists Memoir, 26, p. 83-97.
- Winn, R. D., Jr., Roberts, H. H., Kohl, B., Fillon, R. H., Crux, J. A., Bouma, A. H., and Spero, H. W., 1998, Upper Quaternary strata of the upper continental slope, northeastern Gulf of Mexico: sequence stratigraphic model for a terrigenous shelf edge: Journal of Sedimentary Research, v. 68, no. 4, p. 579-595.

## **VITA**

Casey R. Mobley was born and raised in northern Kentucky. He relocated to Versailles, Kentucky in late 1987. Casey graduated from Woodford County High School with honors in 1994. Enrolling at the University of Kentucky in the fall of 1994, he majored in Physics while attempting to earn an appointment into the United States Naval Academy. Casey reassessed his academic direction when his military career plans met with disappointment, deciding upon a degree in Geology. Following a brief academic hiatus, Casey graduated with a BS in Geology from UK in the summer of 2001.

Casey enrolled at the University of New Orleans as a Masters Degree candidate with a focus in coastal geology in the fall of 2002. His thesis advisor, Dr. Mark Kulp, a fellow UK alum, was instrumental in Casey's decision to attend UNO.

Casey has made New Orleans his permanent home, settling down with his family - fiancée, Michelle, and son, Ryan Alexander. Casey looks forward to a career with ChevronTexaco upon graduation.